

THE APPLICATION OF THE TOTAL EVIDENCE APPROACH FOR PHYLOGENETIC
RECONSTRUCTION OF SELECTED MONOTHALAMOUS FORAMINIFERA OF SAPELO
ISLAND, GEORGIA, USA

by

DENIZ ZUBEYDE ALTIN-BALLERO

(Under the Direction of Susan T. Goldstein)

ABSTRACT

Modern single chambered monothalamids are largely understudied representatives of early-evolving foraminifera despite their widespread presence in marine, freshwater, brackish and even terrestrial habitats. Unlike polythalamids, taphonomic vulnerability, lack of a consistent fossil record and their simple gross morphology makes evolutionary affinities difficult to elucidate. Of thirteen clades delineated by small subunit ribosomal DNA (SSU rDNA) phylogenetics, the Clade E lineage is composed of taxa that do not share a common general morphology but appear to have a loose molecular affinity. Membership of taxa suspected to be in Clade E was tested using Bayesian statistics on the SSU rDNA gene and by multiple genes (SSU rDNA, actin, β -tubulin). Both methods returned a 'core' group (*Psammophaga* spp., *Xiphophaga* spp., *Vellaria* spp.) identified as Clade E whereas remaining taxa are excluded from the clade. Relationships among orphan taxa cannot be determined without an increase in taxon sampling. The multi-gene analysis shifted relationships in the SSU rDNA based tree without an increase in node support.

Ultrastructural data show a consistent architectural theme among all evaluated taxa regardless of phylogenetic placement. All possess an electron-transparent inner organic lining (IOL) containing electron-dense fibers and granules. The IOL is in direct contact with the plasma membrane and test construction materials are released into the IOL exocytotically or by direct transfer via vesicles. All taxa possessed a single nucleus and cytoplasmic stercomata found in some deposit-feeding foraminifera were observed in two. Overall shape, thickness, mineralogic composition and packing of the agglutinated layer, and IOL thickness varied among all taxa and did not correlate with placement in phylogenetic trees. Variability in gross morphology of closely related monothalamids is taxonomically uninformative. Conversely, wall ultrastructure appears to be consistent among the core Clade E and the orphan taxa that cannot be placed into any particular clade at this time. These orphan taxa appear to be close relatives of Clade E based on wall ultrastructure but cannot be considered true members through phylogenetics. Increased taxonomic sampling of monothalamids is required to improve phylogenetic signal in molecular trees and further delineate potential evolutionary patterns of ultrastructural features.

INDEX WORDS: Foraminifera, Monothalamid, Allogromiid, New species, Phylogenetic placement, Clade E, Multi-gene analysis, Total evidence, Electron microscopy, Ultrastructure, Small subunit of the ribosomal DNA (SSUrDNA), Actin, β -tubulin

THE APPLICATION OF THE TOTAL EVIDENCE APPROACH FOR PHYLOGENETIC
RECONSTRUCTION OF SELECTED MONOTHALAMOUS FORAMINIFERA OF SAPELO
ISLAND, GEORGIA, USA

by

DENIZ ZUBEYDE ALTIN-BALLERO

B.S., Montclair State University, 1995

M.S., Montclair State University, 1998

M.S., Montclair State University, 1998

A Dissertation Submitted to the Graduate Faculty of The University of Georgia in Partial

Fulfillment of the Requirements for the Degree

DOCTOR OF PHILOSOPHY

ATHENS, GEORGIA

2013

© 2013

Deniz Zubeyde Altin-Ballero

All Rights Reserved

THE APPLICATION OF THE TOTAL EVIDENCE APPROACH FOR PHYLOGENETIC
RECONSTRUCTION OF SELECTED MONOTHALAMOUS FORAMINIFERA OF SAPELO
ISLAND, GEORGIA, USA

by

DENIZ ZUBEYDE ALTIN-BALLERO

Major Professor: Susan T. Goldstein

Committee: Mark Farmer
Andrea Habura
Joseph McHugh
Sally Walker

Electronic Version Approved:

Maureen Grasso
Dean of the Graduate School
The University of Georgia
December 2013

DEDICATION

I dedicate this dissertation to my child, Linda Felicia Ballero.

ACKNOWLEDGEMENTS

I graciously thank the following individuals for their support in my completion of this doctoral dissertation. Mark Farmer for utilization of equipment and lab space for the molecular portion of this project; Sam Bowser and Sarah Jardeleza for assistance; Elizabeth Richardson, Mary Ard and John Shields for their advisement on electron microscopic techniques, Jan Pawlowski for sharing his alignments, expertise and thoughtful discussions, Paul Schroeder for assistance using the XRD. I thank the UGA Marine Institute (UGAMI), Plant Biology Electron Microscope Facility, UGA Veterinary School Electron Microscope Laboratory and the UGA Center for Advanced Ultrastructural Research for facility access. For thoughtful insights and constructive critiques, I thank my committee Mark Farmer, Andrea Habura, Joseph McHugh and Sally Walker. Most importantly I would like to thank my major professor Susan T. Goldstein for thoughtful discussions and much needed moral support. Finally, I acknowledge the following agencies which generously provided funding for research and the dissemination of the results.

National Science Foundation DEB0445181 to S. S. Bowser and S. T. Goldstein

National Science Foundation OCE0850505 to S.T. Goldstein

Cushman Foundation for Foraminiferal Research

Lerner-Gray Fund of the American Museum of Natural History

Paleontological Society

Geological Society of America

Watts-Wheeler Memorial Fund and John Sanford Levy Fund of the UGA Geology Department

Friends of the University of Georgia Marine Institute

TABLE OF CONTENTS

	Page
ACKNOWLEDGEMENTS	v
LIST OF TABLES	ix
LIST OF FIGURES	x
CHAPTER	
1 INTRODUCTION AND LITERATURE REVIEW	1
Introduction	1
Monothalamid Taxonomy and Classification	2
Monothalamid Gross Morphology and Ultrastructure	5
Morphology versus Molecules: The Total Evidence Approach	10
2 A NEW ALLOGROMIID FORAMINIFERA <i>NIVEUS FLEXILIS</i> , NOV. GEN., NOV. SP., FROM COASTAL GEORGIA USA: FINE STRUCTURE AND GAMETOGENESIS	14
Abstract	15
Introduction	16
Materials and Methods	17
Results: Test Morphology and Fine Structure	21
Results: Cell Body of Non-Reproductive, Vegetative Individuals	23
Results: Reproduction by Gametogenesis and Asexual Reproduction	24
Discussion	29

Systematic Description and Phylogenetic Position.....	35
Conclusions.....	41
Acknowledgments.....	41
3 <i>PSAMMOPHAGA SAPELA</i> N. SP., A NEW MONOTHALAMOUS FORAMINIFERAN FROM COASTAL GEORGIA, U.S.A.: FINE STRUCTURE, GAMETOGENESIS AND PHYLOGENETIC PLACEMENT.....	43
Abstract.....	44
Introduction.....	44
Materials and Methods.....	46
Systematic Description and Phylogenetic Position.....	49
Further Observations on <i>Psammophaga sapela</i>	55
Discussion	63
Acknowledgments.....	70
4 TESTING THE FIDELITY OF SSU BASED PHYLOGENIES IN SELECTED MONOTHALAMOUS FORAMINIFERA: COUPLING MULTI-GENE PHYLOGENETICS WITH ULTRASTRUCTURE.....	71
Abstract.....	72
Introduction.....	73
Materials and Methods.....	76
Results: Phylogenetic Trees.....	81
Results: Gross Morphology and Wall Ultrastructure.....	86
Discussion.....	91
Conclusions.....	113

Acknowledgments.....	114
5 CONCLUSIONS.....	115
REFERENCES	120

LIST OF TABLES

	Page
Table 1.1: Summary of current publications on monothalamid ultrastructure using transmission electron microscopy (TEM).....	9
Table 1.2: Summary of protein coding gene sequences available for Foraminifera	12
Table 3.1: Comparison of fine structural characteristics of selected Clade E foraminiferans.....	67
Table 4.1: GenBank accession numbers for SSU rDNA, actin and β -tubulin sequences obtained in this study.	80
Table 4.2: Summary of gross morphology and wall ultrastructure for taxa examined in this study.....	92

LIST OF FIGURES

	Page
Figure 2.1: Approximate geographic location of sampling site for <i>Niveus flexilis</i>	18
Figure 2.2: Gross morphology of <i>Niveus flexilis</i>	22
Figure 2.3: Wall ultrastructure for <i>Niveus flexilis</i>	25
Figure 2.4: Nuclear ultrastructure and gross reproductive morphology of <i>Niveus flexilis</i>	27
Figure 2.5: Reproductive ultrastructure for <i>Niveus flexilis</i>	28
Figure 2.6: Type specimens for <i>Niveus flexilis</i>	38
Figure 3.1: Approximate geographic sampling locations for <i>Psammophaga sapela</i>	47
Figure 3.2: Type specimens for <i>Psammophaga sapela</i> n.sp.	51
Figure 3.3: Phylogenetic position of <i>Psammophaga sapela</i>	56
Figure 3.4: Gross morphology of <i>Psammophaga sapela</i>	58
Figure 3.5: Wall ultrastructure of <i>Psammophaga sapela</i>	60
Figure 3.6: Nuclear ultrastructure of <i>Psammophaga sapela</i>	62
Figure 3.7: Reproduction in <i>Psammophaga sapela</i>	65
Figure 4.1: Approximate geographic sampling locations	78
Figure 4.2: Phylogenetic tree of selected groups of monothalamids based on SSU rDNA only ..	83
Figure 4.3: Bayesian analysis of “Clade E” monothalamids with selective clade removal	84
Figure 4.4: Bayesian analysis using multiple genetic markers	85
Figure 4.5: Gross morphology and ultrastructure for the “Fusiform” monothalamid	94

Figure 4.6: Gross morphology and ultrastructure for the “Fruitcake” monothalamid.....96

Figure 4.7: Gross morphology and ultrastructure for the “Chocolate silver saccamminid”
monothalamid97

Figure 4.8: Gross morphology and ultrastructure for the “#5 Cigar” monothalamid.....98

Figure 4.9: Ultrastructure for the “Timber dock black and white” monothalamid.....99

Figure 4.10: Ultrastructure for the “*Micrometula*-like” monothalamid.....100

CHAPTER 1

INTRODUCTION AND LITERATURE REVIEW

Introduction

Monothalamous (single chambered) foraminifera represent a seemingly inconspicuous taxonomic group because of their limited fossil occurrences and apparent morphological simplicity. Overall, the gross morphology of monothalamids differs from that of the better known polythalamous taxa in that most possess a single chambered test made of organic material, agglutinated material with an organic bioadhesive (Loeblich and Tappan, 1987) or lack a test all together (Pawlowski and others, 1999a, 1999b). Monothalamids also typically lack distinguishing ornamentation but may have great intraspecific variation, rendering them difficult to identify or characterize. Further, the organic components of the test are vulnerable to taphonomic, particularly bacterial, degradation (Goldstein and Barker, 1988). They are fragile and commonly disintegrate rapidly following death and reproduction (Altin and others, 2009; Altin-Ballero and others, 2013) as evidenced by their absence in most foraminiferal death assemblages. As a result, monothalamids have received less attention by researchers than foraminifera with mineralized tests. For a time, studies on monothalamid diversity and ecology were geographically restricted to higher latitudes in both hemispheres (Bowser and others, 1995, 2002; Cedhagen and Pawlowski, 2002; Gooday, 2002; Gooday and others, 1996; Habura and others, 2006, 2008; Holzmann and others, 2003; Korsun, 2002; Pawlowski and others, 2002, 2003; Wilding, 2002). More recent examination of monothalamid diversity shows they do in

fact have significant occurrences and abundances in the middle latitudes as well (Habura and others, 2004, 2008; LeCroq and others, 2011; Tsuchiya and others, 2013).

Monothalamids have also been recovered in freshwater (Holzmann and others, 2003) and even terrestrial environments (Meisterfield and others, 2001; Lejzerowicz and others, 2010). Such a widespread distribution and significant diversity in modern systems would suggest that monothalamids play an important role in community structure yet relatively little of their biology, ecology and physiology have been examined (Gooday, 2002). Specimens collected for this study were collected from Sapelo Island and nearby environs of the coast of Georgia, USA, and findings therefore contribute to our understanding of mid-latitude monothalamid diversity.

Monothalamid Taxonomy and Classification

The traditional method to study evolutionary relatedness of foraminiferal taxa has been based on homologous, morphological characters of the test wall structure, geologic history and ontogenetic developmental stages (Cushman, 1927, 1928, 1933, 1940, 1948; Loeblich and Tappan, 1964, 1987; Tappan and Loeblich, 1988). According to the traditional classification of Loeblich and Tappan (1964), based strictly on the gross test morphology, the monothalamid foraminifera are separated into two distinct suborders under the Order Foraminiferida. The organic walled monothalamids formed a single suborder, the agglutinated, single-chambered astrorhizids were classified with the polythalamous (multi-chambered) textulariids and the naked athalamids were excluded from Order Foraminiferida altogether (Loeblich and Tappan, 1964). The Loeblich and Tappan 1987 revision of foraminiferal systematics pulled astrorhizids from the textulariids and in 1992, Foraminifera was elevated to Class rendering former suborders as orders (Loeblich and Tappan, 1992). Based on gross morphology of the test, the foraminiferal evolutionary pathway began with an atestate ancestor (no test as an ancestral character state),

followed by ‘simple’ organic monothalamids which gave rise to all other derived foraminiferal lineages including the agglutinated, single-chambered astrorhizids (Loeblich and Tappan, 1987). This linear evolutionary transformation series of increase in test complexity, naked→organic→agglutinated (Tappan and Loeblich, 1988), has successfully been challenged by phylogenetic studies based on DNA sequence analyses (Pawlowski and others, 2003).

With only a sparse fossil record, advances in molecular biology have proved to be an invaluable tool to unravel evolutionary relationships within and across taxonomic boundaries of monothalamid foraminifera. Phylogenetic studies analyzing sequences of the small subunit of the ribosomal gene (SSU rDNA) support the early evolution of monothalamids in agreement with the traditional views based strictly on gross morphology (Pawlowski and others, 2003). Molecular clocks suggest an estimated divergence of Foraminifera, specifically monothalamids, from their cercozoan ancestor of between 690-1150 mya during the Proterozoic Eon, long before their appearance in the fossil record (Pawlowski and others, 2003). Early reports using SSU rDNA sequences found that a taxonomic separation of the astrorhizids and allogromiids based on test composition was incorrect (Pawlowski and Holzmann, 2002; Pawlowski and others, 2003). In fact, the astrorhizids, allogromiids and the atestate freshwater amoeboid protist, *Reticulomyxa filosa* (Pawlowski and others, 1999a, 1999b) all branch among the monothalamids (Pawlowski and others, 2003). Later, actin protein sequence data also recovered a paraphyletic grouping of ‘allogromiids’ which include organic walled (allogromiids), naked (athalamids) and agglutinated forms with primitive test morphology (astrorhizids) (Flakowski and others, 2005). These findings conflict with a hypothesis of a linear transformation series of test complexity because over monothalamid history, the agglutinated test morphology has evolved multiple times (Pawlowski and others, 2003) so atestate morphology in modern allogromiids is not necessarily a

primitive character state but rather a trait secondarily lost over time (Pawłowski and others, 1999a; 1999b). Molecular researchers have conclusively demonstrated that the degree of test complexity and overall test morphology does not reflect evolutionary history in monothalamids.

Of the monothalamids, SSU rDNA sequence analyses have delineated thirteen genetic clades that united taxa that do not share a common morphological theme (Pawłowski and others, 2002). Suffice it to say, taxon sampling was limited in this early work and at the time of this writing, the original thirteen clades have expanded to sixteen (see [foramBARCODING Molecular Database of Foraminifera http://forambarcoding.unige.ch/](http://forambarcoding.unige.ch/)) undoubtedly the result of increased interest and awareness of this group.

The focus of this research is to examine the fidelity of one of the original thirteen genetic clades of Pawłowski and others (2002), ‘Clade E’. Initially, this group was composed of four members of a ‘sand-ingesting’ genus *Psammophaga*, a feature serving as the morphological synapomorphy (Pawłowski and others, 2002). More recently, membership in this clade has grown into a core group including *Nellya rugosa* (Gooday and others, 2011), *Vellaria* spp. (Gooday and Fernando, 1992; Sabbatini and others, 2004), *Psammophaga sapela* (Altin-Ballero and others, 2013) and *Xiphophaga* spp. (Goldstein and others, 2010). Of the currently accepted Clade E taxa, *Psammophaga* spp. and *Xiphophaga* spp. only exhibit a ‘psammophagous’ behavior (of sand and diatoms respectively) therefore sand ingestion alone can no longer be considered a derived characteristic of the group. Later phylogenetic studies incorporating larger taxon sampling broadened membership in this clade. Several undescribed taxa including the “Rod and Gun White Allo” (subsequently described as *Niveus flexilis*, Altin and others, 2009), “Duplin quartzball”, “Timber dock black and white”, “#5 Cigar”, “Chocolate silver saccamminid”, “*Micrometula*-like” and the ‘Fusiform’ were identified as potential Clade E

members (Habura and others, 2008). Although these taxa may be loosely related based on SSU rDNA phylogenetic methods, overall gross morphology of these taxa does not support their relationship. One objective of this study is to determine if the addition of protein coding genetic markers to the routine, single SSU rDNA based analyses would improve the resolution of relationships among members of Clade E or recommend their exclusion. Evolution does not operate on single genes alone; therefore, it is hypothesized that multiple-gene phylogenetic analyses should improve phylogenetic accuracy and resolution in comparison to SSU based trees.

Monothalamid Gross Morphology and Ultrastructure

The diverse morphological characters and mineralized tests render polythalamous taxa (i.e., rotaliids, textulariids) easy to identify and are excellent candidates for preservation in the fossil record making them highly useful as a biostratigraphic tool. Features such as chamber shape, arrangement or coiling pattern, and ornamentation, are highly useful morphological characters that can be applied to polythalamous taxa but not monothalamous forms which only possess a single chamber. Although monothalamid test morphology can vary slightly with respect to the test composition (agglutination, naked, organic), apertural characteristics (number and ornamentation) and chamber shape (elongate, ovoid), these features are limiting when assessing evolutionary affinities within the group because they are found in members of genetically distinct lineages. As a result, gross morphology is not a useful tool to unite clades of monothalamids united by molecular affinities (Pawlowski and others, 2002). For example, of potential Clade E taxa, the ‘fusiform’ taxon possesses two apertures whereas every other genetically close member has a single aperture. Members of Clade E, as delineated by Habura and others (2008) do not even share overall test shapes—the ‘*Micrometula*-like’ taxon is

extremely long and thin, *Vellaria zucchellii* is elongate, *Niveus flexilis* is ovate and psammophagids are generally pyriform in shape. While most taxa have a prominent agglutinated test (e.g., ‘fusiform’, *Niveus flexilis*, *Xiphophaga minuta*) of minerals such as clay, quartz and various other minerals, some are very insignificant (e.g., *Vellaria zucchellii*) and some lack an agglutinated layer all together (e.g., *Vellaria pellucidus*). Members of Clade C also include individuals of great morphological heterogeneity. For example, *Toxisarcon alba* (Wilding, 2002) which has a large, reticulated cell body with agglutinated test that can be abandoned, forms a lineage with a large, round, reflective silver saccamminid (Gooday and others, 1996) and the organic-walled *Gloiogullmia eurystoma*. Other lineages such as Clade G and Clade F also comprise taxa that lack gross morphological affinities (Pawłowski and others, 2002).

Electron microscopy provides useful information at the sub-cellular level, but unfortunately is not a widely utilized tool in monothalamid studies. Relative to the number of monothalamous foraminifera currently described (see Loeblich and Tappan, 1987), little work incorporating transmission electron microscopy (TEM) has been done to date (Table 1.1). Publications on new species descriptions of monothalmids have gained ground; however, most do not include transmission (TEM) or even scanning electron microscopic (SEM) analyses (Gooday and Fernando, 1992; Gooday and others, 2001; Cedhagen and Pawłowski, 2002; Gooday and Pawłowski, 2004; Sabbatini and others, 2004; Sinniger and others, 2008; Cedhagen and others, 2009; Pawłowski and Majewski, 2011; Apothéloz-Perret-Gentil and others, 2013). When SEM or light microscopic data are reported, it is common to find collapsed specimens (Sabbatini and others, 2004; Sinniger and others, 2008; Gooday and others, 2010; Pawłowski and Majewski, 2011), a function of poor fixation techniques. Further, inconsistencies of type specimen preparations, in addition to inappropriate fixation methods, lead to artifacts that also

render morphological comparisons impossible. The limited availability of ultrastructural data, however, is sometimes justified. Evaluation by electron microscopy requires a large number of living specimens for processing that are laboriously picked from sieved sediments in seawater, and they must be maintained alive until undergoing fixation. Sample fixation, embedding, sectioning and staining are time consuming and require manipulation of extraordinarily small items with tiny, expensive instruments. Access to electron microscopes can be limiting and justifiably exorbitant usage fees can be costly to the researcher. Unfortunately, without the availability of ultrastructural information, little can be done morphologically to corroborate molecular phylogenetic trees.

Those ultrastructural morphological components that have previously shown promising phylogenetic signal include fine features and interrelationships of the monothalamid wall (plasma membrane, and the organic lining and agglutinated layer of the test). Previous reports demonstrated that features of the inner organic lining (IOL) differs among monothalamids of distinct molecular lineages. For example, *Allogromia laticollaris* and *Allogromia* sp. (Clade M) possess a wall with a distinct electron-dense granular layer that overlies an IOL that has a conspicuous herringbone pattern (Hedley and others, 1972). Wall ultrastructural studies of several species of *Myxotheca* (Schwab, 1969; Angell, 1971; Goldstein and Richardson, 2002) have also shown a consistent herringbone pattern in the IOL; however, the molecular clade for this genus has not been established at this time. Representatives of Clade E appear to share an IOL that does not uptake heavy metal stains but contains electron-dense fibers and granules (Altin and others, 2009; Goldstein and others, 2010; Altin-Ballero and others, 2013). Interestingly, *Boderia albicollaris* (Clade G) shares features of the IOL with Clade E along with an electron-dense layer seen in Clade M (Schwab, 1977). If clues to evolutionary history of

monothalamids cannot be deciphered from overall appearance or biological behaviors and processes they may be present at the sub-cellular level. To date, ultrastructural studies on foraminifera primarily focused on higher order taxa, namely those that possess calcareous tests (for review, see Hansen, 1999), or examined reproduction (for review, see Goldstein, 1999; Angell, 1971; Goldstein, 1988, 1997; Goldstein and Barker, 1990) or methods of test construction (Bowser and others, 1995, 2002; Goldstein and Richardson, 2002). Results of this study will make a significant contribution to our understanding of ultrastructural features of selected monothalamous foraminifera.

Electron microscopy has proved to be a useful tool aiding in our understanding of monothalamid biological activities which may have phylogenetic significance. The ovoid tests of the taxonomically distinct agglutinated *Cribrothalammina alba* (Clade L) (Goldstein and Richardson, 2002), *Xiphophaga* spp. (Goldstein and others, 2010), *Psammophaga sapela* (Altin-Ballero and others, 2013), *Niveus flexilis* (Altin and others, 2009) and the organic walled *Myxotheca* spp. (Schwab, 1969; Angell, 1971; Goldstein and Richardson, 2002) all possess small vesicles within the cytoplasm arranged near the plasma membrane in contact with the IOL. It appears that new test material is transported to the periphery of the cell in various locations by vesicles to accommodate growth by increasing diameter (widening the single chamber) (Goldstein and Barker, 1988; Goldstein and Richardson, 2002). Conversely, the elongate *Hyperammia* sp. lacks vesicles but contains microtubules running parallel with the plasma membrane allowing the cell to add material at the end containing the aperture (Goldstein and Richardson, 2002). In another example, Clade E was initially united by the biological activity called ‘psammophagy’ or sand ingestion (Pawlowski and others, 2002). Most of the newly

introduced molecular taxa aligning with this group do not ingest sediments, and this feature therefore cannot be considered a synapomorphy for the entire group. The biological activity

Table 1.1 Summary of current publications on monothalamid ultrastructure using transmission electron microscopy (TEM).

SPECIES	CITATION	MOLECULAR CLADE
<i>Allogromia laticollaris</i>	Schwab, 1974, 1976 McEnery and Lee, 1976	M
<i>Allogromia</i> sp.	Hedley and others, 1972	
<i>Astrammia rara</i>	DeLaca, 1986 Bowser and others, 1995	I
<i>Astrammia triangularis</i>	Bowser and others, 2002	I
<i>Boderia albicollaris</i>	Schwab, 1977	G
<i>Cribrothalammina alba</i>	Goldstein and Barker, 1988, 1990 Goldstein, 1997 Goldstein and Richardson, 2002	L
<i>Haliphysema</i> sp.	Hedley and others, 1967	Unknown
<i>Hyperammia</i> sp.	Goldstein and Richardson, 2002	Unknown
<i>Iridia lucida</i>	Cesana, 1972	Unknown
<i>Iridia diaphana</i>	Hedley and others, 1972	Unknown
<i>Myxotheca arenilega</i>	Schwab, 1969	Unknown
<i>Myxotheca</i> sp.	Schwab, 1969 Angell, 1971 Goldstein and Richardson, 2002	Unknown
<i>Nemogullmia longevariabilis</i>	Nyholm and Nyholm, 1975	G
<i>Niveus flexilis</i>	Altin and others, 2009	E
<i>Notodendrodes antarctikos</i>	Bowser and others, 1995	F
<i>Notodendrodes hyalinosphaira</i>	DeLaca and others, 2002	F
<i>Psammophaga crystallifera</i>	Dahlgren, 1962a	E
<i>Psammophaga sapela</i>	Altin-Ballero and others, 2013	E
<i>Shepherdella taeniformis</i>	Hedley and others, 1967 Hedley and others, 1972	Unknown
<i>Xiphophaga minuta</i>	Goldstein and others, 2010	E
<i>Xiphophaga allominuta</i>	Goldstein and others, 2010	E

currently tying members of Clade L together is the development of secondary pore formation in the test prior to gametogenesis. These pores serve as passageways for gametes to exit the parental test in *Ovamina opaca* (Dahlgren, 1962b) and *Cribrothalammina alba* (Goldstein and Barker, 1988, 1990). More recent molecular studies recognize additional Clade L members such as the ‘black and white saccamminid’, ‘rusty saccamminid’ and undetermined saccamminids A279 and 2399 (Habura and others, 2008); however, reproduction of these taxa has not been observed. To circumvent shortcomings on research examining monothalamid reproduction (Goldstein, 1999) data on reproduction were gathered whenever possible. Research employing electron microscopic techniques will increase the understanding of a suite of biological processes that also operate under the influence of evolutionary pressures and can provide insight into allogromiid phylogenies.

Morphology versus Molecules: The Total Evidence Approach

The ultimate goal of a phylogenetic analysis is to establish a well-supported and accurate hypothesis of the evolutionary history of a selected group of organisms at a specified taxonomic level. The means by which to accomplish this goal, using morphological or molecular data sets, is highly debated. Whereas both data sets have advantages and disadvantages in phylogenetics, neither method can be considered more informative or accurate than the other in all circumstances (Hillis and Wiens, 2000). Although collection of molecular data requires living specimens (or in some cases very well preserved fossil material or specimens stored at -80°C) and methods obtaining sequences can be costly, any given gene can provide a very large number of observable characters for comparison in a short period of time (Hillis, 1987). Collecting an equivalent volume of morphological characters and assessing multiple character states can be extraordinarily time consuming and tedious. With an exception of gene selection or alignment

creation, genes can be selected and defined in an objective manner because characters and states are straightforward (Hillis and Wiens, 2000). One problem with molecular data sets can be discordance between trees based on a single genes and species trees based on morphology. If a gene evolves differently from the species (due to phenomena such as lateral gene transfer, paralogy, etc.), when analyzed independently, molecular analyses can return a well-supported but phylogenetically inaccurate tree (Doyle, 1992). Morphology proponents support the idea that a single, observable character is actually a phenotypic expression of multiple genes operating under the influence of evolutionary pressures over time. Evolution operates on many, not single genes therefore the evaluation of a single morphological character is more comprehensive than one based on a single gene alone.

Observable similarities in character states or a morphological feature may not be due to an inherited genetic variation but instead are functions of homoplasy (convergence, parallelism). For example, of the few studies on foraminiferal reproduction, several species show test dimorphism correlating with asexual or sexual phases—but not all taxa that experience an alternation of generations show the same pattern of test dimorphism (Goldstein, 1999). Variations in morphology may also be a function of differences in environmental conditions (Holzmann, 2000; Holzmann and Pawlowski, 1997, 2000). Ecophenotypic variations of test pore size have been reported to occur in *Ammonia* sp. simply living in different oxygen concentrations (Holzmann, 2000). Cryptic speciation, taxa morphologically similar but genetically distinct are common in planktonic foraminifera (i.e., cryptic speciation, Huber and others, 1997; Darling and others, 1997, 1999; deVargas and others, 1999) and was also documented for the benthic, monothalamid *Xiphophaga* sp. (Goldstein and others, 2010).

Variations due to reasons other than inheritance can cause inaccuracies in evolutionary trees based strictly on morphology.

Because both morphological and molecular phylogenetic approaches, have their unique strengths and advantages, evolutionary hypotheses based on both should be significantly more robust than if used alone (Bauldauf and others, 2000; Bauldauf, 2003). Where molecular and morphological trees are incongruent, trees created with both data sets combined show improved phylogenetic accuracy (Hillis and Wiens, 2000).

This current study employs the *Total Evidence Approach* (Carnap, 1950; Kluge, 1989) to resolve evolutionary relationships among those taxa that reportedly belong to Clade E monothalamids (Pawlowski and others, 2002; Habura and others, 2008). Here, evolutionary hypotheses are based on multiple lines of data analyzed simultaneously. In this case, a phylogenetic tree based on SSU rDNA alone is compared with a tree created by concatenating two additional protein coding genes. Results of this work have effectively doubled the existing number of protein-coding actin and β -tubulin sequences available in GenBank (National Institute of Health) at the time of publication of this dissertation (Table 1.2).

Table 1.2 Summary of protein coding gene sequences available for Foraminifera. The numbers refer to published sequences of actin, β -tubulin and RNA polymerase II for different species of Foraminifera available in GenBank (<http://www.ncbi.nlm.nih.gov/genbank/>). Protein sequences obtained in this research include actin and β -tubulin sequences for ‘fruitcake’, ‘fusiform’, ‘chocolate silver saccamminid’, *Niveus flexilis* and *Psammophaga sapela*. Only actin type I was recovered for ‘#5 cigar’.

Gene	Number of Sequences for Foraminifera Total	Number of Sequences for Monothalamids	Additional Monothalamid Sequences Contributed by this Work
Actin Types I and II	25	6	6
β -Tubulin	20	4	5
RNA Polymerase II	16	3	0

Ultrastructural features of the test wall and cytoplasm gathered by transmission electron microscopic analysis coupled with gross morphological features are evaluated and compared with the molecular trees. Current SSU rDNA trees delineate a set of core Clade E taxa but membership of several newfound species based on a single gene is questionable. It is hypothesized that concatenation of multiple genes in a molecular analysis will resolve clade membership and that ultrastructural findings will be congruent with the multi-gene tree.

Research conducted in preparation for this dissertation has met several objectives. First, this work aims to decrease geographic sampling bias and contribute to the diversity assessment of the under-represented monothalamid foraminifera in mid-latitude shallow-water environments. In addition, results obtained here will make significant contributions to the limited number of publications on monothalamid ultrastructure, reproduction and protein-gene sequences currently available. Finally, if evolution operates on many genes simultaneously, and these genes are expressed phenotypically in morphological variations, it is necessary to collect many forms of data to produce robust phylogenetic hypotheses. A combination of morphological and molecular data sets is necessary when evaluating monothalamid evolutionary history.

CHAPTER 2

A NEW ALLOGROMIID FORAMINIFERA NIVEUS FLEXILIS, NOV. GEN., NOV. SP., FROM COASTAL GEORGIA USA: FINE STRUCTURE AND GAMETOGENESIS¹

¹ Altin, D.Z., Habura, A. and Goldstein, S.T., 2009. *Journal of Foraminiferal Research*, v. 39, no. 2, pp. 73-86. Reprinted here with permission from the publisher.

Abstract

Allogromiids (*sensu lato*) occupy diverse habitats, including marine, brackish, freshwater, and terrestrial environments, serve a suite of trophic functions within their communities, and are modern descendents of the earliest diverging foraminiferal lineages. Allogromiids appear to be morphologically simplistic, but they have diverse, intricate shell architectures at the fine structural level. They are not well known from the fossil record and are sometimes difficult to recognize in modern systems. Recent molecular work on small subunit ribosomal DNA (SSU rDNA) sequences by others has delineated 13 genetic clades, most of which unite taxa that do not share a common general morphology. Here, we present ultrastructural and molecular results on an undescribed allogromiid, *Niveus flexilis* nov. gen., nov. sp., collected from low-salinity marshes along coastal Georgia, USA. Partial SSU phylogenetic analyses indicate that this taxon is a member of Clade E Allogromiid Foraminifera.

This taxon is small (<300 μm), generally ovate in shape, and has a single aperture. The flexible test is composed of a thin (<0.5 μm), outer agglutinated layer of fine clay particles predominantly arranged parallel to the shell surface. The outer surface of the test is crenulated and irregular. The agglutinated layer is underlain by a thick (3–8 μm), inner organic lining (IOL), which is in direct contact with the cell membrane. The IOL contains numerous small electron-dense particles along with long, fine fibers generally arranged parallel to the outer surface of the shell. Small vesicles lie just beneath the plasma membrane and appear to release test construction materials at the base of the IOL. The nuclear membrane is surrounded by a thick layer (1.5 μm) of endoplasmic reticulum overlain by a layer of vesicles of unknown function. Gamonts release many small biflagellated gametes through the aperture directly into surrounding seawater. Fine cytological examination of the test suggests that this new allogromiid shares a similar

constructional theme with other Clade E allogromiids examined to date, particularly *Psammophaga* spp. Ultrastructural data for additional Clade E taxa are necessary to identify fine morphological characters that may be synapomorphies for this group.

Introduction

The diversity of morphological characters of the test seen in higher-order groups of Foraminifera (textulariids, globigerinids, rotaliids) is limited in the monothalamous forms. Morphological features commonly used for taxonomic classification, such as chamber arrangement and umbilical ornamentation (Loeblich and Tappan, 1987; Sen Gupta, 1999), are not present in single-chambered allogromiids. Although allogromiid test morphology can vary with respect to the test composition (agglutinated, organic, naked), apertural characteristics (number and arrangement), and test shape (elongate, ovoid), these features are limiting when attempting to assess evolutionary affinities. Allogromiid tests, for example, are often flexible, and shape can vary with activity. Furthermore, molecular studies on monothalamous Foraminifera have shown that traditional taxonomic classification based on gross test morphology is inconsistent with evolutionary phylogenies based on SSU rDNA (Pawlowski and others, 2003), actin (Flakowski and others, 2005), and RNA polymerase II (Longet and Pawlowski, 2007) sequences. Allogromiids and astrorhizids, although traditionally classified separately (Loeblich and Tappan, 1987; Sen Gupta, 1999), are paraphyletic based on molecular sequence comparisons (Pawlowski and others, 2003). Current homology assessment based on gross morphological features of the test does not reveal distinctive characters that reflect evolutionary relatedness consistent with molecular phylogenies (Pawlowski and others, 2002). One goal of this research therefore is to examine the fine structure of test construction in selected Clade E allogromiids, a clade that includes the distinctive *Psammophaga* sp. among others

(Pawlowski and others, 2002; Habura and others, 2008). Do the members of this molecular clade share morphological synapomorphies with regard to test construction?

Recent studies reporting allogromiid fine structure are sparse relative to overall allogromiid diversity (e.g., Bowser and others, 1995, 2002; Goldstein and Richardson, 2002; Bernhard and others, 2006; Goldstein and others, 2006a). Nonetheless, previous reports suggest that closely related allogromiids may share similar ultrastructural characteristics of the test wall, whereas others do not. For example, it appears that at least some prominent Clade E allogromiids share an outer agglutinated layer of predominantly clay platelets underlain by a distinct, finely fibrous inner organic lining (IOL) in direct contact with the plasma membrane (Goldstein and others, 2006a). In order to identify ultrastructural characters with phylogenetic significance, to further examine the fidelity of molecular-based phylogenies, and to provide a foundation for biochemical research, more allogromiid taxa must be examined via electron microscopy. Here, we report fine structural data on test, cell body, and gametogenesis, and we provide a formal taxonomic designation for a new Clade E allogromiid *Niveus flexilis*, which is native to hyposaline marshes of coastal Georgia, USA. This new taxon was reported as the “Rod and Gun White Allogromiid” by Habura and others (2008), who assigned it to Clade E based on its SSU rDNA sequence. This current report is part of a broader study that will test the phylogenetic cohesiveness of Clade E allogromiids by coupling fine structural synapomorphies with multiple genetic markers.

Materials and Methods

Sample Collection and Culturing

Foraminifera used in this study were collected from surface mud at a low-salinity marsh (measured from 10–22 psu) site at the Rod and Gun Marina near Darien, Georgia (31°24'22"N,

81°23'36"W), USA (Fig. 2.1). Surface sediments were collected and sieved over a 20 mesh, stainless-steel sieve (850- μm openings) with filtered seawater of ambient salinity to remove metazoans and detritus. Sediment and associated material finer than 850 μm were placed in a series of transparent plastic tubs, transported to the University of Georgia, and maintained in a low-temperature incubator at 12°C under 12-hour illumination cycles. The new allogromiid, along with several other allogromiids, bloomed in these containers, and populations were maintained in the laboratory for over a year by regularly changing the Instant Ocean (Spectrum Brands, Inc.). Individuals were extracted from these containers for study (fine structure, reproduction) by sieving (63- μm openings, stainless steel) and picking with a fine artist's brush (10-0 or 20-0) and a glass pipette. For light microscopic observations, selected individuals were

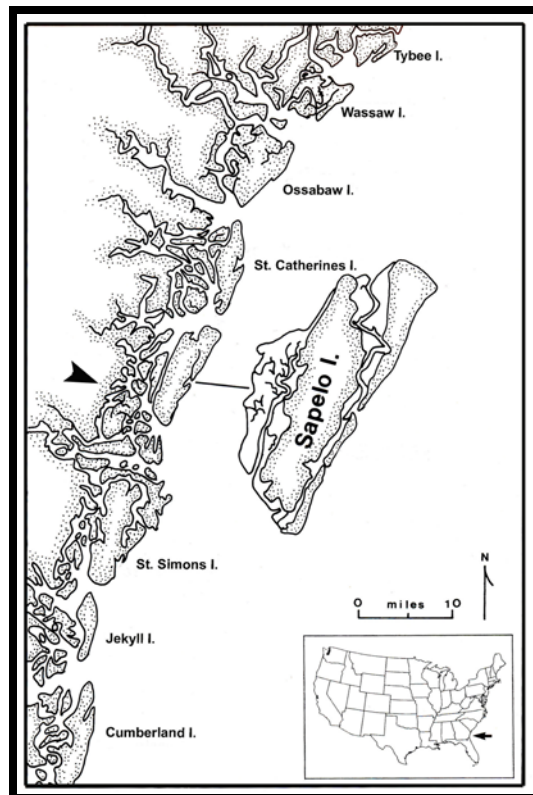


Figure 2.1 Approximate geographic location of the sampling site for *Niveus flexilis*. The salt marshes adjacent to the Rod and Gun Marina near Darien, Georgia (31°24'22"N, 81°23'36"W), USA is the type locality for this species.

placed in plastic culture dishes with Instant Ocean and appropriate live food organisms (*Dunaliella*, *Amphiphora*, *Isochrysis*) and photographed with a Coolpix 990 using transmitted light. Observations were made on both reproductive and non-reproductive individuals, and selected foraminifers were prepared for electron microscopy.

Microscopy

Vegetative foraminifers were prepared for transmission electron microscopy (TEM) using either high-pressure freezing and freeze substitution (HPF/FS) or chemical fixation methods. HPF/FS methods follow those previously reported (Goldstein and Richardson, 2002). Up to 10 living, vegetative individuals were rapidly frozen under high pressure (~15 ms at ~2,100 bars) using a Balzers HPM 010 High Pressure Freezing Machine and immediately placed in liquid nitrogen. Specimens were transferred to a substitution fluid (2% osmium tetroxide, 0.05% uranyl acetate, HPLC-grade anhydrous acetone), stored for 4 days at -80°C , and slowly brought to room temperature (4 hr at 40°C , 4 hr at 20°C , 2 hr at 4°C , 45 min at room temperature). Substitution fluid was removed, and the samples were rinsed in three 15-min changes of HPLC-grade acetone followed by infiltration with Araldite Embed 812 (Epon 812) resin. Specimens were placed in Permamox Petri dishes with a fresh change of resin and polymerized for 48 hr at 60°C .

Reproductive individuals showing specific morphological changes (Goldstein, 1997) were prepared for TEM using chemical fixation protocols slightly modified from previous reports (Goldstein and Barker, 1990; Goldstein and Moodley, 1993). Specimens underwent a primary fixation (2% glutaraldehyde, 0.1 M cacodylate, 0.1 M sucrose, 0.06% ruthenium red) for 1 hr on ice, a 0.1 M cacodylate buffer rinse, and post-fixation preparation with 1% OsO_4 , 0.1 M cacodylate, and 0.1 M sucrose for 1 hr at room temperature, and two 15-min distilled-water

washes followed by a graded ethanol dehydration series (15 %, 30%, 50%, 70%, 80%, 90%, three changes of 100% taking 15 min each) and a propylene oxide rinse (two parts propylene oxide to one part 100% ethanol and 100% propylene oxide, 15 min each). Specimens were infiltrated with an Araldite Embed 812 (Epon 812) resin and a propylene oxide mixture series for a minimum of 1 hr with resin concentrations of 20%, 40%, 60%, 80%, 100%, and a final 100% resin change overnight. Specimens used for TEM were placed in Permamox Petri dishes and were embedded in a fresh resin change cured at 65°C for 48 hr. All TEM preparations were examined under a light microscope, and well-fixed cells were removed with a jeweler's saw and mounted on blocks with glue (Quickbond) overnight. Specimens were trimmed and sectioned (80–90 nm thickness) using a Reichert-Jung Ultracut E microtome. Thin sections were placed on Formvar-coated slot grids, dried overnight, post-stained for three minutes each with uranyl acetate and lead citrate, and viewed on a Zeiss EM 902A operated at 80 kV. Type specimens were prepared using the same methods as TEM preparations, omitting the post-fixation step (osmium tetroxide), after which they were mounted on glass slides.

Living individuals prepared for SEM followed the chemical TEM fixation methods but without ruthenium red. As an alternative to critical-point drying for dehydration, specimens were chemically dried with hexamethyldisilazane (HMDS) following a graded ethanol series (15 min of 1 part HMDS, 2 parts ETOH, 2 parts HMDS, 1 part ETOH, 100% HMDS). Due to the fragile nature of the allogromiid test, HMDS treatment was employed because it reportedly does not introduce artifacts or distort delicate cells (e.g., Botes and others, 2002; Araujo and others, 2003). The individuals were removed from the 100% HMDS using a plastic pipette and placed onto a clean aluminum stub to evaporate the remaining HMDS. Dried individuals were transferred to a separate, carbon-coated aluminum stub by gentle tapping of the stub, allowing

the specimens to fall to the adhesive carbon tab. Specimens were sputter coated with gold (15.3 nm) and viewed on a JEOL JSM-5800 operated at 15 kv.

Results: Test Morphology and Fine Structure

Individuals examined in this study were selected from sieved fine-grained sediments collected along hyposaline *Juncus* marshes adjacent to the Rod and Gun Marina near Darien, Georgia, USA. This particular species bloomed in sieved muds maintained at 12°C with 12-hr illumination cycles for over a year following the original collection date. The overall white color and ovate test shape (Figs. 2.2.1–2.2.2) render them easily distinguishable, and they may turn green while feeding on live *Dunaliella*. In addition, *Niveus flexilis* appears to reproduce readily in culture dishes while being fed live food sources (Fig. 2.2.3). The agglutinated layer is crenulated and composed primarily of clay particles and occasional diatom frustules (Figs. 2.2.4–2.2.6).

In cross-sectional view, the wall is composed of a thin (<0.5 µm), outermost agglutinated layer composed primarily of clay (Figs. 2.3.1–2.3.2) and occasionally interrupted by fragments of diatom frustules. The IOL is characterized by numerous electron-dense granules and fibrils, most of which are oriented parallel to the plasma membrane (Fig. 2.3.2). The IOL lies directly beneath the outermost clay layer, and it is significantly thicker (3–8 µm) than the thin veneer of clay platelets. The clay platelets are cemented together by an organic bioadhesive (Fig. 2.3.4) of unknown biochemical composition. The fibrils are more apparent in the HPF/FS preparations (Figs. 2.3.1-2.3.2, 2.3.5-2.3.6) than in those that were chemically fixed (Figs. 2.3.3, 2.3.4). Thin sections through the IOL cut tangentially to the test surface and cytoplasm show that the fibrils are interconnected with numerous electron-dense granules, imparting a “spider web” appearance (Figs. 2.3.5, 2.3.6). The plasma membrane of the cell body is in direct contact with the

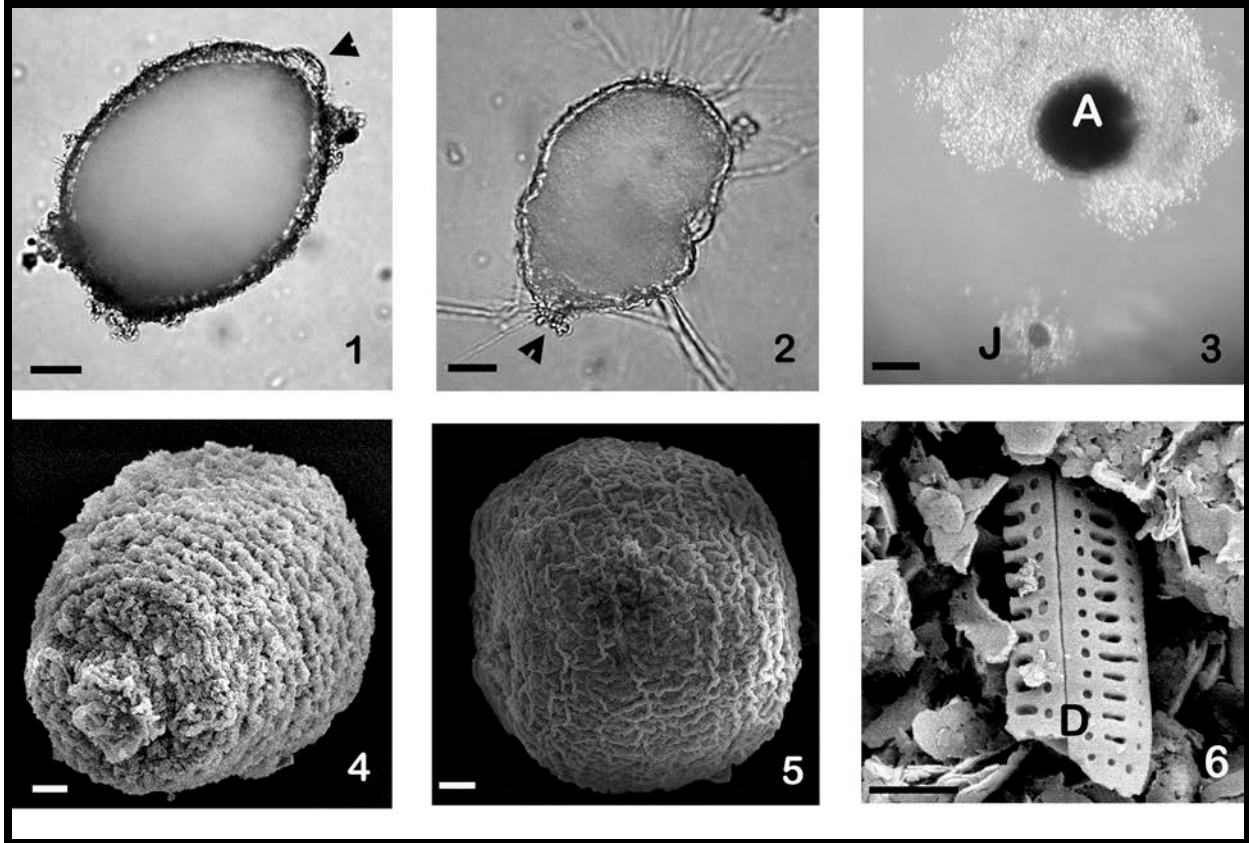


Figure 2.2 Gross morphology of *Niveus flexilis*. **1, 2** Living *Niveus flexilis* n. gen. n. sp., illustrating their ovate shape, white cytoplasm, and single aperture (arrow). Flexible test of *N. flexilis* (note invaginations) and extended granuloreticulopodia (scale bars = 50 μm). **3** Asexually produced juvenile (J) grown in culture compared to an adult (A) (scale bar = 100 μm). Both cells are surrounded by tufts of live *Dunaliella* sp. (food). **4, 5** Scanning electron micrographs of two individuals; **4** apertural view (scale bar = 10 μm), **5** lateral view (scale bar = 20 μm). Both show a distinctive cretulated surface texture. **6** Outer test composed primarily of fine clay particles interrupted by occasional fragments of diatom (D) frustules (scale bar = 1 μm).

IOL and is lined with numerous cytoplasmic vesicles that presumably contain test construction materials. The presence of intact vesicles within the IOL suggests (Fig. 2.3.3) that these migrate directly into the IOL where the contents are released. Vacuoles, however, have been observed merging with the plasma membrane opening directly into the IOL (Fig. 2.3.1), suggesting that they may release contents directly by fusing with the membrane. One chemically fixed specimen appears to have an encysted euglenozoan embedded in the IOL (Fig. 2.4.1), and the cyst resembles *Diplonema* sp. based on the presence of plicate veins that would surround a feeding apparatus (see Triemer and Ott, 1990; M. A. Farmer, oral communication, 2008). In a cross-

sectional view through the aperture, the IOL remains thick and fibrous (Fig. 2.4.2). The crenulated nature and flexibility of the wall are noted by the invagination of the entire wall (Fig. 2.3.1).

Results: Cell Body of Non-Reproductive, Vegetative Individuals

The cytoplasm contains redundant vesicles of varying electron density that range from $<1\ \mu\text{m}$ to $5\ \mu\text{m}$ in size. The variations in electron density are a function of differential uptake of heavy metal stains, suggesting different biochemical composition and thus function. The heavily vesiculated cytoplasm is interrupted by several larger, electron opaque vacuoles ($10\text{--}15\ \mu\text{m}$ in diameter), which are commonly surrounded by a single layer of smaller vesicles ($\sim 0.25\text{--}0.5\ \mu\text{m}$ in diameter) around the periphery (Fig. 2.3.1). Vesicles are conspicuously aligned directly beneath the plasma membrane (Figs. 2.3.1–2.3.3) in a manner similar to other allogromiid taxa (Goldstein and Richardson, 2002). Mitochondria with tubular cristae are numerous and evenly distributed throughout the main cell body. Individuals examined in the vegetative stage contain a single, spherical nucleus approximately $\sim 8\text{--}10\ \mu\text{m}$ in diameter (Fig. 2.4.3). The nuclear membrane is surrounded by a thick layer ($1.5\ \mu\text{m}$) of endoplasmic reticulum overlain by a layer of vesicles of varying electron density and of presumably different but unknown functions (Figs. 2.4.3–2.4.4). Similar nuclear features have been reported in other allogromiid taxa (Goldstein, 1997; Goldstein and Richardson, 2002) that are genetically distinct and do not appear related to Clade E taxa (Pawlowski and others, 2002; Goldstein and others, 2006a). The pores of the nuclear membrane are visible in cross section (Fig. 2.4.4). Uninucleate individuals are presumably haploid gamonts or possibly representatives of the schizont stage, if present. Nuclear chromatin does not accumulate directly beneath the nuclear membrane but appears evenly dispersed throughout the interior nucleoplasm (Fig. 2.4.3).

Results: Reproduction by Gametogenesis and Asexual Reproduction

Marked changes occur at the gross morphological level in individuals undergoing gametogenesis, and these are broadly similar to those described in other foraminiferans (Goldstein and Moodley, 1993; Goldstein, 1997). Any foraminiferans in which the cytoplasm deviated from opaque and white (the typical vegetative appearance) or green (from feeding on *Dunaliella*) were regarded as potentially reproductive and observed closely. Cytoplasmic changes associated with gametogenesis include the occurrence of (1) translucent patches interspersed within the white cytoplasm; (2) individuals that were translucent to tan in color with distinct, dark, spherical vacuoles; and (3) cytoplasm that appeared dense and concentrated into one portion of the test. Several individuals were observed undergoing gametogenesis followed by gamete release, and one individual appeared to complete this process within 2 hr. Initially, the cell was identified as potentially reproductive due to the presence of translucent patches throughout the otherwise opaque cell body. Changes in cytoplasmic coloration may represent expulsion of digestive and waste materials in preparation for cytoplasmic differentiation (Jepps, 1942; Arnold, 1955; Goldstein, 1988). Cytoplasmic streaming diffused the translucent patches, and within 1 hr, dark vacuoles appeared, and the cytoplasm became more translucent.

Vacuoles became more numerous and formed a ring around the periphery of the cell within 0.5 hr after their first appearance. Initially, the vacuoles migrate throughout the cytoplasm via streaming, but movement ceases at some point prior to gamete release. One hour following the first appearance of the dark vacuoles, the cytoplasm begins to glisten and sparkle. This marks the onset of the “buzzing” stage, whereby complete gametic differentiation has occurred and gametes are actively swarming throughout the parental test (Goldstein and Moodley, 1993; Goldstein, 1997). Gametes are released directly into surrounding seawater through the single

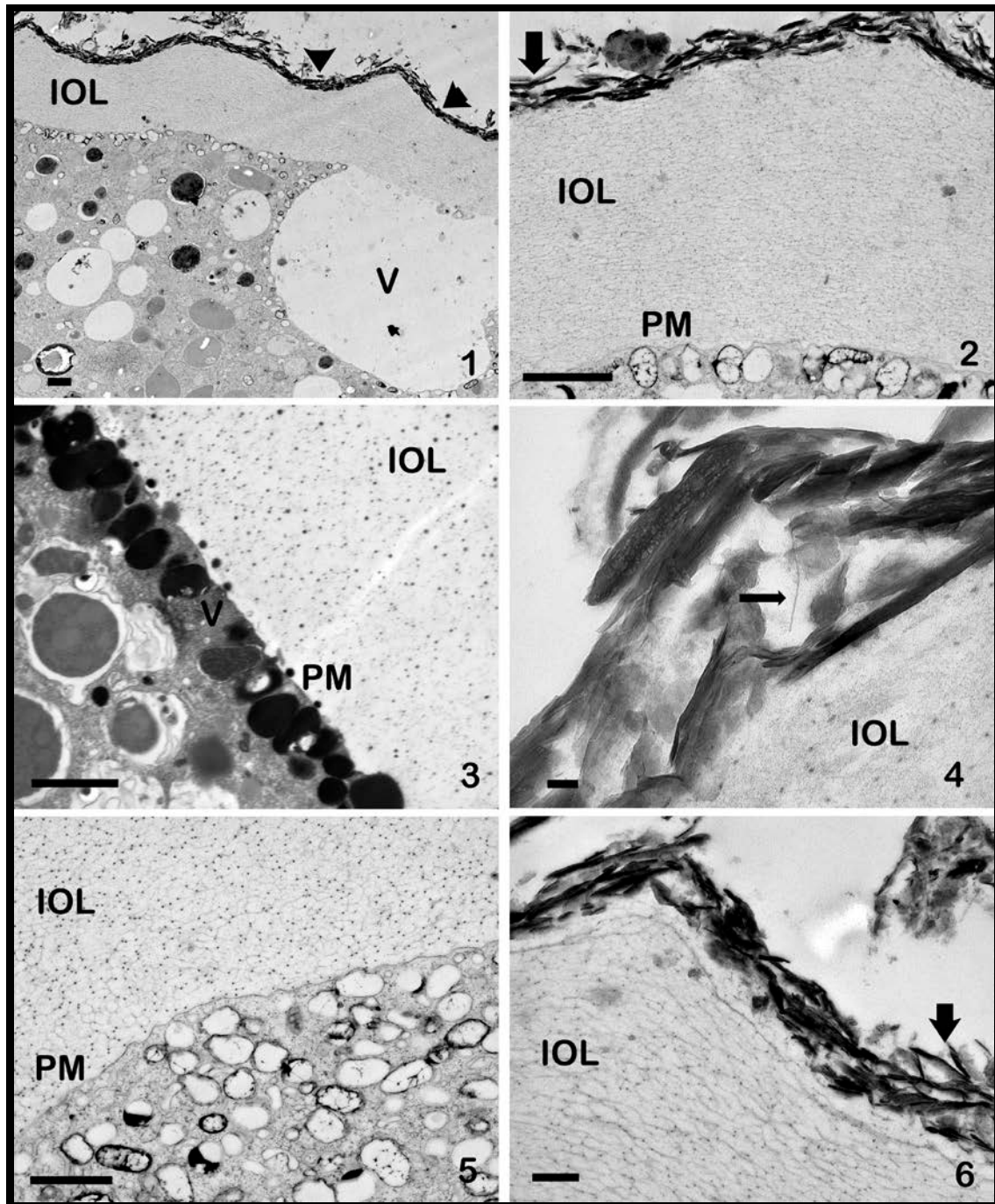


Figure 2.3 Wall ultrastructure for *Niveus flexilis*. Transmission electron micrographs (TEM) showing cross-sectional views of the thin veneer of clay platelets underlain by a thick inner organic lining (IOL) and cytoplasm bound by a plasma membrane (PM). **1, 2** IOL is marked by numerous electron-dense granules and fibrils, most of which are oriented parallel to the plasma membrane (PM) (HPFS, scale bars = 1 μ m). Cytoplasm contains numerous large vacuoles (V) surrounded by a layer of smaller vesicles similar to those lining the plasma membrane (PM). Note crenulated agglutinated surface. **3** Electron-dense granules are evident in chemical fixation preparations (scale bar = 1 μ m). PM is in direct contact with the IOL, lined with numerous vesicles (V) presumably containing test construction materials. **4** Strand of bioadhesive connecting clay platelets (scale bar = 0.1 μ m). **5, 6** Tangential sections illustrating the “spiderweb”-like pattern of dense IOL fibrils and the abundance of vesicles just beneath the plasma membrane (PM) (HPFS scale bars = 1 μ m). Clay minerals (arrow) align parallel to the cell surface.

aperture between 10 and 20 min after the buzzing stage (Fig. 2.4.6). Following gamete release, the parental test may contain residual cytoplasm and vacuoles (Fig. 2.4.7). The parental test during the buzzing stage is significantly weaker compared to the vegetative state or the previous vacuolar stage, and buzzing cells were easily crushed with a fine brush. In fact, intact tests of dead individuals of this taxon are never found in sediment samples despite the large number of living individuals observed.

Asexual reproduction was observed in a single individual that had been maintained in a small-volume culture (with food organisms) for approximately three weeks. Juveniles were identical to the adults, except they were smaller and lacked an outer agglutinated test layer (Fig. 2.2.3). Juveniles commonly embedded themselves in algal mats or constructed feeding cysts composed of *Dunaliella* sp. These individuals were grown in culture in the absence of clay or other test construction materials, indicating that an agglutinated layer is not a requirement for survival, at least in culture. Ultrastructural observations on an asexually produced juvenile revealed that it was undergoing the earliest stages of gametogenesis (Fig. 2.5.1). This earliest stage of gametogenesis (nuclear divisions and flagellar development) therefore was not signaled by any gross morphological cytoplasmic changes. At this point, nuclear divisions had occurred and developing flagella were located in expanding vacuoles. The plasma membrane, however, distinctly separated the IOL from the cytoplasm and remained lined with vesicles. In addition, the presence of numerous vesicles throughout the cell body indicated that cytoplasmic differentiation was not yet complete.

Cytoplasmic changes corresponding to the so-called vacuolar and buzzing stages are corroborated by ultrastructural data. Gametic differentiation, an expansion of the vacuolar system, and flagellar development were identified during the vacuolar stage (Fig. 2.5.2). The

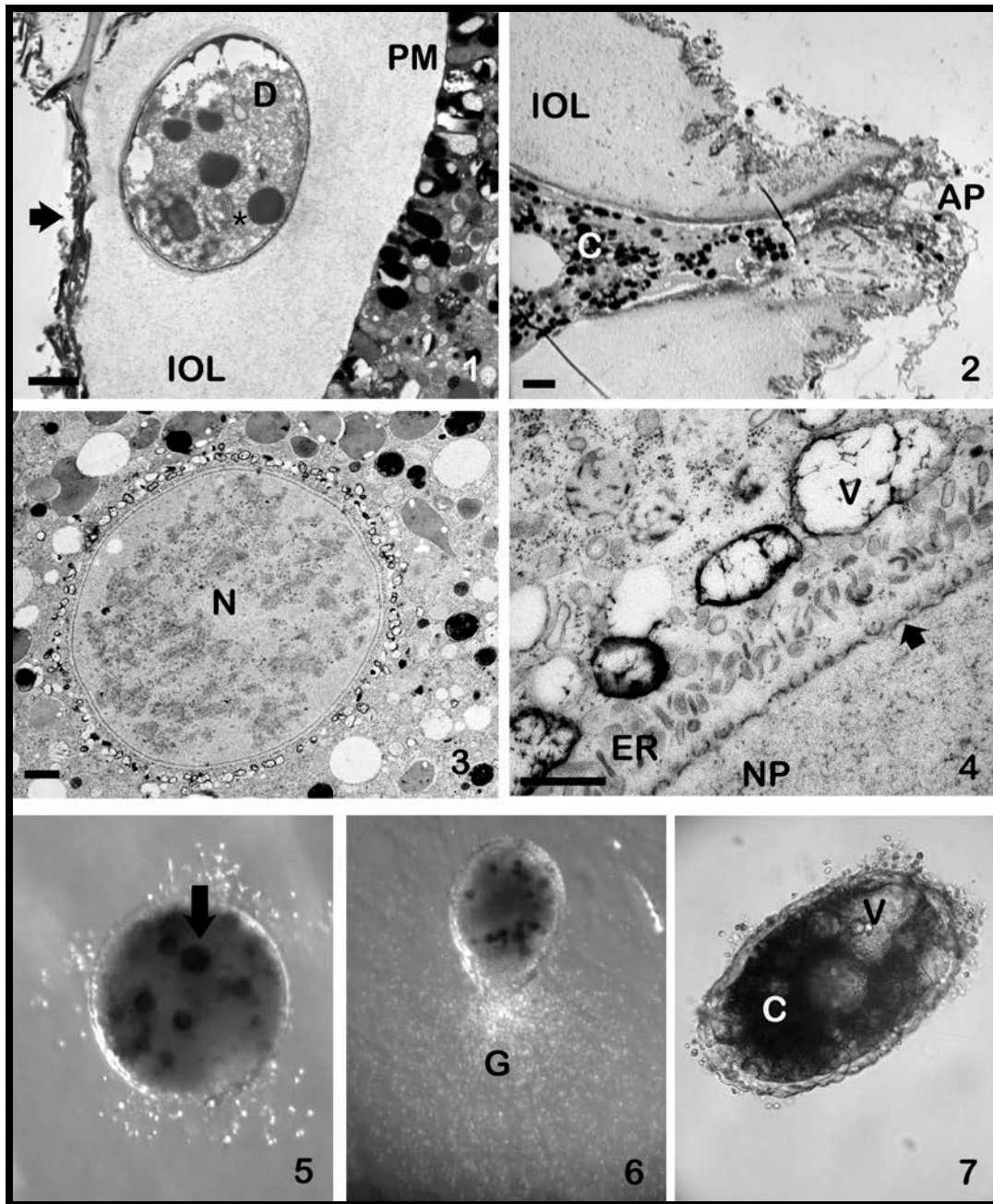


Figure 2.4 Nuclear ultrastructure and gross reproductive morphology of *Niveus flexilis*. 1 Transmission electron micrograph (TEM) (chemical preparation) cross sections of wall with possible encysted *Diplonema* sp. (?) (D) embedded in the inner organic lining (IOL). Note, dark, fibrous structure (left of asterisk) resembles plicate vanes that would surround a feeding apparatus. 2 Apertural (AP) region shows a thickened IOL and numerous electron-dense vesicles in the cytoplasm (C). 3 Survey view of nucleus (N) in a uninucleate gamont (HPFS) with diffuse, evenly spaced chromatin and distinct ring of small vesicles surrounding the nuclear membrane. 4 Higher magnification view (HPFS) of the nuclear membrane separated from the vesicular layer (V) by a thick layer of endoplasmic reticulum (ER) (scale bars = 1 μ m). 5–7 Light micrographs just prior to, during, and after gamete release following gametogenesis (scale bar measurements not taken). During gametogenesis, cytoplasm changes from opaque white to translucent beige with obvious vacuoles (arrow). Thousands of biflagellated gametes (G) are released through the aperture directly into surrounding seawater. Residual cytoplasm (C) and vacuoles (V) remain in the test after gamete release.

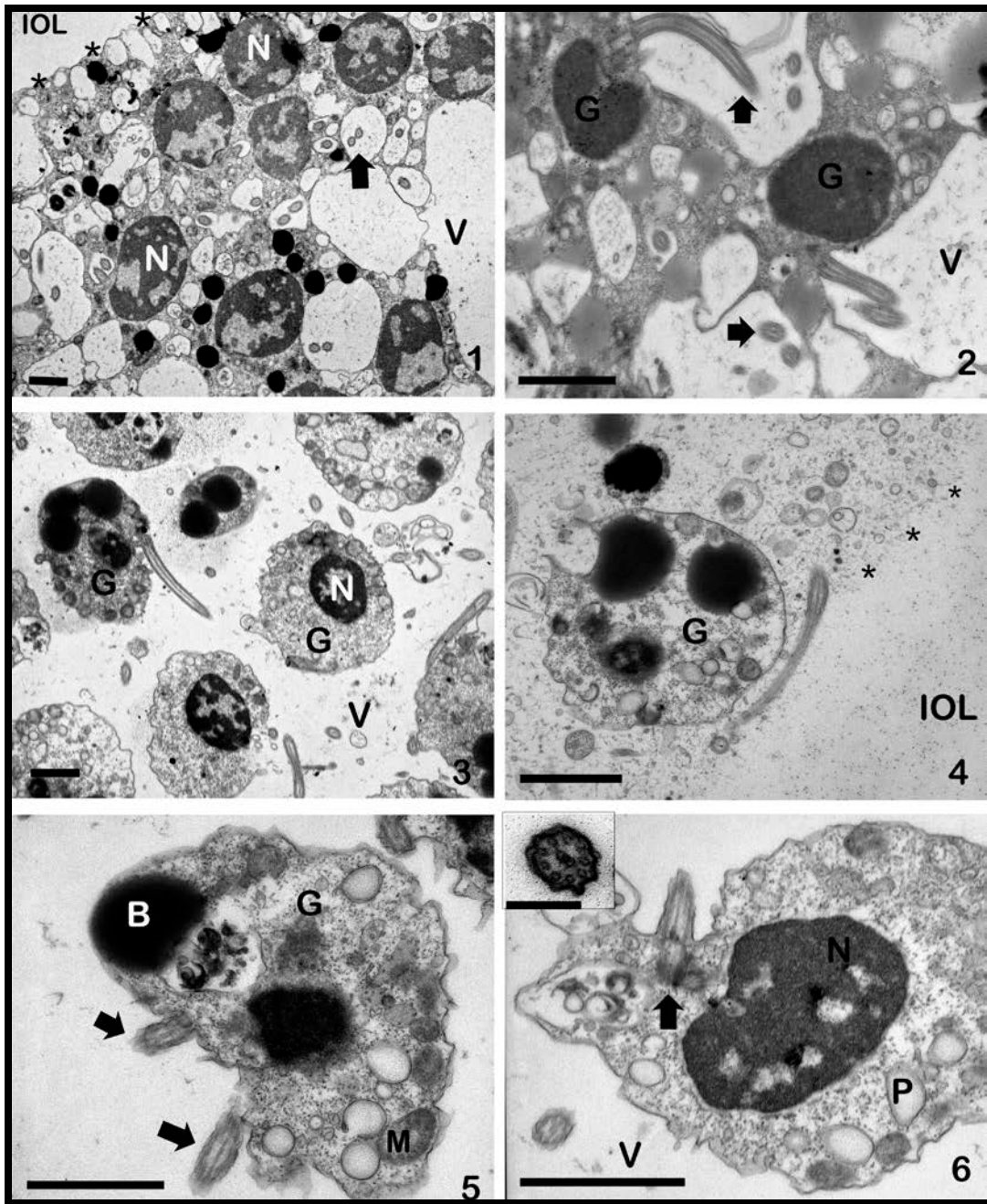


Figure 2.5 Reproductive ultrastructure for *Niveus flexilis*. 1 Asexually produced juvenile (grown in culture) undergoing early stages of gametogenesis. Several nuclei (N) are completely differentiated, and pairs of developing flagella (arrows) are located in expanding vacuoles (V). The plasma membrane (arrow) remains lined with vesicles, indicating cytoplasmic differentiation is not yet complete. 2 The “vacuolar” stage (also see light micrograph Fig. 2.4.5) is marked by gametic (G) differentiation and the expansion of the vacuolar system containing flagella. 3, 4 Cell captured during the “buzzing” stage just prior to gamete (G) release, illustrating complete uninucleate (N) gametic differentiation and vacuolar expansion (V). Plasma membrane is no longer visible in contact with the IOL (asterisks). 5, 6 Biflagellated gametes (arrows) with part of the flagellar root within an expanding vacuolar system (V). Common organelles include mitochondria (M), peroxisomes (P), and large, numerous electron-dense bodies. All images, scale bar = 1 μm , chemical fixation. 6 (inset) Cross section of a flagellum with 9+2 arrangement of microtubules (scale bar = 0.1 μm).

flagella are contained within the vacuoles, and they expand, ultimately separating gametes from each other and the remaining cytoplasm (e.g., Bé and others, 1983). The continued expansion of the vacuoles completely separates gametes and provides space for flagellar activity, ultimately allowing them to move within the parental test (Fig. 2.5.3). At this stage, the parental plasma membrane no longer exists (Fig. 2.5.4). Mitochondria and vesicles commonly line the well-defined plasma membrane of the gametes. Gametes possess two apically inserted flagella (Figs. 2.5.5-2.5.6) that exhibit the characteristic 9+2 microtubular arrangement (Fig. 2.5.6 inset) consistent with other eukaryotes. Flagella are rooted into a groove at one end of the gamete, but morphological details of the flagellar root system have not been examined at this time. It is suspected that root system ultrastructure may reveal insights into the evolutionary history of Foraminifera as in other protistan groups (e.g., algae; Melkonian, 1978, 1979).

Discussion

Historically, allogromiids have been considered primitive among Foraminifera because of their generalized morphology, organic (non-mineralized) test (Loeblich and Tappan, 1987), or lack of test all together (Pawlowski and others, 1999a, 1999b). Traditional foraminiferal systematics has been based on homologous morphological characters of the test wall structure and ontogenetic developmental stages combined with the fossil record (Cushman, 1948; Loeblich and Tappan, 1964, 1987; Tappan and Loeblich, 1988). Allogromiids and astrorhizids, however, possess an external morphology that is comparatively simple relative to their multichambered counterparts, resulting in systematic placement within only two orders, respectively (Sen Gupta, 1999). Phylogenetic studies based on rDNA sequences infer that allogromiids and astrorhizids do not comprise two distinct clades but branch amongst one another as a single, early diverging paraphyletic group (Pawlowski and others, 2002, 2003). A

number of freshwater (Pawlowski and others, 1999a, 1999b; Holzmann and Pawlowski, 2002; Holzmann and others, 2003) and terrestrial (Meisterfield and others, 2001) allogromiids branch throughout many lineages of allogromiids (*sensu lato* = allogromiids + astrorhizids + atestate foraminifers). Many of the molecular clades defined by Pawlowski and others (2002) are composed of taxa that do not share any gross morphological affinities. The disagreement between molecular phylogenetics and morphologically based systematics, the lack of gross morphological continuity among molecular clades, and the minimal number of comparable characters render allogromiid evolutionary history difficult to elucidate. Comparative morphological examination of ultrastructure (test and cell body) may yield phylogenetic signals that are not apparent at the gross morphological level. At this time, there is little ultrastructural data available to assess the value of fine structure for phylogenetic inference.

This newfound taxon is spherical to ovoid in shape and possesses a thin, agglutinated outer covering composed primarily of clay platelets. The agglutinated materials of some species of allogromiids have been reported to vary in size, mineralogy, and position along the test (Cushman, 1948; Wood, 1949). The agglutinated materials of all individuals of *Niveus flexilis* observed, however, were homogeneous in size, composition (primarily clay with occasional fragments of diatom frustules), and position (parallel to plasma membrane). The biochemistry of the test has not been evaluated, but it is presumed that the agglutinated particles are cemented together with strands of bioadhesives embedded in an organic matrix (e.g., Fig. 2.3.4). Such strands were visible in specimens fixed in the presence of ruthenium red. Past work on organic cements in astrorhizids has revealed the composition to be an acidic mucopolysaccharide (DeLaca, 1986; Goldstein and Barker, 1990; Langer, 1992; Bowser and Bernhard, 1993; =the protein-carbohydrate complex tectin of Buchanan and Hedley, 1960). The organic cement of

other allogromiids is susceptible to bacterial degradation (Goldstein and Barker, 1988), resulting in a poor representation of allogromiids and astrophorids in the fossil record (Loeblich and Tappan, 1964) and in modern death assemblages. In this study, taphonomic implications were evidenced by the distinct absence of dead individuals or empty tests in sediment samples.

Examination of the wall ultrastructure revealed that *Niveus flexilis* shares characteristics with members both within and outside its designated molecular Clade E (all clade designations are those of Pawlowski and others, 2002). The most obvious, unique characteristic of the wall is the extremely thick IOL, ranging from 3 μm to 8 μm (see Fig. 2.3.2; Figs. 2.4.1-2.4.2) and the extremely thin agglutinated layer consisting of a veneer of clay ($\sim 0.5 \mu\text{m}$). These wall characteristics differ greatly from those of other allogromiids (for comparison, see taxa evaluated by Goldstein and Richardson, 2002). When viewed with reflected light with a dissecting microscope, *N. flexilis* appears to have an organic, non-agglutinated test similar to descriptions of *Allogromia crystallifera* (Dahlgren, 1962b) and *Psammophaga simplora* (Arnold, 1982). Viewed under transmitted light, the IOL is apparent and resembles a clear halo surrounding the main cell body. The agglutinated layer (Figs. 2.2.1- 2.2.2) is visible along the outermost margin as a thin, dark clay layer. In ultrathin section (TEM), the IOL does not take up heavy metal stains, with the exception of spherical electron-dense granules and fine fibers that predominantly run parallel to the cell surface and that uptake ruthenium red during chemical fixation (Fig. 2.3). Other allogromiids that share a thick IOL characterized by electron-dense granules and fine fibers include the Clade E “Gam Forams” (Goldstein and others, 2006b), the sand-ingesting Clade E *P. simplora* (Arnold, 1982; Goldstein and others, 2006a), and two Clade L allogromiids: *Cribrothalammina alba* (Goldstein and Richardson, 2002) and *Ovammia opaca* (Dahlgren, 1964). The IOL observed in *N. flexilis*, however, is significantly thicker and less fibrous than that

of the Clade L allogromiids (i.e., ~1.3 μm in *C. alba* reported by Goldstein and Richardson, 2002). It appears that Clade E allogromiids, as defined by SSU rDNA phylogeny, share similar wall fine structure, but additional taxa must be evaluated to determine if these ultrastructural characteristics are truly diagnostic for the clade.

Mechanisms for wall construction and cell growth appear to differ among allogromiids (Goldstein and Richardson, 2002). For example, *Hyperammia* sp. (Goldstein and Richardson, 2002) and *Shepherdella taeniformis* (Hedley and others, 1967, 1972) possess long sets of microtubules that run down the entire length of the test just below the plasma membrane and that may function in directional growth along the aperture or possibly serve as structural support to accommodate the elongate shape. Other taxa, including *Myxotheca* sp. (Angell, 1971; Goldstein and Richardson, 2002), *Cribrothalammina alba* (Goldstein and Richardson, 2002), *Ovammia opaca* (Dahlgren, 1962a, 1964), the Sapelo “Gam Foram” (Goldstein and others, 2006b), and *Niveus flexilis* reported here, all contain numerous vesicles just beneath the plasma membrane. It appears that new test material is transported to the periphery of the cell in various locations by vesicles to allow for an increase in diameter, thus widening the single chamber (Goldstein and Barker, 1988; Goldstein and Richardson, 2002). Sub-plasma membrane vesicles have been reported in the filopod *Gromia oviformis* (Hedley and Bertaud, 1962; Hedley and Wakefield, 1969), which is a genetically close relative to the Foraminifera based on a variety of genetic markers (Archibald and others, 2003; Berney and Pawlowski, 2003; Longet and others, 2003, 2004; Nikolaev and others, 2004), suggesting that this morphology is an ancestral character state. Vesicles have also been found surrounding large vacuoles (Fig. 2.3.1) and conspicuously around the nucleus (Figs. 2.4.3-2.4.4) in *N. flexilis*. Ultrastructural observations show that the vesicles uptake varying levels of stain as indicated by their differences in electron opacity, suggesting

their biochemical makeup and function must differ. Because the wall and organic cement of agglutinated coverings are products of cellular biochemistry, Loeblich and Tappan (1987) suggested that the chemical compositions of these biogenic deposits are of major systematic importance, yet biochemical studies of foraminiferal vesicles have not been reported to date.

Vegetative cells of *Niveus flexilis* contain a single, large nucleus, ~11 μm in diameter, and the nucleoplasm just beneath the nuclear membrane is void of chromatin, which appears concentrated toward the interior of the nucleus (Fig. 2.4.3). Vesicles that surround the nuclear membrane have been reported in other allogromiid taxa, such as *Myxotheca* sp. (Goldstein and Richardson, 2002), *Cribrothalammina alba* (Goldstein and Barker, 1988; Goldstein and Richardson, 2002), and *Shepherdella taeniformis* (Hedley and others, 1967), which are genetically distinct and do not appear related to “Clade E” taxa (Goldstein and others, 2006a, 2006b). An extranuclear ring of elongate vesicles has also been reported in *Hyperammina* sp. (Goldstein and Richardson, 2002), and they appear quite similar in morphology to the endoplasmic reticulum in *N. flexilis*. Dahlgren (1964) published a thorough description of nuclear features of *Ovamina opaca*, including the presence of an extranuclear vacuole surrounding an irregularly shaped nucleus reportedly serving as an area where the nucleus communicates with the endoplasmic reticulum. Nyholm and Nyholm (1975) described the nucleus and environs in *Nemogullmia longevariabilis* as having pores that were hexagonal in shape and that varied in dimension and distribution, and they reported the presence of a thin fibrous perinuclear layer and nucleosomic aggregates scattered throughout the nucleoplasm. None of these features was observed in more recently examined allogromiid taxa, including *N. flexilis*.

It appears that similar cytological themes on reproduction span many foraminiferal orders (Goldstein, 1997); however, more data are necessary to confidently distinguish potentially phylogenetically relevant characters from reproductive data. Both asexual reproduction and gametogenesis were observed in cultured specimens of *Niveus flexilis* during this study. This species shares similar reproductive morphology at the light and electron microscopic level with multilocular foraminiferal taxa. For example, the rotaliid *Ammonia beccarii* forma *tepida* (Goldstein and Moodley, 1993) and the miliolid *Triloculina oblonga* (Goldstein, 1997) both share a similar vacuolar stage where the gamont has already undergone the nuclear divisions associated with gametogenesis and the buzzing stage indicative of complete gametic differentiation and the swarming of gametes within the parental test. Within minutes of the onset of buzzing, all three species release gametes directly into surrounding seawater, as done in most, but not all species of Foraminifera (Meyers, 1940; Grell, 1967, 1973; Goldstein, 1997).

The onset of asexual reproduction was not signaled by any cytological changes in the agamont but merely by the presence of gamontic juveniles in culture. Possibly, this species undergoes either a classical or triphasic alternation of generations. However, because the fate of subsequent generations was not followed during this study, it was not determined whether the young of asexually reproducing individuals were agamonts or schizonts. Because no cytoplasmic changes at the gross level were identified in *Niveus flexilis*, individuals that appear to be vegetative may have already begun gametogenesis. It is also interesting to note that a complete alternation of generations occurred in the absence of test construction materials, suggesting that an agglutinated layer is not a requirement for growth and reproduction. Sliter (1968) observed growth and reproduction as well as chamber addition in the textulariid *Trochammina pacifica*, also in the absence of agglutinating materials.

Systematic Description and Phylogenetic Position

Phylogenetic and morphological observations place *Niveus flexilis* in the following systematic position.

Domain EUKARYA (Woese and others, 1990)

Supergroup RHIZARIA (Cavalier-Smith, 2002)

Phylum GRANULORETICULOSA (Lee, 1990)

Class FORAMINIFERA (Loeblich and Tappan, 1992)

Order ASTRORHIZIDA (Brady, 1881)

Superfamily ASTRORHIZACEA (Brady, 1881)

Family SACCAMMINIDAE (Brady, 1884)

Genus *Niveus* nov. gen. (Altin, Habura and Goldstein)

Type species. *Niveus flexilis* nov. sp. (Altin, Habura and Goldstein)

Description. Test free, monothalamous, round to ovate in shape; possesses a finely agglutinated test with single aperture, a flexible collar and lacks internal septae. The outer, agglutinated layer is remarkably thin (0.4–0.7 μm), and primarily composed of clay and occasional fragments of diatom frustules adhered by an organic matrix. Under transmitted light, the test is translucent and underlain by a thick (3–8 μm), transparent inner organic lining. Test is free of perforations during all observed stages of reproduction.

Remarks. The round to ovoid shape, presence of a collar and lack of minerals within the cytoplasm differentiates the genus *Niveus* from *Psammophaga* (Arnold, 1982) which is pyriform to ovoid in shape, lacks a collar and has cytoplasmic mineral inclusions. In *Ovammmina* (Dahlgren, 1962), the presence of an entosolian tube and accessory reproductive pores for gamete release are absent during all observed reproductive stages in the genus *Niveus*.

Cytoplasm of all vegetative cells is opaque white under direct light, with the exception of those feeding, which may adopt the color of their food.

Niveus flexilis nov. sp.

Holotype Fig. 2.6.1, Paratypes Figs. 2.6.2-2.6.9.

Description. This modern species is small, ranging up to ~300 μm in diameter, ovate in shape, has a single aperture with a flexible collar, and lacks internal septae (Figs. 2.2.1-2.2.4). The flexible, translucent test is agglutinated and composed of a thin (0.4–0.7 μm), outer agglutinated layer of fine clay particles that are predominantly arranged parallel to the shell surface (Fig. 2.2.6). The outer surface of the test is crenulated and irregular (Figs. 2.2.4-2.2.5) and is underlain by an (3–8 μm) inner organic lining (IOL). The cytoplasm in vegetative gamonts or agamonts is opaque white in reflected light but can appear tan in transmitted light. In culture, the cytoplasm can become green or brown in color after feeding on *Dunaliella* sp. or *Amphiphora* sp., respectively. This allogromiid foraminiferan can be uninucleate as a gamont or multinucleate as the asexually reproducing agamont, indicative of an alternation of reproductive generations. Pseudopodia reticulate from a short peduncle emerging from the single aperture.

Remarks. Morphological characteristics that both tie *Psammophaga simplora*, *Allogromia crystallifera*, and *Niveus flexilis* as an evolutionary clade and delineate them as separate species may be present at the ultrastructural level. The taxon described here is similar to both *P. simplora* (Arnold, 1982) and *A. crystallifera* (Dahlgren, 1962b) as they all possess a non-mineralized, monothalamous test with a single, unadorned aperture. The collar about the aperture of *N. flexilis* is absent in both *P. simplora* and *A. crystallifera*. The apertural region of *P. simplora* is tapered and lacking a neck, where *A. crystallifera* has a prominent neck, and *N. flexilis* a short neck. A thickened IOL beneath the agglutinated layer in the apertural region is

consistent among all three. Under transmitted light, all three taxa appear to have an organic test because the agglutinated layer is extremely thin. Ultrathin sections of *N. flexilis* and *P. simplora* (Altin, unpublished observations, 2007) reveal a thin, distinct layer of clay with intermittent fragments of diatom frustules. Dahlgren (1962b) described *A. crystallifera* as having a double-layered, hyaline wall (the inner layer thicker and colorless) and did not mention any external agglutinated matter. The test of *A. crystallifera* must be examined with electron microscopy to determine whether the thinner, darker outer layer includes agglutinated materials. The major differences between the walls of *Psammophaga* sp. and *N. flexilis* are the meticulous layering of the clay particles parallel to the surface of the IOL and the profoundly crenulated agglutinated layer in the latter. In populations of *Psammophaga* sp. from Sapelo Island, Georgia, the outer surface of this test is smooth, not crenulated, and clay particles are deposited loosely and in varying orientations (Altin, unpublished observations, 2007). Arnold (1982) suggested that the degree of organization of the agglutinated particles may be an evolutionarily derived character state. The overall test shape of all three taxa differs: *P. simplora* is pyriform or lachrymiform (Arnold, 1982), *A. crystallifera* is elliptical (Dahlgren, 1962b), and *N. flexilis* is distinctly ovate.

Features of the cytoplasm and organelles are characters worth considering for phylogenetic affinities. The color of the cytoplasm of *Niveus flexilis* is opaque and white, consistent among all individuals with the exception of those containing undigested algal food material. Both *Psammophaga simplora* (Arnold, 1982) and *Allogromia crystallifera* (Dahlgren, 1962b) were described as having white cytoplasm, though as many individuals were found to be gray or pink, respectively (Dahlgren, 1962b; Arnold, 1982).

The major distinction that separates *N. flexilis* from both *P. simplora* and *A. crystallifera* is the lack of ingested mineral grains maintained within the cytoplasm. Although *A. crystallifera*

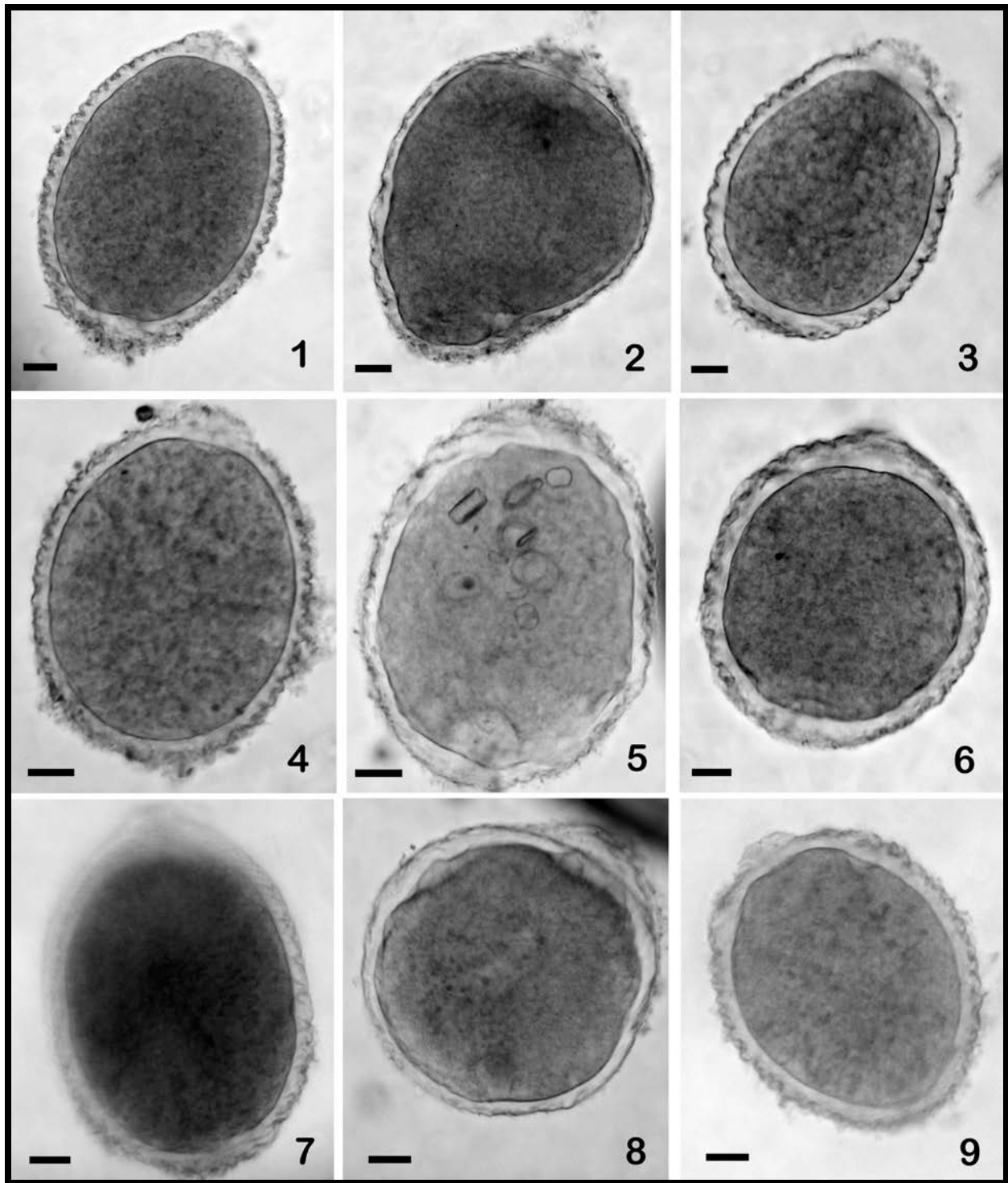


Figure 2.6 Type specimens for *Niveus flexilis*. **1** Holotype (USNM 538118a) and **2-9** paratypes (USNM 538118b-538118i respectively) for *Niveus flexilis* nov. gen., nov. sp. embedded in epon-araldite epoxy resin and mounted on glass slides. Holotype test is characterized by an ovoid shape, a thick, transparent inner organic lining (IOL), a thin agglutinated layer composed of clay minerals, and a single aperture with collar. Scale bars = 50 μ m.

maintains the majority of sand grains near the aperture (Dahlgren, 1962b), *P. simplora* possesses a conspicuous volume of sediment as indicated by the derivation of its name (Arnold, 1982). In addition to SSU sequences, this behavioral characteristic tied members of Clade E together (Pawlowski and others, 2002). Our results suggest that sand ingestion may not be a synapomorphy for the clade as suggested by Pawlowski and others (2002); alternatively, the characteristic may have been secondarily lost over time. A distinct electron-dense ring along the cortex of the nucleus appears to separate *P. simplora* and *A. crystallifera* from *N. flexilis*. The cortical nucleoplasm was described as a polygenomic zone of chromosomes or basophilic components in *P. simplora* (Arnold, 1982). This peripheral region in *A. crystallifera* was reported to consist of large quantities of basophil material, consisting of granules of varying shapes and sizes that created a distinct boundary from the inner nucleoplasm (Dahlgren, 1962b). These observations have been confirmed via transmission electron microscopy in *Psammophaga* sp. from Sapelo Island, Georgia (Altin, unpublished observations, 2007). Unlike these taxa, the nucleoplasm of *N. flexilis* contains evenly dispersed chromatin throughout. Ultrastructure of the wall, including the IOL and cement, plasma membrane, and other features of the cytoplasm of *P. simplora* and *A. crystallifera*, cannot be compared with *N. flexilis* as they have not been examined at the ultrastructural level at this time.

The sum of the gross and fine morphological features of the test and cell body in this study supports the erection of *Niveus* as a new genus. Fine morphology in this report clearly distinguishes *Niveus* from previously described Clade E allogromiids at the generic level (Dahlgren, 1962b; Arnold, 1982) and is in agreement with the most current phylogenetic reconstructions based on SSU rDNA sequences (Habura and others, 2008).

Etymology. The generic designation *Niveus* is a translation from the Latin snow, reflecting the overall shape and color of this taxon reminiscent of a snowball (Figs. 2.2.1-2.2.2). The flexible nature of the test during both vegetative and reproductive phases is reflected in the specific designation *flexilis*.

Type locality. Hyposaline *Juncus roemerianus* salt marshes adjacent to the Rod and Gun Marina, Darien, Georgia, (31°24'22"N, 81°23'36"W), USA (Fig. 2.1).

Type specimens. Type specimens (Figs. 2.6.1-2.6.9) have been deposited at the Smithsonian Institute, Washington D.C., USA, under the following catalog numbers: holotype (Fig. 2.6.1) USNM 538118a, paratypes (Figs. 2.6.2-2.6.9), USNM 538118b-USNM 538118i respectively.

Phylogenetic relationships. Phylogenetic analyses using partial SSU rDNA sequences place *Niveus flexilis* into allogromiid Clade E along with *Psammophaga* sp., *Allogromia crystallifera* (Pawlowski and others, 2002), and other newfound allogromiid taxa conspicuously found along Georgia's salt marshes and mudflats (Goldstein and others, 2006a; Habura and others, 2008). The most recent phylogenetic tree for allogromiids places *N. flexilis* as a sister to a "Duplin quartzball"–"Fusiform allogromiid" clade at some evolutionary distance from *Psammophaga* spp. and *A. crystallifera*. The GenBank accession number for *N. flexilis* (EU213257) was previously reported as the "Rod and Gun White Allogromiid" in Habura and others (2008). Further examination of allogromiids along Sapelo Island, Georgia, revealed the presence of several other morphologically diverse undescribed taxa with molecular affinities for Clade E (Habura and others, 2008). Some of these include the "Timber Dock black and white saccamminids," the "2005 gam foram," the "Chocolate silver saccamminids," the "Fusiform allogromiid," and a taxon with morphological similarity to *Micrometula*. The addition of these

newfound species within the analysis resulted in a decrease in resolution of Clade E as compared with Pawlowski and others (2002). However, all of the Clade E foraminiferans shared sequence features in the “Region II” insert (Bowser and others, 2006) that excluded other foraminiferans, indicating that common membership in a single clade was the most likely interpretation of the molecular data.

Conclusions

The extent to which morphological characters at the ultrastructural level are useful phylogenetic indicators for Clade E allogromiids is not yet known. Current phylogenetic analyses of allogromiid foraminifers typically utilize a single genetic marker (i.e., SSU) to infer an evolutionary history. Various analyses employ different statistical methods to interpret the SSU sequences, alternative roots for the resulting trees, and include varying numbers of taxa. These differences may return inconsistent evolutionary hypotheses, at least at this taxonomic level, as seen in the relationship of members of Clade E. Morphological data at the fine structural level are essential, as allogromiids tend to lack many of the characters commonly used in foraminiferal classification. Fine cellular morphological data are critical to test the fidelity of phylogenetic trees of allogromiids based solely on the sequences of a single gene. Because any phylogenetic tree is an evolutionary hypothesis, an increase in the number of characters, whether they are additional genetic markers, taxa, or ultrastructural morphology, may increase the resolution of the Clade E allogromiids.

Acknowledgments

We would like to thank Sam Bowser and Mark Farmer for assistance, Elizabeth Richardson for her advisement on electron microscopic techniques and the two anonymous reviewers for their thoughtful comments on this manuscript. This research was funded by

National Science Foundation (NSF) grant DEB0445181 to S.S. Bowser and S.T. Goldstein, the Cushman Foundation for Foraminiferal Research for the Loeblich and Tappan Student Research Award to D.Z. Altin, and the Friends the of University of Georgia Marine Institute Student Research Award to D.Z. Altin. This is contribution number 972 of the University of Georgia Marine Institute, Sapelo Island, Georgia.

CHAPTER 3

PSAMMOPHAGA SAPELA N. SP., A NEW MONOTHALAMOUS FORAMINIFERAN FROM
COASTAL GEORGIA USA: FINE STRUCTURE, GAMETOGENESIS AND
PHYLOGENETIC PLACEMENT²

² Altin-Ballero, D.Z., Habura, A. and Goldstein, S.T., 2013. *Journal of Foraminiferal Research*, v. 43, no. 2, pp. 113-126. Reprinted here with permission from the publisher.

Abstract

We describe a new monothalamous species, *Psammophaga sapela*, collected from salt marshes and mudflats along the coast of Georgia, U.S.A. Partial small subunit ribosomal DNA (SSU rDNA) phylogenetic analyses assign this species to “Clade E,” one of a series of clades of monothalamous foraminifera. *Psammophaga sapela* joins three previously described species in this genus: *P. simplora* Arnold, the type species, *P. magnetica* Pawlowski and Majewski and the reassigned *Allogromia crystallifera* Dahlgren. This new species is of moderate size (up to ~ 550 μm), is generally pyriform in shape, and has a single, flexible aperture, which may occur at the end of a very short neck. The flexible test is composed of a relatively thick (10-15 μm), smooth, outer agglutinated layer of fine clay particles arranged loosely parallel with respect to the plasma membrane of the cell body. The agglutinated layer is underlain by a moderately thick (2–5 μm), inner organic lining (IOL), which is in direct contact with the cell membrane. The IOL contains numerous small electron-dense particles along with elongated, fine fibers similar to other previously reported Clade E taxa. Small vesicles lie just beneath the cell membrane and merge with the plasma membrane to release test construction materials at the base of the IOL. This species is gametogamous, where gamonts release biflagellated gametes either through the aperture or within membrane-bound packets that open following release. Budding was also observed. True to its generic name *Psammophaga* (sand eating), this taxon avidly ingests and maintains sediment grains of orthoclase, pyrrhotite, basaluminite, pseudobrookite, anatase and ilmenite, the latter rendering this taxon magnetic.

Introduction

Modern monothalamous foraminifera represent descendants of the earliest diverging foraminiferal lineages (Pawlowski and others, 2003) and are found in virtually all marine as well

as some freshwater (Pawlowski and others, 1999a, 1999b; Holzmann and Pawlowski, 2002; Holzmann and others, 2003) and terrestrial environments (Meisterfield and others, 2001; Lejzerowicz and others, 2010). Of the single-chambered taxa, the genus *Psammophaga* is noteworthy for its broad geographic distribution and occurrence in a range of shallow marine settings (Arnold, 1982; Goldstein and others, 1995; Gooday and others, 1996; Larkin and Gooday, 2004; Gooday and others, 2005; Sergeeva and Anikeeva, 2006; Anikeeva, 2007; Sabbatini and others, 2007; Pawlowski and Holzmann, 2008; Pawlowski and others, 2008; Pawlowski and Majewski, 2011). Here we describe the fine structure of the wall, cell body and nucleus and include observations on reproduction (gametogenesis, budding) for *Psammophaga sapela* nov. sp. which is common on the Georgia coast (U.S.A.).

The type species, *Psammophaga simplora* Arnold 1982, was described from shallow-water habitats of Monterey Bay, California. The etymology of the generic name reflects the avid ingestion of sediment grains which are retained in the cytoplasm as inclusions while these foraminifera undergo normal biological activities. This characteristic unites the several described species of this genus and is similar to the avid packing of diatoms in the related genus *Xiphophaga* Goldstein and others 2010). Although ribosomal small subunit DNA (SSU rDNA) analyses suggest that these taxa are phylogenetic members of Clade E (Pawlowski and others, 2002; Habura and others, 2008), this ‘particle ingesting’ character is not synapomorphic for the entire clade as it is currently recognized. Rather, the homogeneity of Clade E becomes problematic with the addition of closely-related but non-sediment ingesting species to phylogenetic analyses utilizing just SSU rDNA sequences (Habura and others, 2008). This report is part of a larger project aimed at testing the phylogenetic cohesiveness of Clade E by coupling fine structure with multiple genetic markers.

Materials and Methods

Sample Collection and Culturing

Foraminifera used in this study were collected from several sites in the Sapelo Island, Georgia area: a low-salinity salt marsh (~10–22 ‰) at the Rod and Gun Marina near Darien, Georgia mudflats at the historical site on Sapelo locally known as “Chocolate,” the type locality, as well as mudflats near the Sapelo lighthouse and tidal creeks of Cabretta Island (Fig. 3.1).

Salinity overall at these Sapelo sites may range up to 30+ ‰ depending on season and rainfall.

Surface sediment collection and processing followed that of Altin and others (2009). For light microscopic observations, selected individuals were placed in plastic culture dishes with Instant Ocean adjusted to ambient salinity and appropriate live food organisms (*Dunaliella*,

Amphiphora, *Isochrysis*) and photographed using either transmitted or reflected light. If left isolated in a culture dish with no movement or extraneous sediment overnight, *Psammophaga sapela* egests most of its mineral inclusions. These inclusion-free individuals were ideal for fixation and subsequent sectioning. Observations were made on both reproductive and non-reproductive individuals, and selected foraminifers were prepared for electron microscopy.

Microscopy and Identification of Mineral Inclusions

Vegetative and reproductive foraminifera were prepared for transmission electron microscopy (TEM) using either high-pressure freezing and freeze substitution (HPF/FS) or chemical fixation methods. HPF/FS methods follow those previously reported (Goldstein and Richardson, 2002; Altin and others, 2009). Reproductive individuals that showed specific morphological changes (Goldstein, 1997) were prepared for TEM using chemical fixation protocols of previous reports (Goldstein and Barker, 1990; Goldstein and Moodley, 1993; Altin and others, 2009). All TEM preparations were examined under a light microscope, and well-

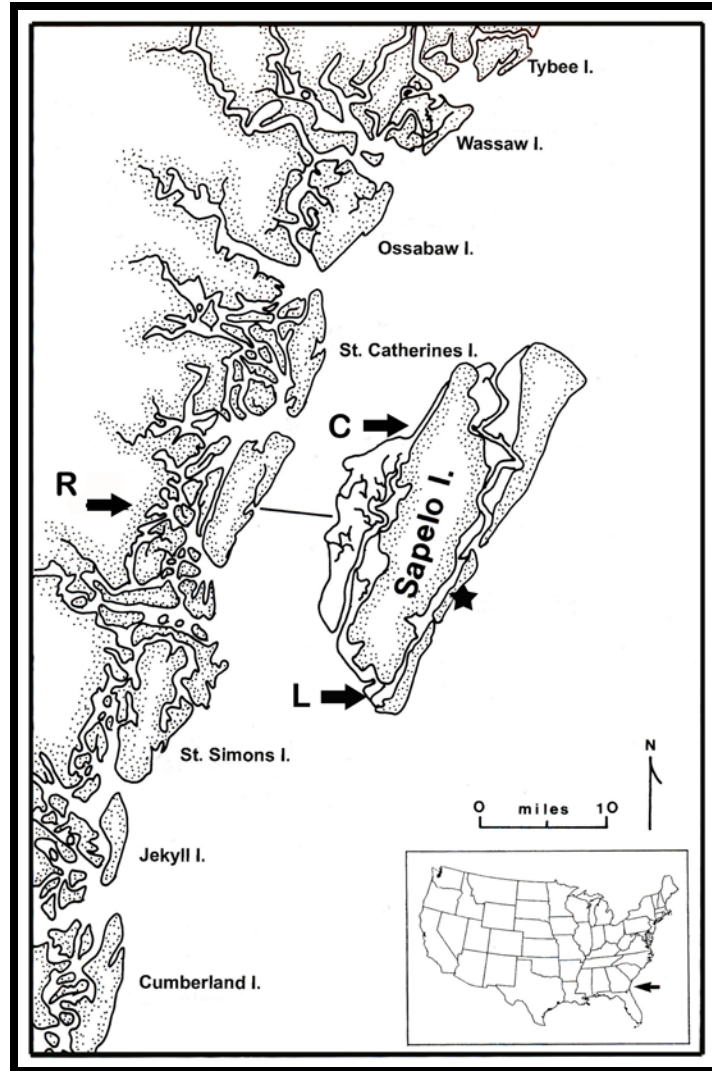


Figure 3.1 Approximate geographic sampling locations for *Psammophaga sapela*. Approximate geographic locations of the sampling sites (arrows) along the salt marshes and mudflats adjacent to the Rod and Gun Marina (R) near Darien, Georgia (31°24'22"N, 81°23'36"W), Chocolate (C) Beach (31°30'21"N, 81°15'25"W), the Sapelo lighthouse (31°23'22.64"N, 81°17'10.00"W) and tidal creeks of Cabretta Island (31°26'20.21"N, 81°14'14.74"W, Sapelo Island, Georgia. Insert map at lower right shows position of Sapelo Island (arrow) within contiguous United States.

fixed cells were removed with a jeweler's saw and mounted on acrylic blocks with glue (Quickbond). Blocks containing selected specimens were trimmed, then sectioned (80–90 nm thickness) using a Reichert-Jung Ultracut E microtome and a diamond knife. Thin sections were placed on Formvar-coated slot grids, dried overnight, post-stained for three minutes each with uranyl acetate and lead citrate, and viewed on a Zeiss EM 902A operated at 80 kV. Type

specimens were prepared using the same methods as TEM preparations, omitting the post-fixation step (osmium tetroxide), after which they were mounted on glass slides (see Goldstein and others, 2010).

Living individuals prepared for SEM followed the chemical TEM fixation protocols. As an alternative to critical-point drying for dehydration, specimens were chemically dried with hexamethyldisilazane (HMDS) (see Altin and others, 2009). Specimens were sputter coated with gold (15.3 nm) and viewed on a JEOL JSM-5800 operated at 15-20 kv. In some cases, however, the use of HMDS produced dehydration artifacts and SEM was repeated using standard critical-point drying methods (e.g., Bozzola and Russell, 1998).

In addition, selected individuals were examined with epifluorescence microscopy following DAPI (4'-6'-diamidino-2-phenylindole) staining. Individuals which had purged their ingested sand grains were fixed in 4% paraformaldehyde, stained with 5 µg/ml DAPI (protocol provided by J.M. Bernhard, Woods Hole Oceanographic Institution) to count the number of nuclei in whole specimens without sectioning.

To identify the minerals ingested by *P. sapela*, approximately 100 individuals were isolated from sediment collected from the mudflat at the Lighthouse site on Sapelo Island, and the mineral inclusions were isolated by digesting the cells with repeated washings in 30% hydrogen peroxide and de-ionized water. The sediment was dried, placed on a zero-background quartz plate and analyzed with a Bruker D-8 Advance x-ray diffractometer, using cobalt radiation, a 0.2 mm slit, and scanned from 4–80° 2-theta.

Sample Preparation for Molecular and Phylogenetic Analysis

Approximately 20 individuals were placed in a culture dish with sterile Instant Ocean for 24 hrs to complete digestion of food and purge digestive wastes. Individuals were thoroughly

cleaned with a fine artist's brush in a series of six sterile Instant Ocean washes to remove any obvious epibionts or other potential external contaminants. Cells were stored in RNALater (Ambion), and genomic DNA was extracted using the DNeasy Plant Mini Kit (Qiagen, Valencia, California). The 3' region (Domain III) of the SSU rDNA was amplified by nested PCR primers (S14F3A, B; S14F1, S20R; Pawlowski, 2000). PCR amplifications were performed on a Techne Genius thermocycler using ExTaq premix (TaKaRa) with cycle parameters as previously reported in Habura and others (2004). PCR products were analyzed by agarose gel electrophoresis, cloned in pGEM-T Easy vectors (Promega, Madison, WI) and replicated in JM104 *Escherichia coli* cells. Cloned inserts were extracted and purified with the SpinPrep mini kit (Qiagen, Valencia, CA) and a minimum of six clones was sequenced in both directions (Geneway Research, Hayward, California) using M13 forward and reverse primers. Sequences were manually aligned with a subset of one shared by Jan Pawlowski and edited in Geneious (Drummond and others, 2010). Unambiguously aligned positions were analyzed by Bayesian analysis using Mr. Bayes, version 3.1 (Huelsenbeck and Ronquist, 2001) under the GTR + I + G evolutionary model, run with two sets of four chains using the random tree option for five million generations. Trees were sampled every thousand generations with the first 1,250 discarded as burn-in. Remaining trees were used to generate a consensus tree. Trees were edited with TreeView 1.6.6 (Page, 1996) and MEGA version 5 (Tamura and others, 2011). The sequences of five clones of *Psammophaga sapela* have been deposited in GenBank under the accession numbers JX645722 through JX645726.

Systematic Description and Phylogenetic Position

The traditional classification of monothalamous foraminifera based on wall characteristics (e.g., Astrorhizida, Allogromiida; Loeblich and Tappan, 1987) is inconsistent with

current molecular phlogenetic studies (Pawlowski and others 2002, 2003). At this time, assigning classical familial and ordinal taxonomic affinities to monothalamous foraminifera are not evolutionarily informative. Phylogenetic and morphological observations place *Psammophaga sapela* in the following systematic position.

Supergroup RHIZARIA Cavalier-Smith, 2002

Phylum FORAMINIFERA d'Orbigny, 1826

Genus *Psammophaga* Arnold, 1982

Psammophaga sapela nov. sp.

Figs. 3.2.1 – 3.2.8

Etymology. The species name *sapela* refers to the geographic location (Sapelo Island, Georgia) where this taxon is remarkably common.

Type locality. Mudflats near the historical site “Chocolate” on, Sapelo Island, Georgia (31°30'21"N, 81°15'25"W), U.S.A. This species is common on mudflats and in tidal creeks of Sapelo Island and nearby marshes of coastal Georgia.

Type specimens. Type specimens have been deposited at the Smithsonian Institute, Washington D.C., U.S.A., under the following catalog numbers— holotype: USNM 542380 (Fig. 3.2.1), paratypes: USNM 542381 (Fig. 3.2.2) and USNM 542382a-f respectively (Figs. 3.2.3-3.2.8).

Diagnosis. Test free, single-chambered, pyriform, elongate or spherical in shape with a single unornamented, terminal aperture. Test is composed of primarily clay particles agglutinated by an organic adhesive. Cytoplasm is translucent, gray or milky white. Mineral inclusions retained throughout the entire cytoplasm during normal biological activities. Reproduction is

gametogamous. Biflagellated gametes are released through the aperture directly or within packets. Reproduction by budding has been observed.

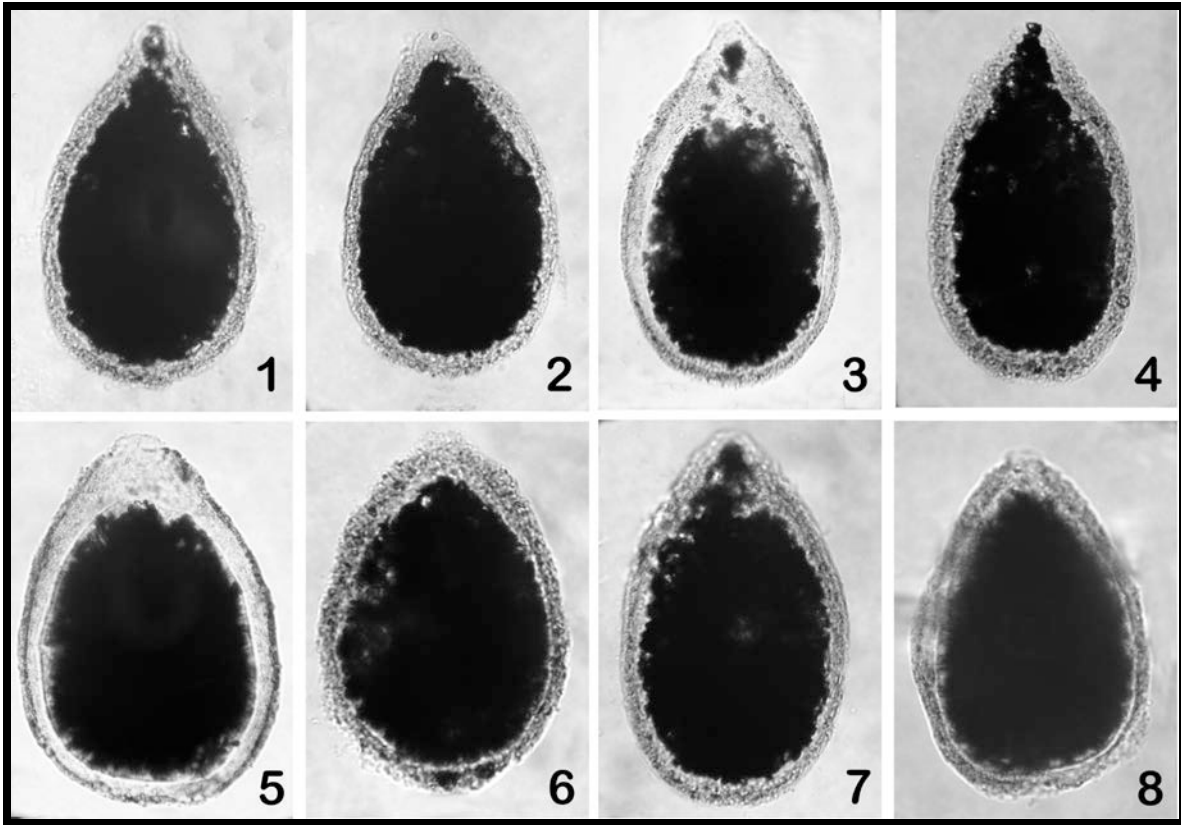


Figure 3.2 Type specimens for *Psammophaga sapela* n. sp. 1 Holotype (USNM 542380). and 2–8 paratypes (USNM 542381, 542381, 542382a-f respectively) embedded in epon-araldite epoxy resin and mounted on glass slides. Holotype test is characterized by a pyriform shape, a thin agglutinated layer composed of clay minerals, a single unornamented aperture, and cytoplasmic inclusions of sand grains evenly dispersed throughout the cytoplasm. Dark appearance of the cytoplasm is due to the generous amount of ingested sediment grains. Measurements from aperture to abapertural end: 1, 420 μm ; 2, 420 μm ; 3, 564 μm ; 4, 372 μm ; 5, 492 μm ; 6, 312 μm ; 7, 8 396 μm .

Description. Of moderate size (up to ~ 550 μm in length), *Psammophaga sapela* is generally pyriform, elongate or spherical in shape, and has a single, flexible and unornamented aperture which may occur at the end of a very short neck. The transparent to translucent test is flexible and composed of two layers: an outer agglutinated layer (10-15 μm thick) of fine clay particles that are aggregated within an organic bioadhesive, and an inner organic lining (IOL) that measures 2-5 μm in thickness and thins toward the aperture. No outer organic lining is present. The cytoplasm in the uninucleate, vegetative gamont is translucent in reflected light and

contains abundant cytoplasmic inclusions of mineral grains that typically appear to fill the entire test. Pseudopodia reticulate from a short peduncle that emerges from the single aperture. The test is free of perforations during all stages of gametogenesis. Sexual reproduction produces biflagellated gametes that are released into the surrounding seawater directly as swarms of individual gametes or as aggregated packets of gametes that subsequently open following release from the aperture. Budding also occurs.

Remarks. We examined Arnold's (1982) entire collection of prepared *Psammophaga simplora* material, including type specimens. Nonetheless, morphological comparisons of *P. simplora* and *P. sapela* are difficult. Arnold's types include a holotype and 10 paratypes, all of which are sections of individuals prepared cytologically for light microscopy and mounted on glass slides. Further, some of the paratypes were selected specifically to illustrate the sequence of nuclear stages associated with gametogenesis (see also Arnold, 1984) rather than the overall morphology of this species. Arnold's (1982) type specimens are among >100 randomly oriented individuals that were fixed, concentrated into lots of ~20 individuals, embedded in paraffin, and serially sectioned. Occasional gaps in the serial sections are probably a result of the numerous mineral inclusions, not all of which could be removed with HF (Arnold, 1982), that interfered with sectioning. The collection includes no intact (i.e., un-sectioned) specimens. The holotype of *P. simplora* is an equatorial section that includes both the aperture and the nucleus. Mineral inclusions are concentrated near the aperture, but are absent in the abapertural region that includes the nucleus. The distribution of mineral inclusions within the cell body of *P. simplora*, however, is probably a variable feature because other individuals in the collection have mineral inclusions dispersed throughout as in *P. sapela* except that the latter also has the ability to egest most or all of these inclusions. Other described species of *Psammophaga* include *P. crystallifera*

(Dahlgren, 1962a) and *P. magnetica* Pawlowski and Majewski, 2011. The former has mineral inclusions that are “mostly concentrated around the apertural end” (Dahlgren, 1962a), and Pawlowski and Majewski (2011) reported the same for *P. magnetica*. Arnold (1982) described *P. simplora* as lacking a peduncle, a feature that is present in *P. sapela* and *P. crystallifera* (Dahlgren, 1962a); though not mentioned, a peduncle is illustrated in *P. magnetica* (see figs. 2D and 2E of Pawlowski and Majewski, 2011). Of the described species of *Psammophaga*, the species *P. sapela* most closely resembles that of *P. simplora* in shape and in that both populations include pyriform, spherical, and elongate individuals; *P. magnetica* and *P. crystallifera* are both described as predominantly elongate. Although morphologically similar, *P. simplora* and *P. sapela* differ significantly in life cycle features. Both are gametogamous but *P. simplora* releases fairly large amoeboid gametes (5-6 μm ; Arnold, 1982), whereas *P. sapela* releases small ($\sim 1.5 \mu\text{m}$) biflagellated gametes either directly or in small tethered packets. Budding occurs in both *P. simplora* and *P. sapela*, and the forming bud initially lacks an aperture. *Psammophaga crystallifera* undergoes “transverse division,” and the parent forms a second aperture at the distal end prior to division (Dahlgren, 1962a). A multinucleate agamont and associated asexual reproduction were not observed in *P. sapela*.

Psammophaga simplora and *P. sapela* inhabit geographically and ecologically distinct settings. *Psammophaga sapela* has been reported previously from marsh and mudflat settings of coastal Georgia as *P. simplora* by Goldstein and others (1995), Pawlowski and others (2002), Pawlowski and Holzmann (2008), and Habura and others (2008) and as *Psammophaga* sp. by Goldstein and Alve (2011). The latter authors showed that juveniles of this species are common constituents of the foraminiferal propagule bank at two mudflat sites on Sapelo Island, Georgia, and that they grew readily at 12° and 22° C, and at salinities of 22 and 36 ‰. Individuals rarely

grew at an experimental salinity of 12 ‰, suggesting that this species is limited by very low salinities. *Psammophaga simplora* occurs in cooler waters of Monterey Bay, California, U.S.A. among stands of the surfgrass *Phyllospadix* Hooker (Arnold, 1982).

Phylogenetic relationships. Phylogenetic analyses using partial SSU rDNA sequences place *Psammophaga sapela* into Clade E (Pawlowski and others, 2002 formerly reported as *P. simplora*) along with *P. crystallifera* (Pawlowski and others, 2002), *Xiphophaga allominuta* and *X. minuta* Goldstein and others, 2010 (the latter two reported as the “2005 and 2003 Gam Foram” respectively in Habura and others, 2008). Clade E members including *P. sapela*, share common sequence features of the “Region II” insert, a foraminiferan-specific expansion of the SSU that shows sequence heterogeneity between different foraminiferal clades (Bowser and others, 2006; Goldstein and others, 2010). Clones of *P. sapela* form a distinct clade from other members of this genus including *P. magnetica*, *P. crystallifera* (Pawlowski and Majewski, 2011) and *Psammophaga* sp. 2359 (Pawlowski and others, 2003; Fig. 3.3).

Previous molecular studies on *P. simplora* utilized DNA obtained from specimens of *Psammophaga* collected along Sapelo Island mudflats (GenBank Accession number AJ317985; see Pawlowski and others, 2002, 2003; Pawlowski and Holzmann 2008) of which identification was based solely on gross morphology. Intact type specimens of *P. simplora* do not exist and genomic DNA has not yet been obtained from potential topotypes in Monterey Bay, California. At this time, the phylogenetic position of *P. simplora* cannot be established. The previously published SSU rDNA sequences designated as *P. simplora* Arnold 1982 (Pawlowski and others, 2002, 2003; Pawlowski and Holzmann, 2008) are actually from *P. sapela* as described here.

Further Observations on *Psammophaga sapela*

Psammophaga sapela is common on mudflats and in tidal creeks and ponded low-marsh habitats of Sapelo Island and neighboring barrier islands and mainland marshes of coastal Georgia. As typical of the genus, *P. sapela* ingests and retains abundant mineral inclusions in addition to occasional diatom frustules within its cell body (Figs. 3.4.1-3.4.3) and appears to prefer heavier minerals. X-ray diffraction identified anatase, ilmenite, orthoclase, zircon, pyrrhotite, basaluminite, and pseudobrookite as the primary mineral inclusions. Quartz, probably the most abundant mineral in these intertidal settings, is rare to absent among these inclusions. Individuals of this species are readily drawn to a magnet, reflecting the abundance of ilmenite retained within the cell body. However, attempts to “pick” these foraminifera from bulk sediment with a magnet commonly resulted in severe cell damage.

Test Morphology and Fine Structure

This monothalamous foraminiferan extends pseudopodia solely through the single, unornamented aperture (Figs. 3.4.4-3.4.9), through which food, sediment grains, and gametes also pass. The aperture (~6 μm in diameter) is presumed to be sufficiently flexible to allow for the passage of sediment grains of various sizes. The exterior portion of the test wall is composed of a relatively thick (10-15 μm), imperforate, outermost agglutinated layer composed primarily of clay platelets, rare fragments of diatom frustules and larger mineral grains, and an organic bioadhesive (Figs. 3.4.10-3.4.12; Figs. 3.5.1-3.5.4) The loosely packed, somewhat randomly oriented clay platelets (Fig. 3.5.4) are cemented together by an organic bioadhesive that contains electron-dense fibrils, visible when stained with ruthenium red, suggesting that it is rich in acidic

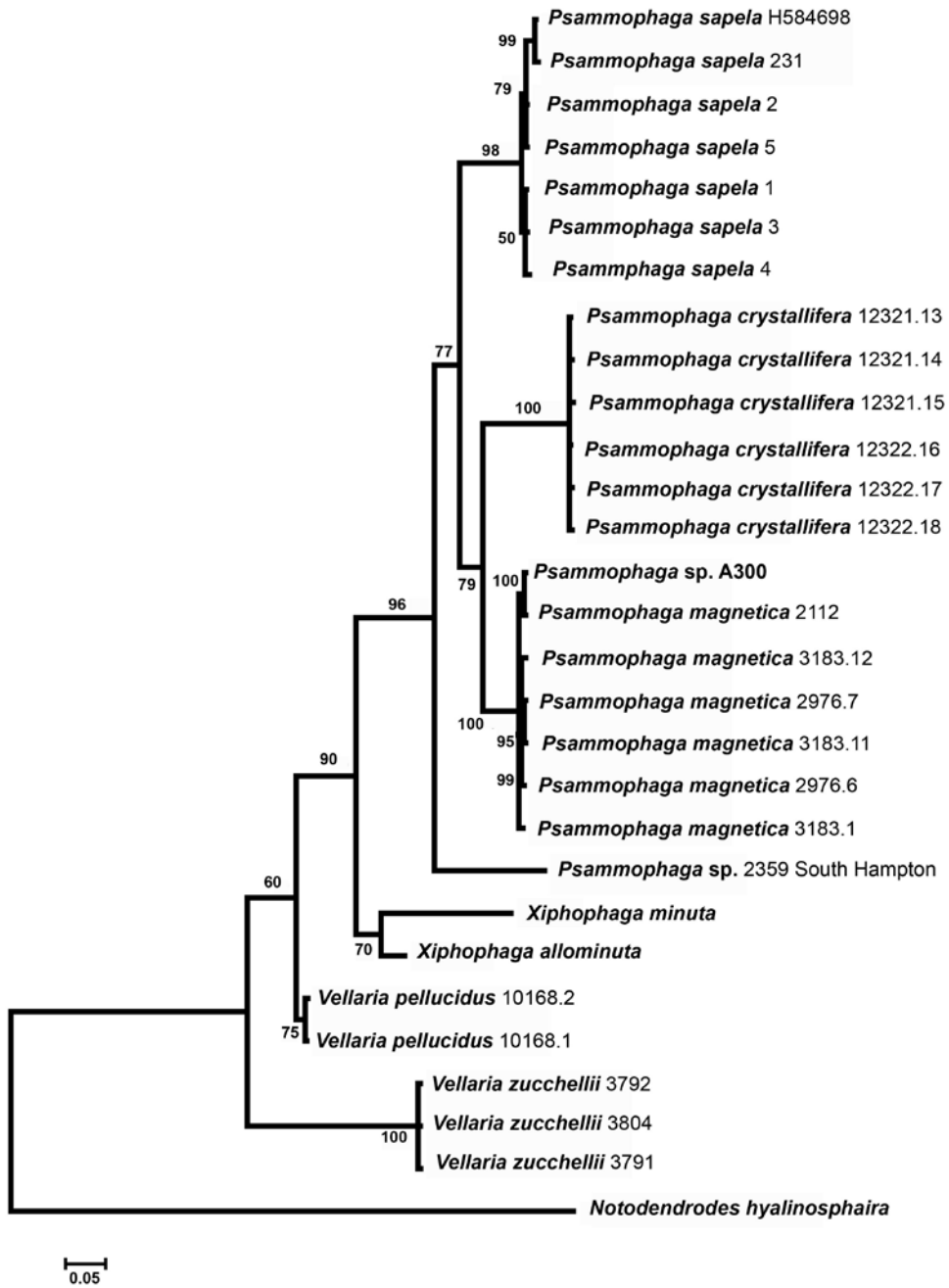


Figure 3.3 Phylogenetic position of *Psammophaga sapela*. Bayesian analysis of 1080 positions illustrating phylogenetic position of *Psammophaga sapela* within selected members of Clade E, using *Notodendrodes hyalinosphaira* DeLaca and others, 2002 (Clade F) as the outgroup. Posterior probabilities for nodes with a value of ≥ 60 are shown.

mucopolysaccharides (e.g., Goldstein and Barker, 1988). Otherwise, the complete biochemical composition of the bioadhesive has not been determined. The presence of bacterial colonies within the bioadhesive (Fig. 3.5.3) is not uncommon in *P. sapela*.

The IOL is significantly thinner than the overlying agglutinated layer, and is characterized by numerous electron-dense granules and fibrils, most of which are oriented parallel to the plasma membrane (Figs. 3.5.1-3.5.4) of the cell body. This membrane is in direct contact with the IOL and is lined with numerous cytoplasmic vesicles of unknown function that presumably contain test construction materials (Fig. 3.5.3). These vesicles have been captured merging with the plasma membrane (Fig. 3.5.2) signifying that they exocytotically expel Golgi-derived materials directly into the base of the IOL. Growth in *P. sapela* occurs by expansion at all points along the wall in a manner similar to that of some other, but not all, agglutinated monothalamous foraminiferans (Goldstein and Barker, 1990; Bowser and others, 1995; Goldstein and Richardson, 2002; Altin and others, 2009; Goldstein and others, 2010). The IOL extends into the aperture where it contains a higher proportion of electron-dense granules than in the main cell body and tapers toward the distal edge of the aperture (Figs. 3.5.5-3.5.6). Clay platelets are commonly found within the aperatural cytoplasm (Figs. 3.5.5-3.5.6).

Cell Body: Vegetative and Reproductive Individuals

Both vegetative and sexually reproductive individuals of *Psammophaga sapela* contain numerous vesicles of varying electron density that range from <1 μm to ~5 μm in size. The variations are a function of differential uptake of heavy metal stains, suggesting different biochemical compositions and thus function. In the vegetative state, vesicles are conspicuously

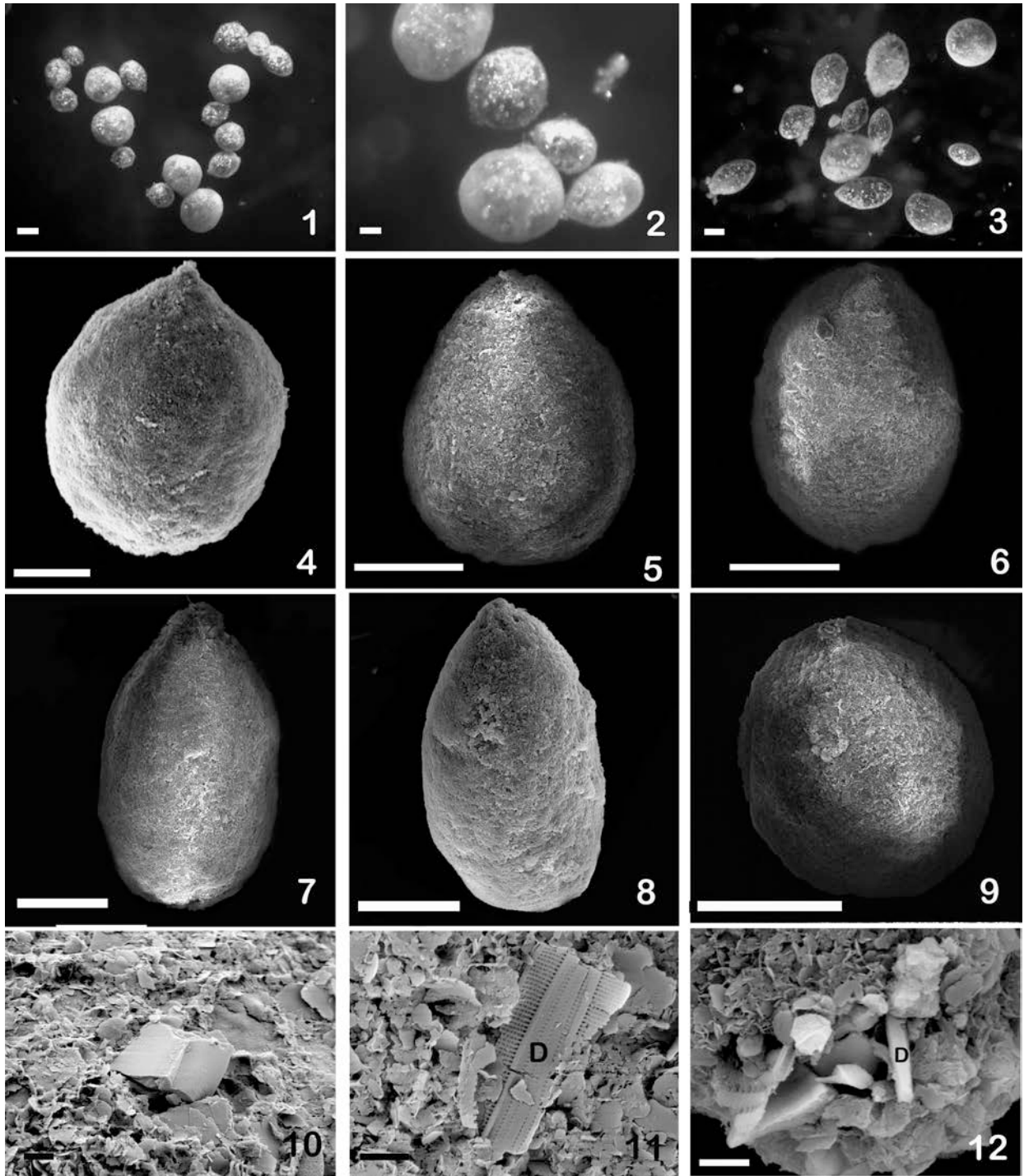


Figure 3.4 Gross morphology of *Psammophaga sapela*. 1–3 Light micrographs of living *Psammophaga sapela*, illustrating their pyriform to spherical shape, translucent cytoplasm and test, and cytoplasmic inclusions. Scale bars: 1, 3 = 50 μm ; 2 = 20 μm . 4–9 Scanning electron microscopic images (SEM) of complete test showing variations in overall shape. Scale bars = 100 μm . 10, 11 High magnification SEM images of agglutinated material. Test is composed primarily of loosely aggregated clay platelets interrupted by occasional diatom frustule fragments (D). Scale bars = 2 μm . 12 SEM image of apertural region with a diatom (D) inserted in aperture. Scale bar = 10 μm .

aligned directly beneath the plasma membrane (see above; Figs. 3.5.1–3.5.3). Additional vesicles also occur prominently just external to the nuclear membrane (Figs. 3.6.1-3.6.2)

Individuals examined in the vegetative stage contain a single, fairly large, spherical nucleus approximately ~20–40 μm in diameter (Figs. 3.6.1-3.6.6). Uninucleate individuals (Fig. 3.7.1) are presumably haploid gamonts or possibly representatives of the schizont stage. The nuclear membrane is surrounded by a layer (0.5 μm thick) of endoplasmic reticulum and a vesicular layer of varying electron density and of presumably different but unknown functions (Figs. 3.7.1-3.7.3). Like *P. simplora* the vegetative nucleus of *P. sapela* exhibits a thick, conspicuous cortical ring of chromatin (7 μm thick) and an interior of weakly staining nucleoplasm (Arnold, 1982; Fig. 3.6.1).

Any specimens of the new species in which the cytoplasm deviated from translucent and/or gray were regarded as potentially reproductive and observed closely. The ‘whitening’ of the cytoplasm corresponds to the purification from the purging of food and waste debris in the cell body in preparation for gametic differentiation (Jepps, 1942; Arnold, 1955; Goldstein and Moodley, 1993; Altin and others, 2009; Goldstein and others, 2010). Cytoplasmic inclusions become concentrated towards the central portion of the cell body, and large vacuoles form within the peripheral cytoplasm shortly after this whitening (Figs. 3.7.2-3.7.3).

At the fine structural level, the overall appearance of the cytoplasm of individuals in the early stages of gametogenesis (Figs. 3.6.4-3.6.5) differs significantly from that of the vegetative individuals. Vegetative cytoplasm is highly vesiculated, whereas reproductive individuals possess electron-translucent spheres surrounded by numerous mitochondria with typical tubular cristae (Figs. 3.6.4-3.6.5). These membrane-bound spheres appear to contain cytoplasmic groundmass lacking any food, wastes, organelles or vesicles with the exception of the numerous

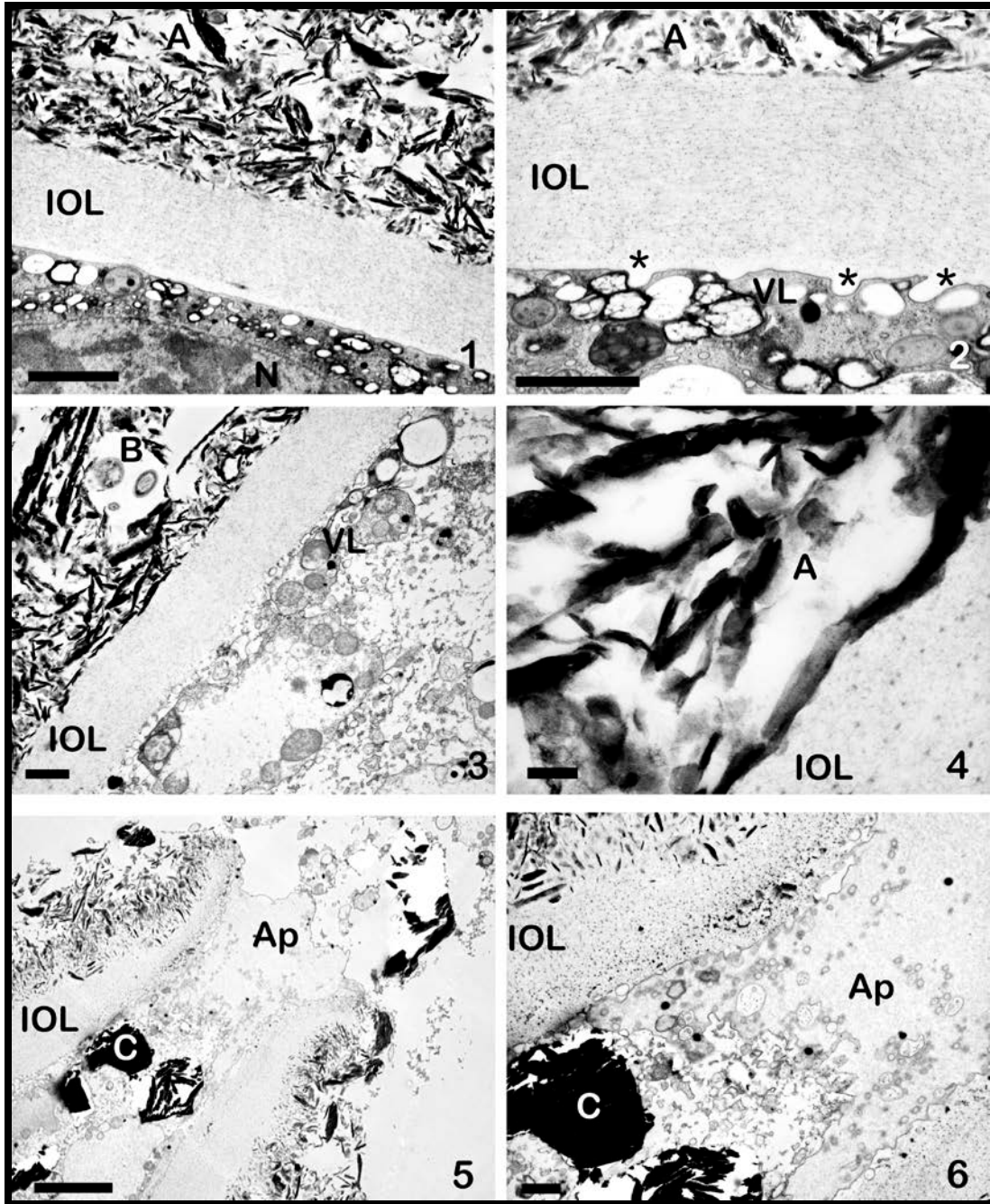


Figure 3.5 Wall ultrastructure of *Psammophaga sapela*. 1, 2 Transmission electron micrographs (TEM) showing cross-sectional views of the agglutinated layer (A), inner organic lining (IOL), and vesicular layer (VL). Agglutinated materials primarily of clay are unordered and loosely packed. The nucleus (N) may be in close proximity to the plasma membrane which is lined with vesicles that merge with the plasma membrane (asterisks). High pressure freeze substitution (HPFS) preparations; scale bars = 2 μm . 3 TEM showing bacterial colony (B) embedded in the organic matrix. Chemical preparation; scale bar = 2 μm . 4 Higher magnification TEM showing details of the agglutinated layer (A) and IOL, in particular the electron-dense granules and fibers among the electron-translucent matrix. Glutaraldehyde and osmium tetroxide fixation; scale bar = 0.1 μm . 5, 6 TEM views of the apertural region (Ap), IOL and ingested clay minerals (C). Apertural IOL contains a higher proportion of electron-dense granules than the remainder of the cell body. Glutaraldehyde and osmium tetroxide fixation, scale bars: 5 = 2 μm , 6 = 1 μm .

contiguous mitochondria. They most likely represent the earliest cytoplasmic differentiation stages of gametogenesis given the high energy demand indicated by the large number of mitochondria present.

Fine features of the reproductive nucleus differ dramatically from those of the vegetative state. The perinuclear vesicles common in the latter stage are noticeably absent in the earliest stages of gametogenesis (Figs. 3.6.4-3.6.6). Vegetative nuclear activity ceases at the onset of gametogenesis and thus the presence of the extranuclear ring of vesicles is biologically unnecessary. Nuclear chromatin does not accumulate directly beneath the nuclear membrane as it does in the non-reproductive gamont, but appears evenly dispersed throughout the nucleoplasm. (Fig. 3.6.4).

As in other monothalamous taxa, the cytoplasm begins to glisten and sparkle marking the onset of the “buzzing” stage, when complete gametic differentiation has occurred and gametes are actively swarming throughout the parental test (Goldstein and Moodley, 1993; Goldstein, 1997; Altin and others, 2009). Unlike the vegetative test, the parental test during the buzzing stage is significantly weaker and is easily crushed with a fine brush.

The gametes observed of *P. sapela* are biflagellated (Figs. 3.7.7-3.7.8), which is common in foraminiferal reproduction (Goldstein, 1997, 1999), and measure ~1.5µm diameter (excluding flagella). Individual gametes are either released from the parental test directly into surrounding seawater through the single aperture commonly between 10 and 20 min after the onset of the buzzing stage (Figs. 3.7.4-3.7.5) or collectively in several gametic ‘packets’ (30-40 µm diameter) each containing hundreds of gametes. These packets subsequently open, releasing gametes that actively swim away into seawater (Fig. 3.7.6). Following gamete release, the parental test contains residual cytoplasm, vacuoles and mineral inclusions. Asexual reproduction

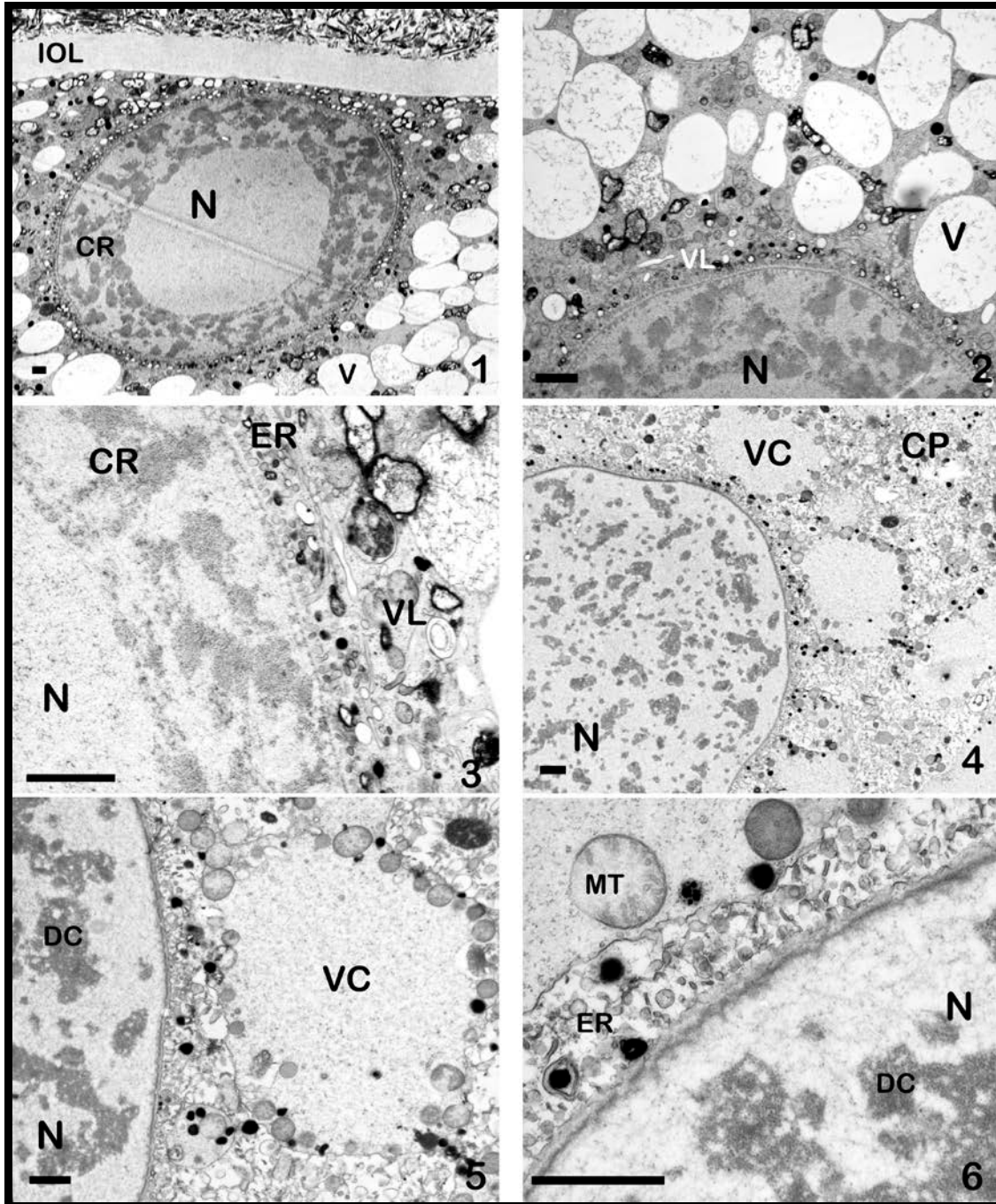


Figure 3.6 Nuclear ultrastructure of *Psammophaga sapela*. 1–3 Transmission electron micrographs (TEM) of a vegetative gamont showing inner organic lining (IOL) and nucleus (N). A distinct chromatin ring (CR) surrounds the periphery of nucleoplasm and in turn is overlain by individual layers of endoplasmic reticulum (ER) and vesicles (VL) of unknown function. Vegetative cytoplasm contains numerous and apparently empty, vacuoles (V). HPFS preparations; scale bars = 1 μm. 4–6 TEM micrographs of the Zerfall nucleus (N) and environs at its earliest stage of gametogenesis. The endoplasmic reticulum (ER) is present but the previously surrounding vesicular layer is absent. The chromatin is diffuse (DC) throughout the nucleus (N). The cytoplasm (CP) contains several vacuolated cytoplasmic (VC) packages heavily surrounded by mitochondria (MT). This local, energy-rich environment may represent the earliest morphological changes associated with gametogenesis. Glutaraldehyde and osmium tetroxide fixation; scale bars = 1 μm.

by budding (Fig. 3.7.9) was also observed and seems to be more common during the winter months. The aperture forms following separation from the parent.

Discussion

Historically, single-chambered foraminiferans have been considered primitive among foraminifera because of their generalized morphology, organic and/or agglutinated (non-mineralized) test (Loeblich and Tappan, 1987), or lack of test all together (Pawlowski and others, 1999a, 1999b). For example, external morphology is comparatively simple relative to their multichambered counterparts, resulting in a confusing taxonomic classification among monothalamous foraminifera (e.g., Pawlowski and others, 2002). Further, they are rare in the fossil record because their non-mineralized tests are prone to taphonomic degradation (Loeblich and Tappan, 1964). The presence of bacterial colonies within the bioadhesive (Fig. 3.4.3) is not uncommon in *Psammophaga sapela* and other monothalamous agglutinated taxa, and may accelerate post-mortem disintegration of the wall (e.g., Goldstein and Barker, 1990) resulting in an underrepresentation in the fossil record (Loeblich and Tappan, 1964). As with most agglutinated monothalamids, intact tests of dead *P. sapela* are seldom found in sediment samples despite the large number of living individuals.

As in *Psammophaga simplora*, *P. sapela* ingests numerous sand grains, which are much larger than the clay particles used for test construction. When retained, sediment in *P. sapela* is concentrated towards the center of the cell body during gametogenesis; however, in *P. simplora* ingested sediment grains are moved towards the periphery (Arnold, 1982). There could be several advantages for sediment ingestion in *Psammophaga* Arnold (1982). One possible function would be to add ballast and stability to the foraminiferan. For example, the Clade E foraminiferan *Psammophaga crystallifera* specifically distributes ingested sediments towards the

apertural end presumably to add weight to the individual so that it can stand upright on the sediment surface and aid in anchoring itself in soft mud (Dahlgren, 1962a). Only five members of Clade E, *P. simplora*, *P. sapela*, *P. crystallifera*, *Xiphophaga minuta* and *X. allominuta* demonstrate a marked avidity for the ingestion of either mineral particles from the surrounding environment or intact diatoms. The genus *Xiphophaga* ingests pennate diatoms for food but also possibly for chloroplast sequestration (Goldstein and others, 2010). Bacteria make up a large part of the diet of at least some foraminiferans (Lee, 1980; Langezaal and others, 2005), and the primary objective of sediment uptake is for feeding on the microbiota that adheres to sediment grains. The sand ingesting characteristic is not a synapomorphy for Clade E allogromiids because it is a feature absent in *Niveus flexilis* (Altin and others, 2009) though it may have been secondarily lost over time.

General morphology and fine structural features vary among Clade E species (Table 3.1). The agglutinated materials of some monothalamous species have been reported to vary in size, mineralogy, and position along the test (Cushman, 1948; Wood, 1949) yet test construction materials in *P. sapela* were composed primarily of clay, loosely packed, somewhat randomly arranged but homogeneous in size and composition. This predominance of clay platelets of fairly uniform size suggests selectivity in the process by which material is chosen for test construction. To date, all Clade E members examined via transmission electron microscopy (TEM), with the possible exception of *P. crystallifera*, adhere agglutinated materials within an organic matrix, presumably an acidic mucopolysaccharide (DeLaca, 1986; Goldstein and Barker, 1990; Langer, 1992; Bowser and Bernhard, 1993). The agglutinated layer in the wall of *N. flexilis* is meticulously layered, and clay platelets are arranged parallel to the surface of the IOL, whereas clay platelets are arranged more loosely in *P. sapela* and *X. minuta*. Further, the profoundly

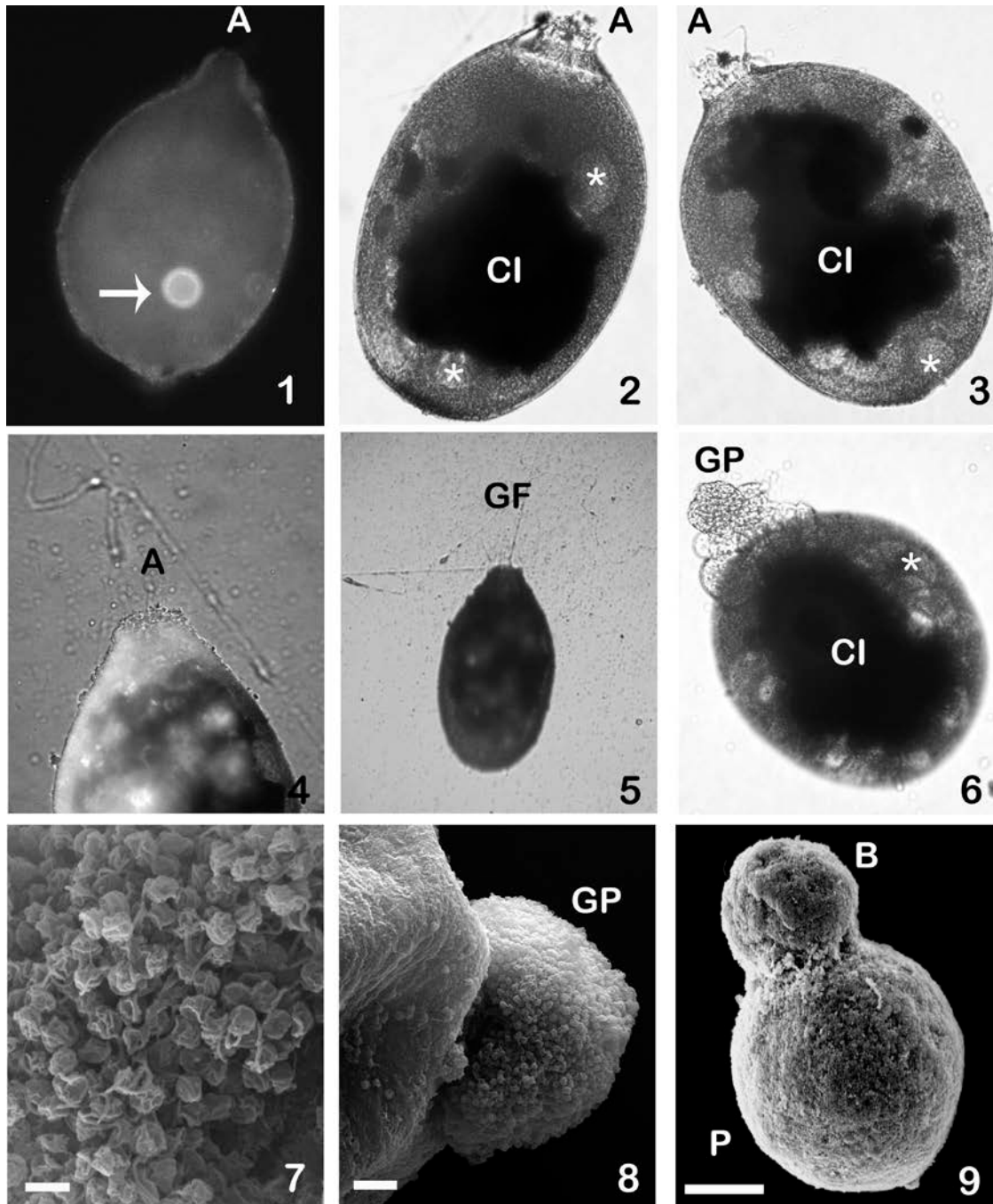


Figure 3.7 Reproduction in *Psammophaga sapela*. 1 Fluorescence micrograph of a uninucleate (arrow) gamontic individual. Note placement of aperture (A). Maximum diameter not more than 350 μm . 2, 3 Two living individuals just prior to gametogenesis, indicated by the presence of large vacuoles (asterisks) surrounding the central cell body where cytoplasmic inclusions (CI) of mineral grains are concentrated towards the center. 4 A living individual just prior to gametogenesis. Note few gametes are being released from the aperture (A). 5 Field of gametes (GF) released directly into surrounding seawater while maintaining pseudopodial network. No scale; maximum diameter not > 350 μm . 6 Gametes can also be compiled into packets (GP) which disaggregate after release into surrounding seawater via the aperture. Note peripheral vacuoles (asterisk) are present. Scale bar = 50 μm . 7, 8 Higher and lower SEM magnifications of gametes released as a packet (GP) from the aperture. Scale bars: 7 = 2 μm 8 = 10 μm . 9 SEM of asexually reproducing individual. Note parental test (P) and budding offspring (B). Scale bar = 50 μm .

crenulated agglutinated layer in *N. flexilis* is absent in *P. sapela* and *X. minuta* (see Goldstein and others, 2010).

Examination of the *P. sapela* wall ultrastructure revealed similarities with other monothalamous taxa including members of Clade E. The IOL is relatively thick, ranging from 2-5 μm (for comparison, see taxa evaluated by Goldstein and Richardson, 2002). In ultrathin section (TEM), the IOL does not take up heavy metal stains, with the exception of spherical electron-dense granules and fine fibers that predominantly run parallel to the cell surface. Other monothalamids that share a thick IOL characterized by electron-dense granules and fine fibers include *Xiphophaga* spp. *N. flexilis* and the Clade L *Cribrothalammina alba* Goldstein and Barker 1988 (Goldstein and Richardson, 2002). The IOL observed in *P. sapela*, however, is not as thick as *N. flexilis* and less fibrous than that of the Clade L taxa (i.e., IOL thickness is ~ 1.3 μm in *C. alba*, Goldstein and Richardson, 2002). In many monothalamous foraminiferans, distinct layers of vesicles that vary in electron density line the plasma membrane. Commonly, the vesicles merge with the plasma membrane, suggesting that enlargement of the test during cell growth occurs along the entire margin between the test and cell body (Goldstein and Richardson, 2002). Similar vesicles have been reported in the rhizarian *Gromia oviformis* Dujardin 1835 (Hedley and Bertaud, 1962; Hedley and Wakefield, 1969), which is a close relative of the foraminifera based on a variety of genetic markers (Archibald and others, 2003; Berney and Pawlowski, 2003; Longet and others, 2003, 2004; Nikolaev and others, 2004; Rothe and others, 2009; Burki and others, 2010). Avnimelech (1952), Dahlgren (1962a) and Loeblich and Tappan (1987) inferred that the wall and organic cement of agglutinated taxa are a function of cellular biochemistry and must be of major systematic importance.

Table 3.1 Comparison of fine structural characteristics of selected Clade E foraminiferans. The symbol N/A indicates information has not been reported at this time.

Species	<i>Psammophaga crystallifera</i>	<i>Niveus flexilis</i>	<i>Psammophaga simplora</i>	<i>Psammophaga sapela</i>	<i>Xiphophaga minuta</i> , <i>X. allominuta</i>
Citation	Dahlgren (1962a)	Altin and others (2009)	Arnold (1982)	This Report	Goldstein and others (2010)
Overall Shape	ellipsoidal	ovate	pyriform to lachrymiform; spherical to sausage-like	pyriform to spherical or elongate	ovate to spherical
Size	500–700 μm	~300 μm	250–350 μm	100–550 μm	150–250 μm
Aperture Number and Ornamentation	Single, unadorned, may have apertural tube	Single, unadorned collar	Single, unadorned, occasional short neck	Single, unadorned	Single, unadorned neck
Cytoplasm Color	White, pale pink	white	translucent, gray, milky white	translucent, gray, milky white	colorless to golden brown due to diatom ingestion
Agglutinated Layer Composition and Thickness	“very thin”	clay and occasional diatom frustule fragments, 0.5 μm	Clay, “wall” reported as 6–10 μm , may include IOL	clay, occasional diatom frustule fragments and infrequent minerals, 10–15 μm	clay and occasional diatom frustule fragments, 7–9 μm
Inner Organic Lining	Direct contact with plasma membrane, “Thicker than outer layer” TEM N/A	Direct contact with plasma membrane, 3–8- μm thick, Electron-dense granules and fibers present	Direct contact with plasma membrane, Complete wall thickness reported as 6–10 μm TEM N/A	Direct contact with plasma membrane, 2–5- μm thick, electron-dense granules and fibers present	Direct contact with plasma membrane, 1- μm thick, electron-dense granules and fibers present
Vesicles Below Plasma Membrane	N/A	Completely released into IOL	N/A	Merge with plasma membrane and release contents into IOL	Merge with plasma membrane and release contents into IOL
Cytoplasmic Inclusions	Minerals situated within apertural cytoplasm only	Not present	Minerals concentrated near aperture, concentrate around periphery during gametogenesis	Minerals throughout, remain throughout cell body during gametogenesis.	Pennate diatoms throughout, some egested during gametogenesis.

Gamontic Nucleus and Diameter	Chromatin arranged in cortical ring	Chromatin evenly dispersed throughout nucleoplasm, 10 μm	Chromatin arranged in cortical ring, 8–10 μm	Chromatin arranged in cortical ring, 20–30 μm	Chromatin around periphery but not in ring, located near abapertural end, 15–22 μm
Perinuclear Endoplasmic Reticulum Layer	N/A	Present	N/A	Present	Present
Perinuclear Vesicular Layer	N/A	Present	N/A	Present	Present
Reproduction and Gamete Diameter	Transverse division only reported	Gametogamous, biflagellated gametes ~2 μm , Asexual reproduction also reported	Gametogamous, amoeboidal gametes 5–6 μm	Gametogamous, biflagellated gametes ~1.5 μm , Gamete packets ~40–50 μm released through aperture also reported, Asexual reproduction by budding.	Gametogamous, biflagellated gametes 1.5–2 μm

The vegetative cells examined in *P. sapela* contain a single, large nucleus, ~20–40 μm in diameter, and the nucleoplasm just beneath the nuclear membrane contains a thick cortical layer of chromatin (Figs. 3.6.1–3.3.3). This same cortical layer is also present in *P. simplora*, *Allogromia laticollaris* Arnold 1955 and *P. crystallifera*, whereas chromatin is evenly displaced in *N. flexilis* and randomly packaged in *Xiphophaga* spp. Perinuclear chromatin has also been reported in genetically distinct, non-Clade E allogromiids, including *Ovammina opaca* Dahlgren 1962b (Dahlgren, 1964) and *Saccammina alba* Hedley 1962 (Goldstein 1988). It is not yet known if the distribution of chromatin (also reported as basophilic granules see Dahlgren, 1962a and Arnold, 1982) is of phylogenetic significance or if it represents normal nuclear morphology. Vesicles that surround the nuclear membrane have been reported in other Clade E taxa (see *N. flexilis* of Altin and others, 2009 and *Xiphophaga* spp. of Goldstein and others, 2010) but is also

found in other monothalamous taxa, such as *Myxotheca* sp. of Schaudinn (1893) reported in Goldstein and Richardson (2002), *C. alba* (Goldstein and Barker, 1988; Goldstein and Richardson, 2002), and *Shepherdella taeniformis* Hedley and others 1967, which are genetically distinct and do not appear related to Clade E taxa (Pawlowski and others, 2002). In addition to the peri-nuclear vesicular ring, a layer of endoplasmic reticulum is also commonly found surrounding the nucleus of *P. sapela* presumed to be at the earliest stages of gametogenesis (Figs. 3.6.4-3.6.6), has a different fine morphology than those in the vegetative state. The surrounding endoplasmic reticulum and vesicular layers are conspicuously absent, possibly denoting a cessation of vegetative biological function and instead of being assembled as a cortical ring, the nuclear chromatin is evenly dispersed throughout the nucleoplasm. This individual most likely represents the early stages of “Zerfall” as first described by Føyn (1936) that marks the onset of gametogenesis.

Given the numerical abundance of extant foraminiferal taxa, complete reproductive life cycles are known for relatively few (see Goldstein, 1999). This may reflect the need for numerous specimens observed over long periods of time and the difficulties involved in culturing foraminifera. Interestingly, similar cytological themes on reproduction span many foraminiferal orders despite their early divergence and long evolutionary history (Goldstein, 1997). Some reproductive features shared by Clade E allogromiids (Altin and others, 2009; Goldstein and others, 2010)— for example, the formation of large cytoplasmic vacuoles prior to gametogenesis, the ‘buzzing stage’ (e.g., Goldstein and Moodley, 1993) whereby gametes swarming within the parental test and the direct release of gametes via the aperture during gametogamy—are also features of sexual reproduction in many foraminiferal orders (Meyers, 1940; Grell, 1967, 1973; Goldstein, 1997). Similarly, the release of biflagellated gametes directly

into surrounding seawater is a method that crosses phylogenetic boundaries indicating that it is a conserved characteristic (Goldstein, 1997).

Acknowledgments

We thank Mark Farmer for utilization of equipment and lab space for the molecular portion of this project; Sam Bowser for assistance; Elizabeth Richardson, Mary Ard and John Shields for their advisement on electron microscopic techniques; Jan Pawlowski for sharing his Clade E alignment; and Paul Schroeder for identifying the minerals ingested by *P. sapela* using XRD. The thoughtful recommendations of S. S. Bowser, J. Pawlowski and one anonymous reviewer significantly improved this manuscript. This research was funded in part by National Science Foundation grants DEB0445181 to S. S. Bowser and S. T. Goldstein, and OCE0850505 to STG; and by graduate research awards to D. Z. Altin-Ballero including the Loeblich and Tappan Award (Cushman Foundation for Foraminiferal Research), Lerner-Gray Award (American Museum of Natural History), Rodney M. Feldmann Award (Paleontological Society), Student Research Award (Geological Society of America), Levy Award for Marine Geology and Watts-Wheeler Grants-In-Aid (UGA Geology Department) and the Friends the of University of Georgia Marine Institute Award. This is contribution number 995 of the University of Georgia Marine Institute, Sapelo Island, Georgia.

CHAPTER 4

TESTING THE FIDELITY OF SSU BASED PHYLOGENIES IN SELECTED
MONOTHALAMID FORAMINIFERA: COUPLING MULTI-GENE PHYLOGENETICS
WITH ULTRASTRUCTURE³

³ Ballero, D.Z.A., Habura, A. and Goldstein, S.T., To be submitted to Journal of Eukaryotic Microbiology.

Abstract

Of the thirteen molecular lineages of monothalamous (predominantly single chambered, non-mineralized) foraminifera, Clade E is of great interest because although members are retained loosely by SSU rDNA based phylogenies, they lack similarities in their gross morphology. Bayesian and maximum likelihood analyses of the small subunit of the ribosomal DNA gene (SSU rDNA), aligned using secondary structure predictions alone and with concatenated actin and β -tubulin genes were performed to test membership of selected monothalamids within Clade E. Gross morphology of the test and ultrastructural features of the wall were evaluated and compared with phylogenetic trees.

Both SSU rDNA and multi-gene analyses return a monophyletic 'core' Clade E grouping composed of *Psammophaga* spp., *Xiphophaga* spp. and *Vellaria* spp. Both Bayesian and maximum likelihood analyses return an expanded group that included previously reported Clade E taxa (*Niveus flexilis*, *Nellya rugosa*) among others, however, this group had posterior probabilities and bootstrap support. Most of the orphaned taxa excluded from Clade E continue to show nebulous phylogenetic affinities among the monothalamids but they appear to have close relations to Clade E than to other clades.

Despite the loose molecular affinities for the taxa evaluated in this study, there is a consistency with respect to the fine structure of the wall. All possessed an electron transparent inner organic lining (IOL) with electron-dense granules and fibers that separates the agglutinated layer from the plasma membrane of the cell body. Similar fine structural themes among the orphaned taxa along with Clade E members suggests they are related in some capacity. Mineralogy, packing and thickness of the agglutinated layer, thickness of the IOL and cytological features (plasma membrane and environs, presence of stercomata or cytoplasmic

inclusions) varies among the taxa evaluated in this study. Clay is a common mineral in agglutinated monothalamids examined here but some species can incorporate additional minerals of different chemical composition and of much larger size. Overall gross morphology and mineralogy of the test are not taxonomically significant characteristics because there are no obvious trends observed, even within the ‘core’ Clade E taxa. Our findings suggest that taxon sampling must be increased to resolve the phylogenetic trees based on molecular data sets and resolve any potential morphological evolutionary trends. Ultrastructure of the wall may be an invaluable tool for revealing the evolutionary history of monothalamous foraminifera but the available data remain limited. This study offers robust ultrastructural data for several new, undescribed species and doubles the current available actin and β -tubulin sequences for monothalamous foraminifera.

Introduction

Monothalamous foraminifera represent a seemingly inconspicuous taxonomic group because of their limited fossil occurrences and apparent morphological simplicity. Overall, the gross morphology of monothalamids differs from that of the better known polythalamous taxa in that most possess a single chambered test made of organic material and/or agglutinated material with an organic bioadhesive (Loeblich and Tappan, 1987) or lack a test all together (Pawlowski and others, 1999a, 1999b). The tests of these foraminiferans are also fragile and commonly disintegrate rapidly following death and reproduction (Goldstein and Barker, 1988; Altin and others, 2009; Altin-Ballero and others, 2013) as evidenced by their absence in most foraminiferal death assemblages. A limited fossil record combined with little gross morphological variation makes evolutionary reconstructions of monothalamids much more difficult than their multi-chambered counterparts (Pawlowski and others, 2013). Aspects of the gross morphology of the

polythalamous foraminifera, such as chamber arrangement, chamber shape, umbilical ornamentation and mineralogy of the test for example, coupled with a highly detailed fossil record, make them a useful stratigraphic tool and taxonomic classification relatively easy. Phylogenetic analyses of the small subunit of the ribosome (SSU rDNA) from modern monothalamids estimate the divergence of foraminifera from their ancestor in the Proterozoic Eon between 1150 million years ago to 650 (Pawłowski and others, 2003). Extant taxa therefore represent living clues to help answer biological, ecological and evolutionary questions in the present as well as in deep time.

Researchers have utilized DNA sequence evidence to delineate thirteen genetic clades of monothalamous foraminifera, many of which unite members that do not share a common morphological theme (Pawłowski and others, 2002). Membership in Clade E, the focus of this study, initially consisted of four members of the ‘sand-ingesting’ genus *Psammophaga* (Pawłowski and others, 2002). Subsequent phylogenetic studies incorporating larger taxon sampling broadened potential membership in this clade. Several undescribed taxa including the “Rod and Gun White Allo” (subsequently described as *Niveus flexilis*, Altin and others, 2009), and as yet undescribed species known as “Duplin quartzball”, “Timber dock black and white”, “#5 Cigar”, “Chocolate silver saccamminid”, “*Micrometula*-like and the Fusiform” were identified as potential Clade E members because they tended to cluster with psammophagids in SSU rDNA trees (Habura and others, 2008). More recently, membership in this proposed clade has grown to include *Nellya rugosa* (Gooday and others, 2011), *Vellaria* spp. (Gooday and Fernando, 1992; Sabbatini and others, 2004), *P. sapela* (Altin-Ballero and others, 2013) and *Xiphophaga* spp. (Goldstein and others, 2010). Of the currently accepted Clade E taxa, only *Psammophaga* spp. and *Xiphophaga* spp. exhibit a ‘psammophagous’ behavior of consuming

siliceous particles (sand and diatoms, respectively). Therefore sand ingestion alone can no longer be considered a shared-derived characteristic of the group. Although these taxa may have molecular affinities based on SSU rDNA analysis, the overall gross morphology of these taxa does not support their relationship. In this study, we investigated whether clues to evolutionary history may be found in the ultrastructural architecture of the wall and test (e.g., Hedley and others, 1972; Bowser and others, 1995, 2002; Goldstein and Richardson, 2002).

Phylogenetic studies on monothalamids explore their diversity (Habura and others, 2008; Pawlowski and others, 2008; LeCrocq and others, 2011), evolutionary history (Pawlowski and others, 2002, 2003) and center on new species descriptions (Meisterfield and others, 2001; Gooday and Pawlowski, 2004; Sabbatini and others, 2004; Sinnigar and Pawlowski, 2008; Cedhagen and others, 2009; Gooday and others, 2010, 2011; Pawlowski and Majewski, 2011; Altin-Ballero and others, 2013; Apothéloz-Perret-Gentil and others, 2013). However, these studies were performed using a single gene, the SSU rDNA. Increasing the number of genes in a phylogenetic analysis can decrease potential stochastic error resulting from data involving single genes (Swofford and others, 1996). Multiple gene-based analyses have primarily been used to establish the phylogenetic position of foraminifera among all eukaryotes (Takishita and others, 2005; Burki and Pawlowski, 2006; Moreira and others, 2007; Burki and others, 2008; Parfrey and others, 2010) and in assessing the phylogenetic position of a species within foraminifera (Habura and others, 2006) but have not been applied to evaluating clade-level phylogenetics in monothalamids. This work attempts to improve phylogenetic resolution of potential members of Clade E monothalamous foraminifer through a multi-gene analysis by concatenating two protein-coding genes (actin, β -tubulin) with the SSU rDNA gene. Ultrastructural observations on the

test and wall of several potential Clade E taxa are also examined and compared with molecular findings to show that wall features may correlate with phylogenetic findings.

Materials and Methods

Sample Collection and Culturing

Foraminifera used in this study were collected from several sites in the Sapelo Island, Georgia, USA, region bound by 31°33'N 31°21'N and 80°24'W 81°13'W. Sampling locations include a low-salinity salt marsh (~10–22 ‰) at the Rod and Gun Marina near Darien, a hypo-saline mudflat site (~6 ‰) along the North River, a historical site on Sapelo locally known as “Chocolate,” mudflats near the Sapelo lighthouse and tidal creeks of Cabretta Island (Fig. 4.1). Salinity overall at these Sapelo sites may range > 30 ‰ depending on season and rainfall. Surface sediment collection and processing followed that of Goldstein and Richardson (2002) and Habura and others (2008). For light microscopic observations, selected individuals were placed in plastic culture dishes with Instant Ocean adjusted to ambient salinity and appropriate live food organisms (*Dunaliella*, *Amphiphora*, *Isochrysis*) and photographed using either transmitted or reflected light.

Microscopy

Vegetative and reproductive foraminifera were prepared for transmission electron microscopy (TEM) using either high-pressure freezing and freeze substitution (HPF/FS) or chemical fixation methods following protocols reported previously (Goldstein and Richardson, 2002; Altin and others, 2009, 2013). All TEM preparations were examined after embedment using a light microscope, and well-fixed cells were removed with a jeweler's saw and mounted on acrylic blocks with glue (Quickbond). Blocks containing selected specimens were trimmed, then sectioned (80–90 nm thickness) using a Reichert-Jung Ultracut E microtome and a diamond

knife. Thin sections were placed on Formvar-coated slot grids, dried overnight, post-stained for three minutes each with uranyl acetate and lead citrate, and viewed on a Zeiss EM 902A operated at 80 kV or a JEOL JEM1210 at 120 kV.

Living individuals prepared for SEM followed the chemical TEM fixation protocols. As an alternative to critical-point drying for dehydration, specimens were chemically dried with hexamethyldisilazane (HMDS) (see Altin and others, 2009). Specimens were sputter coated with gold (15.3 nm) and viewed on a JEOL JSM-5800 operated at 15-20 kv. In some cases, however, the use of HMDS produced dehydration artifacts and SEM was repeated using standard critical-point drying methods (e.g., Bozzola and Russell, 1998).

Sample Preparation for Molecular and Phylogenetic Analysis

Approximately 20 individuals were placed in a culture dish with sterile Instant Ocean for 24 hrs allowing the foraminifera to complete digestion of food and purge digestive wastes. Individuals were thoroughly cleaned with a fine artist's brush in a series of six sterile Instant Ocean washes to remove any obvious epibionts or other potential external contaminants. Cells were stored in RNALater (Ambion), and genomic DNA was extracted using the DNeasy Plant Mini Kit (Qiagen, Valencia, California). Successful amplification of three target genes, the 3' region (Domain III) of the SSU rDNA was amplified by nested PCR primers (S14F3A, B, S14F1, S20R; Pawlowski, 2000), actin type I (Act73D, ActN2, ActF1, 1024R, 1350_R, 1354R, 1354rCe; Flakowski and others, 2005) and B-tubulin (BTub1F, BTub2F, BTub1R; Habura and others, 2005). PCR amplifications were performed on a Techne Genius thermocycler using ExTaq premix (TaKaRa) with cycle parameters as previously reported (Habura and others, 2004, 2005; Flakowski and others, 2005). PCR products were analyzed by agarose gel electrophoresis, cloned in pGEM-T Easy vectors (Promega, Madison, WI) and replicated in JM104 *Escherichia*

coli cells. Cloned inserts were extracted and purified with the SpinPrep mini kit (Qiagen, Valencia, CA) and four to six clones were sequenced in both directions (Geneway Research, Hayward, California) using M13 forward and reverse primers. Actin, β -tubulin and SSU rDNA sequences that were not amplified in this study were obtained from GenBank (National Institute of Health).

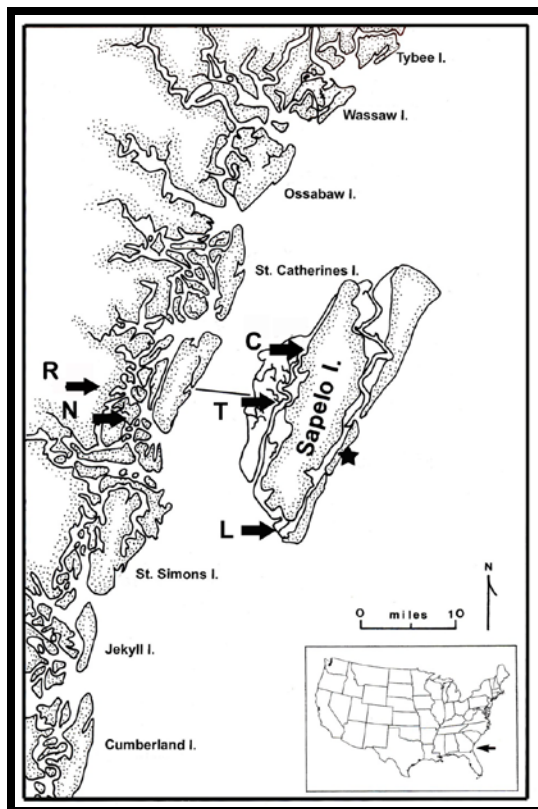


Figure 4.1 Approximate geographic sampling locations. Approximate geographic locations of the sampling sites (arrows) along the salt marshes and mudflats adjacent to the Rod and Gun Marina (R) near Darien, Georgia (31°24'22"N, 81°23'36"W), Chocolate (C) Beach (31°30'21"N, 81°15'25"W), the Sapelo lighthouse (31°23'23"N, 81°17'10"W), North River (N) site (31°23'34"N, 81°24'07"W), Timber Dock (T) site (31°27'35"N, 81°16'40"W) and tidal creeks of Cabretta Island (31°26'20"N, 81°14'15"W, Sapelo Island, Georgia. Insert map at lower right shows position of Sapelo Island (arrow) within contiguous United States.

All sequences were first tested using the BLAST (<http://blast.ncbi.nlm.nih.gov/Blast.cgi>) database to verify that the obtained sequences were full length and of foraminiferal origin. PCR amplification using previously reported actin primers (Flakowski and others, 2005) yielded sequence from two actin paralogs (type I and type II) as well as various actin deviating proteins

of various sizes. Actin and tubulin sequences retained for analysis contained the 5' and 3' primer binding sites and were of equivalent size to previously published foraminiferal sequences. Protein sequences were manually aligned with previously published sequences obtained from GenBank using Geneious 4.5.5 (Drummond and others, 2010). Translation residues were used simultaneously as a guide to align protein nucleotides across all available actin and β -tubulin sequences. All SSU rDNA sequences were also initially aligned manually using Geneious 4.5.5 (Drummond and others, 2010) and compared with a curated alignment provided by Jan Pawlowski. All five divergent regions were evaluated for secondary structure using the online servers MFOLD <http://mfold.rna.albany.edu/?q=mfold> (Zuker, 2003) and PFOLD <http://www.daimi.au.dk/~compbio/pfold/> (Knudsen and Hein, 1999, 2003). Folding temperatures were set at 25°C and pairings were not forced for all regions except region III. This region of the SSU rDNA gene is structurally complex containing several stem-loop structures which required constraining a short (4 nucleotides) segment at the base of helix 43 (Habura and others, 2004). Folding predictions were examined for structural similarities (folds, loops) and complimentary base pairing. Sections structurally inconsistent across all Clade E taxa were presumed to be homoplasy and eliminated from further analysis. One representative clone of SSU rDNA was concatenated to actin and β -tubulin consensus sequences for the multi-gene analysis. Protein sequences that could not be successfully amplified were marked as missing data. Actin and β -tubulin sequences for several taxa and SSU rDNA clones for 'Fruitcake' have been deposited in GenBank under accession numbers listed in Table 4.1.

A total of 2468 unambiguously aligned positions, including 756 from SSU rDNA, 725 from actin type 1 and 987 from β -tubulin were analyzed in the multi-gene phylogeny. The Clade E SSU rDNA alignment was combined with the non-Clade E alignment generously provided by

Dr. Jan Pawlowski (University of Geneva). Alignments for both the multi-gene and SSU rDNA trees were analyzed by Bayesian statistics using Mr. Bayes, version 3.1 (Huelsenbeck and Ronquist, 2001) under the GTR + I + G evolutionary model, run with two sets of four chains using the random tree option for a minimum of two million generations. Trees were sampled every thousand generations with the first 50% (multi-gene tree) or 25% (SSU rDNA tree) of the sampled trees discarded as burn-in. Remaining trees were used to generate a consensus tree which was edited with TreeView 1.6.6 (Page, 1996) and MEGA version 5.1 (Tamura and others, 2011). Maximum likelihood analyses were conducted on the SSU rDNA and multi-gene alignments using MEGA 5.1 (Tamura and others, 2011) under the general time reversible (GTR) model with uniform rates of substitution among sites. Tree reliabilities were estimated using 1000 bootstrap replicates.

Table 4.1 GenBank accession numbers for protein SSU rDNA, actin and β -tubulin sequences obtained in this study. Genomic DNA from the following Clade E taxa was not obtained: *Vellaria zucchellii*, *Vellaria pellucidus*, *Nellya rugosa*, and *Psammophaga magnetica*.

Taxon	SSU rDNA	Actin Type 1 DNA/AA	β -Tubulin DNA/AA
<i>Niveus flexilis</i>	KF841623-KF841626	KF728642-KF728646	KF728617-KF728619
<i>Psammophaga sapela</i>	Previous	KF728647-KF728648	KF728620-KF728625
'Fruitcake'	KF706684-KF706689	KF728649-KF728652	KF728626-KF728630
'Fusiform'	Previous	KF728636-KF728641	KF728612-KF728616
'Chocolate silver saccamminid'	Previous	KF728631-KF728635	KF728609-KF728611
<i>Xiphophaga minuta</i>	Previous	Not amplified.	Not amplified.
'Timber dock black and white'	Previous	Not amplified.	Not amplified.
' <i>Micrometula</i> -like'	Previous	Not amplified.	Not amplified.
'#5 Cigar'	Previous	Not amplified.	KF728604-KF728608

Results: Phylogenetic Trees

Selection of Clade E taxa and aligning the SSU rDNA.

The monothalamids selected for this study include taxa that were previously described as having membership in Clade E such as *Nellya rugosa* (Gooday and others, 2010), *Psammophaga magnetica* (Pawlowski and Majewski, 2011), *P. sapela* (Altin-Ballero and others, 2013), *Vellaria zucchellii* (Sabbatini and others, 2004), *Xiphophaga minuta* and *X. allominuta* (Goldstein and others, 2010) and *Niveus flexilis* (formerly reported as the “Rod and Gun White Allo”, Habura and others, 2008). Some taxa however, appeared to have molecular affinity to Clade E (“*Micrometula*-like”, “Chocolate silver saccamminid”, “Duplin quartzball”, “Fusiform”, “Fruitcake”, “Timber dock black and white”, “#5 Cigar”) but membership was nebulous (Habura and others, 2008).

As in all other organisms, the SSU rDNA gene in foraminifera contains rapidly evolving, divergent regions some of which can be used to evaluate phylogenetic questions at the ‘clade’ level (Pawlowski, 2000; Bowser and others, 2006). The sequences were first aligned using the conserved sections followed by a manual alignment of five divergent regions (I-V). As expected, the majority of these regions could be manually aligned in different species of the same genus however this became more difficult when making suprageneric comparisons. Foraminiferal ribosomal genes are littered with large variable insertions, most of which cannot be compared across clades (Bowser and others, 2006). For example, the “Timber dock black and white” monothalamid has significantly shorter divergent sections that were disproportionately A-T rich compared to other members of the proposed group. Others such as “Fruitcake” and *Niveus flexilis* have very large insertions (in regions 2 and 4 respectively) compared to other taxa evaluated in this study. Sequence divergences in the variable regions among the taxa evaluated

in this study were so great that in order to improve the SSU alignment, secondary structure predictions were conducted. Structural folding predictions were not useful to align regions III and IV as wildly different patterns were returned for even closely related taxa. In region III, forced pairing was assigned to evolutionarily conserved sections as previously reported (Habura and others 2004) but this did not return structurally sound folding predictions for comparison. Of the divergent sections of SSU rDNA used in this study, it was possible to align the majority of region V across all taxa which appears to be phylogenetically significant for evaluating clade-level phylogenetics. The difficulty in aligning the variable regions, especially the distal region of helix 39 (Bowser and others, 2006) for some proposed members of this group supports their exclusion from Clade E.

SSU rDNA based phylogenies.

The SSU rDNA phylogenetic analysis returned a reliable, strongly supported (posterior probability (PP) = 0.96) ‘core’ set of taxa that compose Clade E consistent with other researchers (Habura and others, 2008; Gooday and others, 2010; Pawlowski and Majewski, 2011) (Fig. 4.2). It also places *Nellya rugosa*, *Niveus flexilis*, and the undescribed “#5 Cigar”, “*Micrometula*-like” and “Chocolate silver saccamminid” as an extension of Clade E but this grouping was weakly supported (PP= 70; maximum likelihood bootstrap support not shown (BS) = 52). The “Duplin quartzball”, “Fruitcake” and “Timber dock black and white” monothalamids form a polytomy with the aforementioned grouping and Clade D. A similar topology was recovered when select monothalamid clades were eliminated from the analysis (Fig. 4.3.A). Selective removal of Clade F (not shown) produces a tree of similar topology and support as a tree created with the removal of Clade M (Fig. 4.3.A). In all these trees, including those produced by maximum likelihood analysis, the SSU rDNA phylogenies always retained certain sister relationships: *Nellya rugosa*

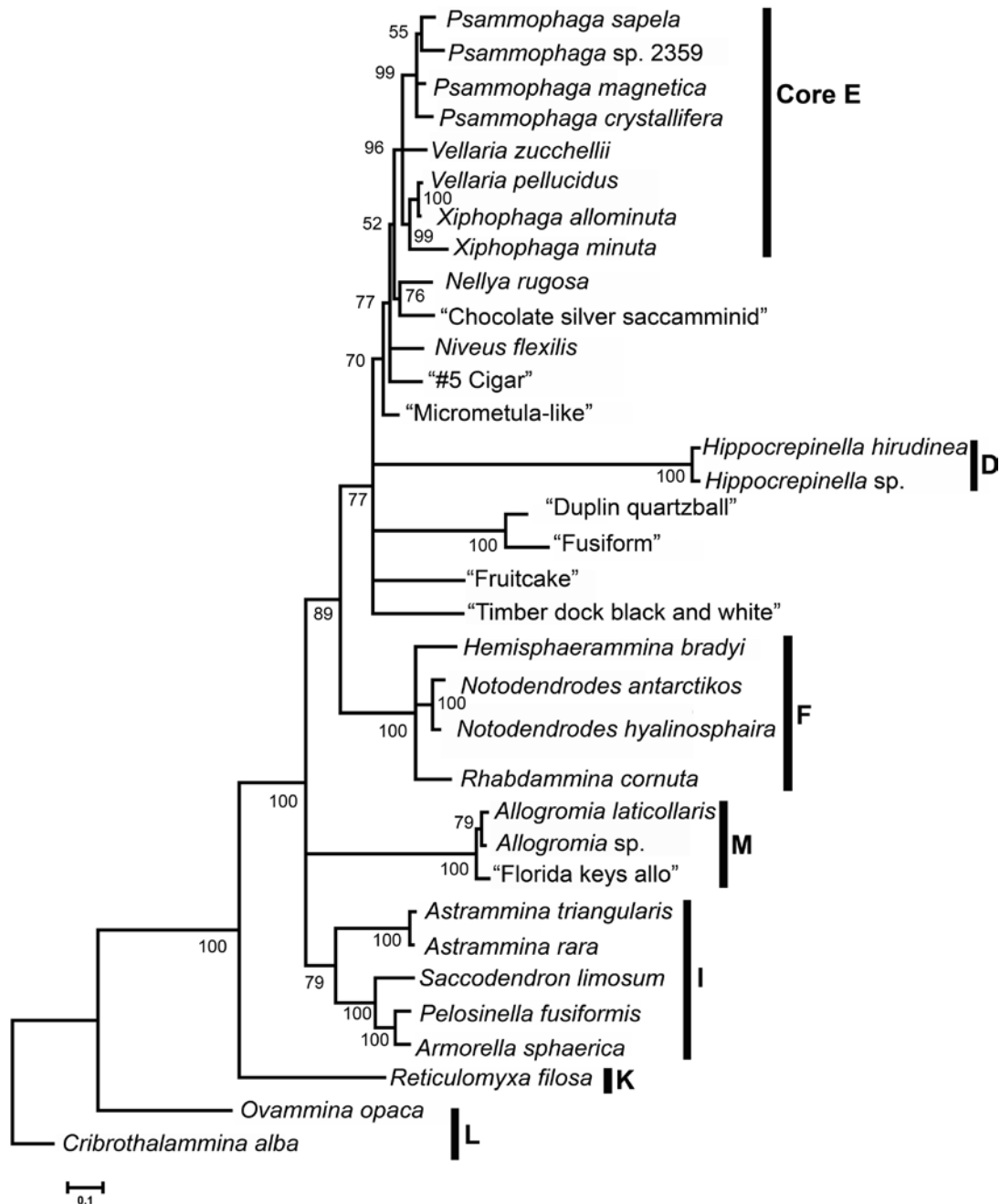


Figure 4.2 Phylogenetic tree of selected groups of monothalamids based on SSU rDNA only. Bayesian analysis is based on 756 unambiguously aligned positions of the SSU rDNA gene with *Cribrorhammina alba* (Clade L) as the outgroup. Posterior probabilities x100 are indicated at the nodes. Results return a set of 'core' Clade E membership including *Xiphophaga* spp., *Vellaria* spp., and *Psammophaga* spp. Potential Clade E members include *Nellya rugosa*, *Niveus flexilis*, the "Chocolate silver saccamminid", "#5 Cigar" and "Micrometula-like". The SSU rDNA tree excludes the "Duplin quartzball", "Fusiform", "Fruitcake" and "Timber dock black and white" from Clade E.

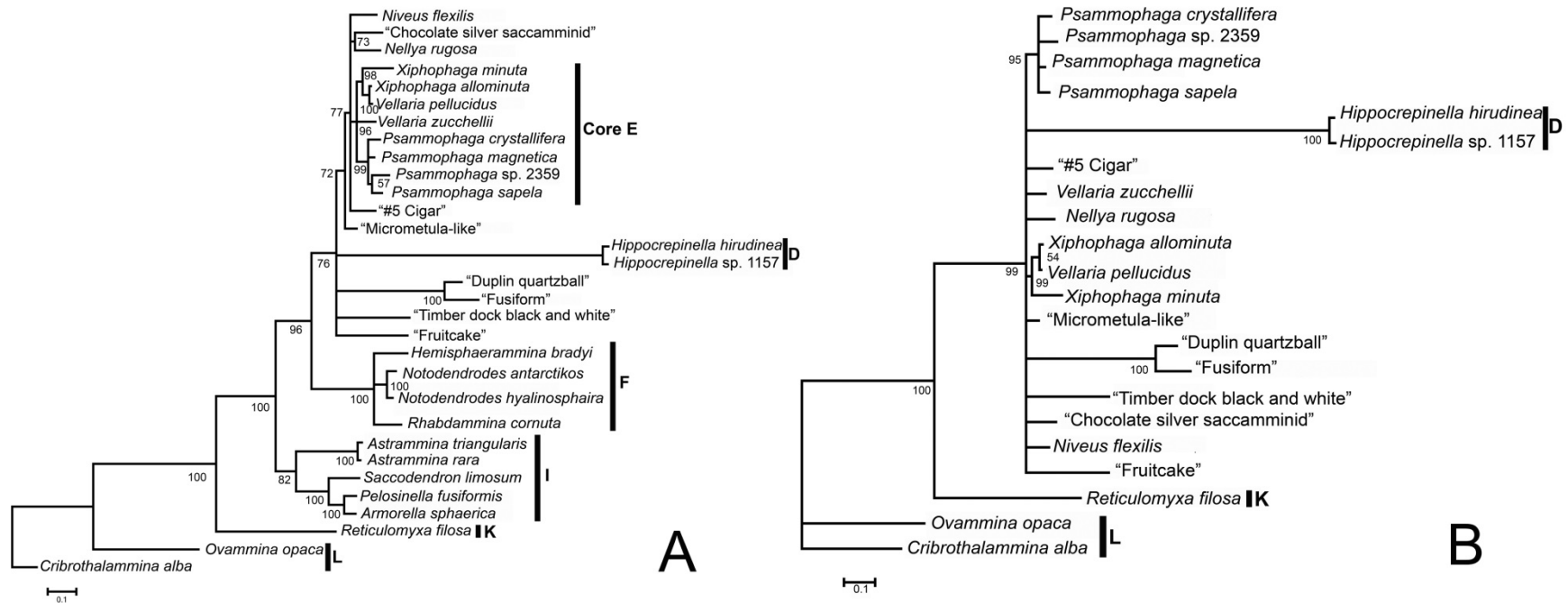


Figure 4.3 Bayesian analysis of "Clade E" monothalamids with selective clade removal. Phylogenetic trees were created from the exact alignment shown in Fig. 4.2 with the removal of Clade M (tree A) and Clades I, M and F (tree B), both with *Cribrothalammina alba* (Clade L) as the outgroup. Removal of Clade M (tree A) results in a similar topology and Bayesian posterior probabilities as the phylogeny shown in Fig. 4.2. Phylogenetic relationships between core and auxiliary Clade E taxa cannot be determined when multiple clades (I, M and F) are eliminated from the analysis (tree B). These results show that taxon sampling greatly influences phylogenetic relationships of monothalamids at the 'Clade' level when using the SSU rDNA gene.

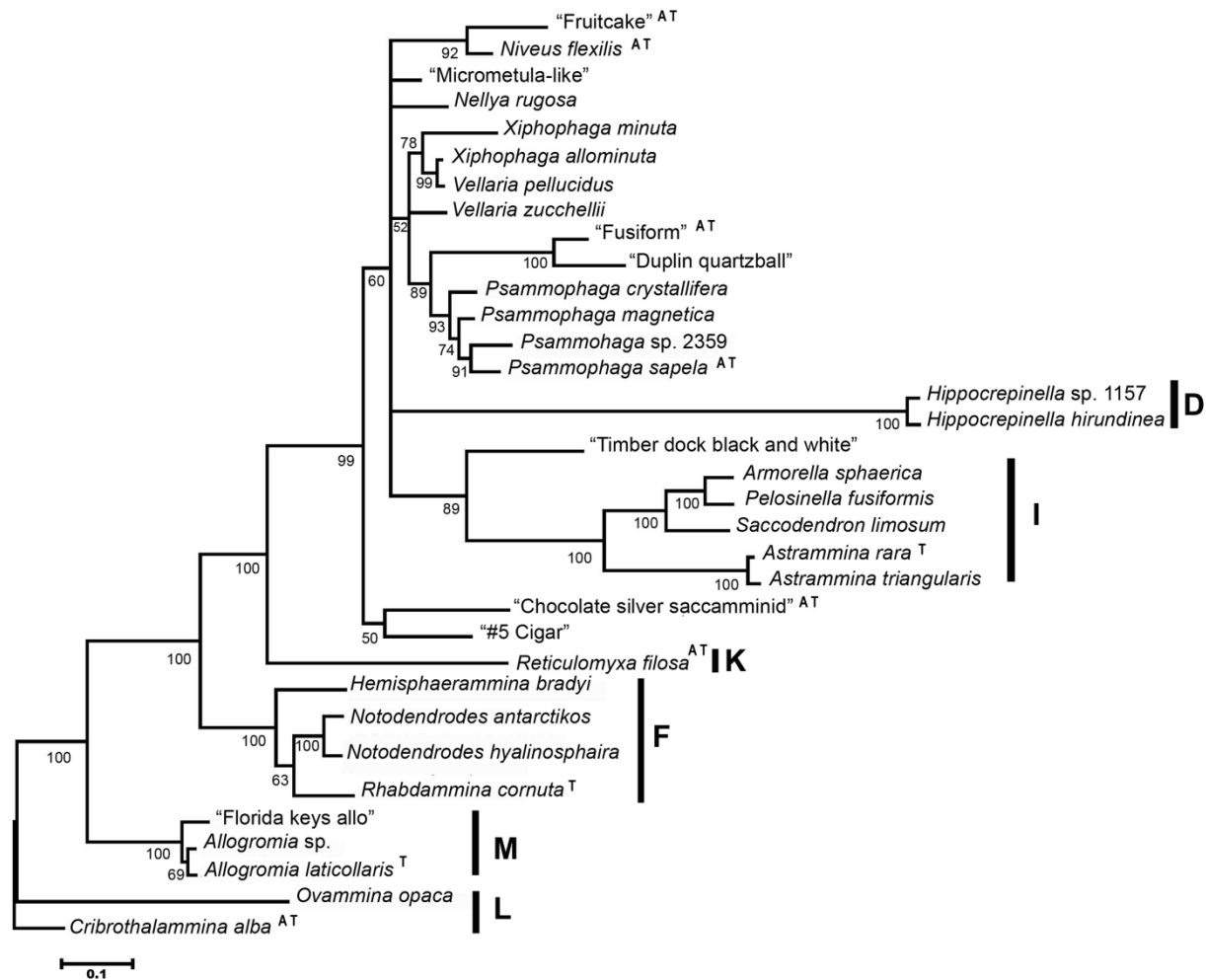


Figure 4.4 Bayesian analysis using multiple genetic markers. Consensus tree of concatenated SSU rDNA, actin (type 1) and β -tubulin ran for 4 million generations with the first 25% sampled trees discarded as burnin. Actin and β -tubulin sequences were available for taxa where A and T superscripts are indicated, and when not represented, was recorded as missing data. Numbers represent Bayesian posterior probabilities x100. *Cribothalammina alba* (Clade L) is the outgroup.

and "Chocolate silver saccamminid" (PP = 76; BS = 45), *X. allominuta* and *V. pellucidus* (PP = 100, BS = 93), "Duplin quartzball" and "Fusiform" (PP = 100, BS = 100). Maximum likelihood relocates the "Duplin quartzball" – "Fusiform" sister taxa basal to clade F (results not shown). As more non-Clade E taxa are removed from the analysis the phylogeny loses more and more resolution. The removal of multiple clades such as I, M and F (Fig. 4.3.B) results in virtually complete collapse of the expanded grouping, including the disruption of the strongly supported 'core' Clade E. It is clear that phylogenetic trees of clade level monothalamids are highly

sensitive to taxon sampling, particularly in regions that exhibit nebulous relationships (i.e., polytomy of the expanded grouping). Key taxa that may break up observed polytomies are missing from the analysis.

Multi-gene phylogeny.

The multi-gene phylogeny was created by concatenating two cytoskeletal proteins actin (type 1, 725 nt) and β -tubulin (987 nt) to the SSU rDNA gene creating a total of 2468 unambiguously aligned positions. The multi-gene Bayesian and maximum likelihood analyses returned different topologies (Fig. 4.4) than the SSU rDNA based trees (Fig.4.2). It reaffirmed the ‘core’ Clade E but with lower support and unexpectedly placed the “Fusiform-Duplin quartzball” sister taxa basal to the psammophagids. It also established a relationship between *Niveus flexilis* and “Fruitcake”, “Timber dock black and white” with Clade I and removed the “Chocolate silver saccamminid” from *N. rugosa* and placed it with “#5 Cigar”. The addition of the cytoskeletal protein data did not appear to improve the single-gene, SSU rDNA based phylogeny nor are results consistent with gross morphological findings.

Results: Gross Morphology and Wall Ultrastructure

The taxa examined in this study represent a group that is potentially related in SSU rDNA analyses. At the gross morphological level, these taxa display a wide diversity but many show similarities at the fine structural level. These findings are summarized along with available morphological data from previous reports of Clade E taxa in Table 4.2. Morphological findings of newfound taxa including “Fusiform” (Figs. 4.5.1-4.5.10), “Fruitcake” (Figs. 4.6.1-4.6.10), “Chocolate silver saccamminid” (Figs. 4.7.1-4.7.6), “#5 Cigar” (Figs. 4.8.1-4.8.6), “Timber dock black and white” (Figs. 4.9.1-4.9.6) and “*Micrometula*-like” (Figs. 4.10.1-4.10.7) are reported in this work but are not formally described at this time. Overall test shape for individuals

potentially considered in “Clade E” can be defined as fusiform, elongate, pyriform, ovate, spherical, round and completely variable within an individual species as seen in “Fruitcake” (Fig. 4.6.1- 4.6-6). All new taxa evaluated in this study possess one aperture with the exception of the “Fusiform” which has two terminal apertures (Fig. 4.5.5). Variations in test mineralogy and packing of the agglutinated materials are noted among taxa examined here. Aside from occasional diatom frustules commonly found in formaminferal cytoplasm, none of the taxa evaluated in this study possessed cytoplasmic inclusions, minerals or otherwise, as in previously reported Clade E taxa (Dahlgren, 1962b; Arnold, 1982; Sabbatini and others, 2004; Goldstein and others, 2010; Pawlowski and Majewski, 2011; Altin-Ballero and others, 2013). Cytoplasmic inclusions differ from stercomata in that they consist of foreign inorganic material (sediments, diatom frustules, etc.) retained in the cytoplasm for a specific purpose (i.e., ballast, Altin-Ballero and others, 2013; sequestration of plastids, Goldstein and others, 2010). In contrast, deposit feeding monothalamid cytoplasm may contain stercomata or waste vacuoles that contain sediments, bacteria and refractory organic matter (Gooday and others, 2008).

“*Fusiform*”. Individuals exhibit a fusiform test shape, wide at the midriff and tapering on either side terminating with apertures (Figs. 4.5.1-4.5.5). Test length always exceeds the width and can range in size from approximately 100 μ m-400 μ m in length. The test is flexible and composed of agglutinated grains of predominantly quartz but also clay, indiscriminate fragments of diatom frustules and occasional dark, unidentified minerals (Figs. 4.5.1-4.5.2). Agglutinated materials are loosely packed (10 μ m thick) within an apparently featureless organic bioadhesive (Figs. 4.5.6-4.5.7, 4.5.9) in which bacterial colonies have also been observed. Fibrous structures have been reported in organic bioadhesives (i.e., *Cribrothalammina alba*, Goldstein and Barker, 1988) of specimens fixed in the presence of ruthenium red stain which

binds to acidic mucopolysaccharides (Luft, 1971), a major organic component of the bioadhesive (Hedley, 1958, DeLaca, 1986). Absence of a fibrous component cannot be ruled out because these specimens were fixed using HPFS in the absence of ruthenium red. The inner organic lining (IOL) is roughly 4-5 μm thick, lies just beneath the agglutinated layer and is in direct contact with the plasma membrane of the cell. Numerous vesicles of differing electron density reside just beneath the plasma membrane and those containing test construction materials have been captured merging with the plasma membrane (Fig. 4.5.8, 4.5.10). The IOL is electron transparent and contains electron-dense fibers and granules that tend to be more dense and numerous toward the apertural ends (Fig. 4.5.8). The cytoplasm may contain large vacuoles and a single nucleus was observed in different specimens (Fig. 4.5.10).

“*Fruitcake*”. This species exhibits variable overall test shape (ovate, spherical) and size (approximate range from 100 μm -350 μm in length) (Figs. 4.6.1-4.6.6) and possesses a single, terminal aperture. The agglutinated material is primarily composed of a fine grained quartz layer in contact with the IOL (Figs. 4.6.7-4.6.9) along with 5-10 larger mineral grains including biotite mica (Fig 4.6.4) and others of unknown composition connected by an organic bioadhesive. Larger minerals often broke free of the test during sectioning (Fig. 4.6.7) leaving a void, thus rendering measurements of the agglutinated layer difficult. The agglutinated layer was much thicker than the IOL which too, is relatively thick (15 μm -20 μm) in comparison to the other Clade E taxa examined. Unlike most other Clade E taxa evaluated to date, the IOL of the “*Fruitcake*” monothalamid lacks the electron-dense granules but is densely fibrous (Fig. 4.6.9). The cytoplasm is composed of very large vacuoles (Fig. 4.6.7) a single nucleus (Fig. 4.6.10) and cytoplasmic packets reminiscent of stercomata (Figs. 4.6.7-4.6.8) indicating this monothalamid may be a deposit feeder (e.g., Gooday and others, 1992).

“Chocolate silver saccamminid”. Members of this species are fairly small (approximate length 100 μm - 150 μm) and possess a pyriform to ovate test shape. The agglutinated layer is composed of clay particles that are tightly packed and predominantly aligned parallel to the plasma membrane (Figs. 4.7.1-4.7.4) over the majority of the cell body. Agglutinated materials near the aperture appear to have undergone compressional forces causing the folding pattern illustrated in Fig. 4.7.2. The IOL contains electron-dense fibers and is remarkably thin (1 μm -2 μm) in comparison to the very thick (20 μm -25 μm) agglutinated layer. The IOL is in direct contact with the plasma membrane and contains fine electron-dense fibrils (Fig. 4.7.4-4.7.5). The cytoplasm contains numerous stercomata (Figs. 4.7.5-4.7.6) in all the sections observed in the transmission electron microscope. Of the Clade E taxa, stercomata have been reported in the *“Chocolate silver saccamminid”* and *“Fruitcake”* to date.

“#5 Cigar”. This taxon is large (up to 2mm in length), elongate with a terminal aperture situation at the tapered end (Fig. 4.8.1). The agglutinated portion of the wall is ~20 μm thick composed predominantly of loosely packed clay particles, some quartz and few dark minerals of unknown composition. The bioadhesive cementing the agglutinated particles appears free of any electron-dense structures (Figs., 4.8.2-4.8.3). The IOL is a thin layer (2 μm), in direct contact with the plasma membrane and contains numerous electron-dense fibrils and particles (Fig. 4.8.4). Specimens observed with electron microscopy show a remarkably mitochondrial rich cytoplasm (Figs. 4.8.3-4.8.5) with many situated directly beneath the plasma membrane. A single nucleus surrounded by a perinuclear ring of endoplasmic reticulum has been observed (Fig. 4.8.5).

“Timber dock black and white”. Several molecular species of ‘black and white saccamminids’ were isolated from marsh sediments along the sampling sites, however, this

particular morphotype is up to 500 μm in length, ovate in shape and has a single, terminal aperture (Fig. 4.9.1 inset). It possesses a thick agglutinated layer of loosely packed quartz grains interrupted by larger dark colored minerals of unknown identity. Bacterial colonies have been observed in the bioadhesive that otherwise lacks structural features (Fig., 4.9.6). The IOL is 1.5 μm thick and contains electron-dense fibers and granules (Figs, 4.9.1-4.9.5) and is in direct contact with the plasma membrane. Vesicles presumably containing test construction materials appear to be released intact into the IOL (Figs. 4.9.3-4.9.4). The cytoplasm just beneath the plasma membrane is mitochondria rich indicating that these regions of the cell are energetically active, possibly the result of cellular growth at the time of fixation.

“*Micrometula-like*”. This taxon is small in size (~ 170 μm long), pyriform to ovate in shape with a single, terminal aperture (Figs. 4.10.1-4.10.3). It possesses an IOL with electron-dense granules and fibers consistent with other Clade E taxa (Fig. 4.10.5). The cytoplasm appears to be separated from the IOL by the presence of an electron opaque transitional zone (Fig. 4.10.5). The cytoplasm uptakes a significant amount of heavy metal stains rendering it visually distinct from the transitional zone (Fig. 4.10.4-4.10.7). The cytoplasm contains large vacuoles and a large, single nucleus with a cortical ring of chromatin (Fig. 4.10.7). The agglutinated layer composed clay minerals arranged in varying orientations is remarkably thin (0.8 μm - 1.5 μm) in comparison to most other Clade E members.

A common theme in ultrastructure of the wall is consistent among all taxa evaluated in this study regardless of phylogenetic position: An inner organic lining (IOL) separates the main cell body from an agglutinated layer. The IOL appears ‘white’ in the micrographs because the structure does not uptake heavy metal stains. Electron-dense fibrils and granules were present in the IOL of all taxa but density could vary among taxa or even within an individual. With the

exception of the presence of a transitional zone in “*Micrometula*-like”, the IOL is in direct contact with the plasma membrane of the cell body. The IOL thickness is variable ranging from remarkably thin 0.5 μm – 1.0 μm as in “*Micrometula*-like” to very thick as observed in “Fruitcake” (15 μm -20 μm). All taxa appear to transmit test construction materials directly to the IOL by either merging with the plasma membrane or completely transferring vesicles into the IOL. The agglutinated layer can differ with respect to mineralogy (predominantly clay, quartz or a mixture), thickness, and degree of organization of packing. Bacterial colonies are common inhabitants of the bioadhesive in the agglutinated layer.

Discussion

The traditional method of determining evolutionary relatedness of foraminiferal taxa has been based on homologous, morphological characters of the test wall structure, geologic history and ontogenetic developmental stages (Cushman, 1927, 1928, 1933, 1940, 1948; Loeblich and Tappan, 1964, 1987; Tappan and Loeblich, 1988). Based on gross morphology of the test, the hypothesized foraminiferal evolutionary pathway began with an atestate ancestor followed by ‘simple’ organic allogromiids which gave rise to all other derived foraminiferal lineages including the agglutinated, single-chambered astrorhizids (Loeblich and Tappan, 1987). This linear evolutionary transformation series of increase in test complexity naked \rightarrow organic \rightarrow agglutinated (Tappan and Loeblich, 1988) has successfully been challenged by phylogenetic studies based on DNA sequence analyses (Pawłowski and others, 2003). The SSU rDNA (Pawłowski and others, 2003) and subsequent actin based phylogenies (Flakowski and others, 2005) indicate that astrorhizids, allogromiids and the atestate constitute a single, paraphyletic group. Over monothalamid history, the agglutinated test morphology has evolved multiple times (Pawłowski and others, 2003) and the atestate morphology in modern forms is not

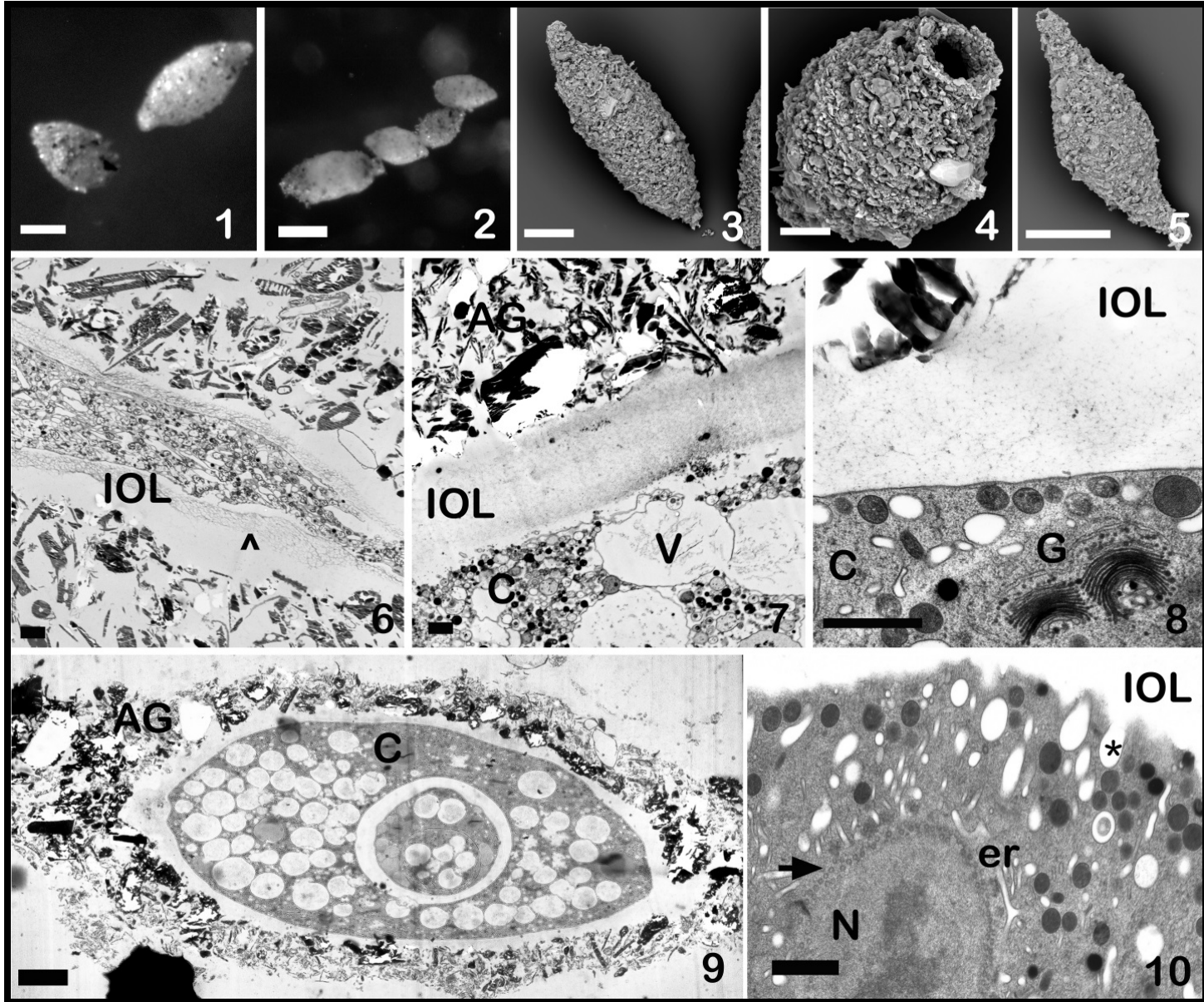
Table 4.2 Summary of gross morphology and wall ultrastructure for taxa examined in this study.

Species	Test Shape/Aperture Number	Test Features	IOL Features	Plasma Membrane	Cytoplasmic Stercomata	Cytoplasmic Inclusions	Citation
#5 Cigar	Elongate with tapered abapertural end/1	Predominantly clay, quartz and dark minerals. Loosely packed. Cement lacks structure. 20 µm thick.	Electron-dense granules and fibers. 2µm thick. Distinct from cement.	IOL is in direct contact with the PM. Vesicles line and observed merging with PM.	Not observed.	Not observed.	This work Figs. 4.8.1-4.8.6.
“Chocolate Silver Saccamminid”	Pyriiform to ovate/ 1	Primarily clay well organized running parallel to the cell body, hence the pearlescent sheen. Very thick 20-25µm. Cement appears finely fibrous.	IOL is fibrous but granules not observed. Very thin 1-2 µm thick). IOL appears continuous with cement.	IOL is in direct contact with the PM. Vesicles line the PM.	Present.	Not observed.	This work Figs. 4.7.1-4.7.6.
“Fruitcake”	Variable Ovate, Elongate/ 1	Fine quartz and larger minerals (biotite) and others. Thickness not measured but at least twice that of the IOL. Cement lacks internal structure.	IOL is densely fibrous but granules not observed 15-20 µm thick. IOL appears continuous with cement.	IOL is in direct contact with the PM. Vesicles directly released into the IOL.	Present.	Not observed.	This work Figs. 4.6.1-4.6.10.
“Fusiform”	Fusiform/ 2	Flexible, quartz, clay, diatoms. 10µm thick. Bacterial colonies.	Electron-dense granules and fibers (not dense) but more fibrous near aperture Distinct from cement. 4-5 µm thick.	IOL is in direct contact with the PM. Vesicles line and merge with the PM.	Not observed.	Not observed.	This work, Figs.4.5.1-4.5.10.
“Micrometula-like”	Pyriiform/ 1	Remarkably thin (.5-1 µm). Clay in varying orientations moderately packed.	Electron-dense granules and fibers. IOL 0.8-1.5µm Distinct from cement.	IOL is separated from cytoplasm by a transitional layer that is different from the cytoplasm and IOL.	Not observed.	Not observed.	This work Figs. 4.10.1-4.10.4.

<i>Niveus flexilis</i>	Round to ovate/ 1	Very thin (0.5µm) agglutinated layer of clay with some diatom fragments. Meticulously layered, well organized.	Electron-dense granules and fibers. Densely fibrous. IOL 3-8 µm. Distinct from cement.	IOL is in direct contact with the PM. Vesicles line the PM. Direct release into IOL	Not observed.	Not observed.	Altin and others, 2009
<i>Nellya rugosa</i>	Oval to Cigar / 1	20 µm wall thickness. Did not report mineralogy.	No data.	No data.	No data	Not observed.	Gooday and others, 2010
<i>Psammophaga crystallifera</i>	Ellipsoidal/ 1	No agglutination. Organic wall “Very thin”	No data.	IOL is in direct contact with the PM.	No data	Present throughout cytoplasm.	Dahlgren, 1962b; Pawlowski and Majewski, 2011
<i>Psammophaga magnetica</i>	Ovoid to elongate/ 1	Wall is < 10µm wide.	No data.	No data.	No data	Present near apertural end.	Pawlowski and Majewski, 2011
<i>Psammophaga sapela</i>	Pyriiform, elongate, spherical/ 1	Clay some diatoms. 10-15µm Bacterial colonies. Cement weakly fibrous.	Electron-dense granules and fibers. IOL 2-5 µm. Distinct from cement.	IOL is in direct contact with the PM. Vesicles line and merge with the PM	Not observed.	Present throughout cytoplasm.	Altin-Ballero and others, 2013
“Timber Dock Black and White”	Ovate/ 1	Loosely packed 15µm thick. Predominantly quartz with clay minerals of closer proximity to the IOL. Larger minerals of dark color. Bioadhesive with bacterium.	Electron-dense granules and fibers. IOL 1.5µm. Distinct from cement.	IOL is in direct contact with the PM. Vesicles line and are directly released into the IOL. Mitochondria found in abundance at PM.		Not observed.	This work Figs. 4.9.1-4.9.6.

<i>Vellaria pellucidus</i>	Variable globular to elongate/ 1	No agglutination. Organic wall 2-3 μm .	No data.	No data.	No data	Not observed.	Gooday and Fernando, 1992; Gooday and others, 2010.
<i>Vellaria zucchini</i>	Elongate/ 1	“Two semitransparent membranes with veneer of plate like particles.”	No data.	No data.	No data	A few mineral inclusions.	Sabbatini and others, 2004
<i>Xiphophaga allominuta</i>	Ovate to spherical/ 1	Clay some diatoms. 7-8 μm thick. Loose packing of varying orientations. Bacterium found in cement.	Electron-dense granules and fibers. Finely fibrous. IOL 1 μm . Distinct from cement.	IOL is in direct contact with the PM. Vesicles line and merge with the PM.	Not observed.	Present; pennate diatoms.	Goldstein and others, 2010
<i>Xiphophaga minuta</i>	Ovate to spherical/ 1	Clay some diatoms. 7-8 μm thick. Loose packing of varying orientations. Bacterium found in cement.	Electron-dense granules and fibers. Finely fibrous. IOL 1 μm . Distinct from cement.	IOL is in direct contact with the PM. Vesicles line and merge with the PM.	Not observed.	Present; pennate diatoms.	Goldstein and others, 2010

Figure 4.5 (Next Page) Gross morphology and ultrastructure for the “Fusiform” monothalamid. **1, 2** Living individuals illustrating the variation in size. **3-5** Scanning electron micrographs of three individuals; **3, 5** Showing distinct tapered ‘fusiform’ shape with tapered ends. **4** View showing one of the two apertures (Scale bars 1, 3, 5 = 100 μm ; 2 = 200 μm ; 4= 20 μm). **6-10** Transmission electron micrographs of the “Fusiform” monothalamid fixed by HPFS methods. **6** Section across aperture showing densely fibrous IOL (^) (scale bar = 1 μm). **7-8** Cross sectional view of the wall. The inner organic lining (IOL) separates the agglutinated layer (AG) from the cytoplasm (C). Cell body contains numerous vacuoles (V). Mitochondria and golgi (G) are abundant in examined specimens. The IOL contains electron-dense fibers and granules (scale bars = 1 μm). **9** Survey view of the complete organism showing relative thickness of the agglutinated layer (AG) to the inner organic lining. Note the abundance of large, circular white vacuoles within the cytoplasm (C) (HPFS, scale bar = 10 μm). **10** Wall building materials are transported to the IOL by small vesicles that merge with the plasma membrane (asterisk). Chromatin displacement within the nucleus (N) is centralized. Tangential section of nuclear pores (arrow) of the nuclear membrane is surrounded by a layer of endoplasmic reticulum (er) (scale bar = 1 μm).



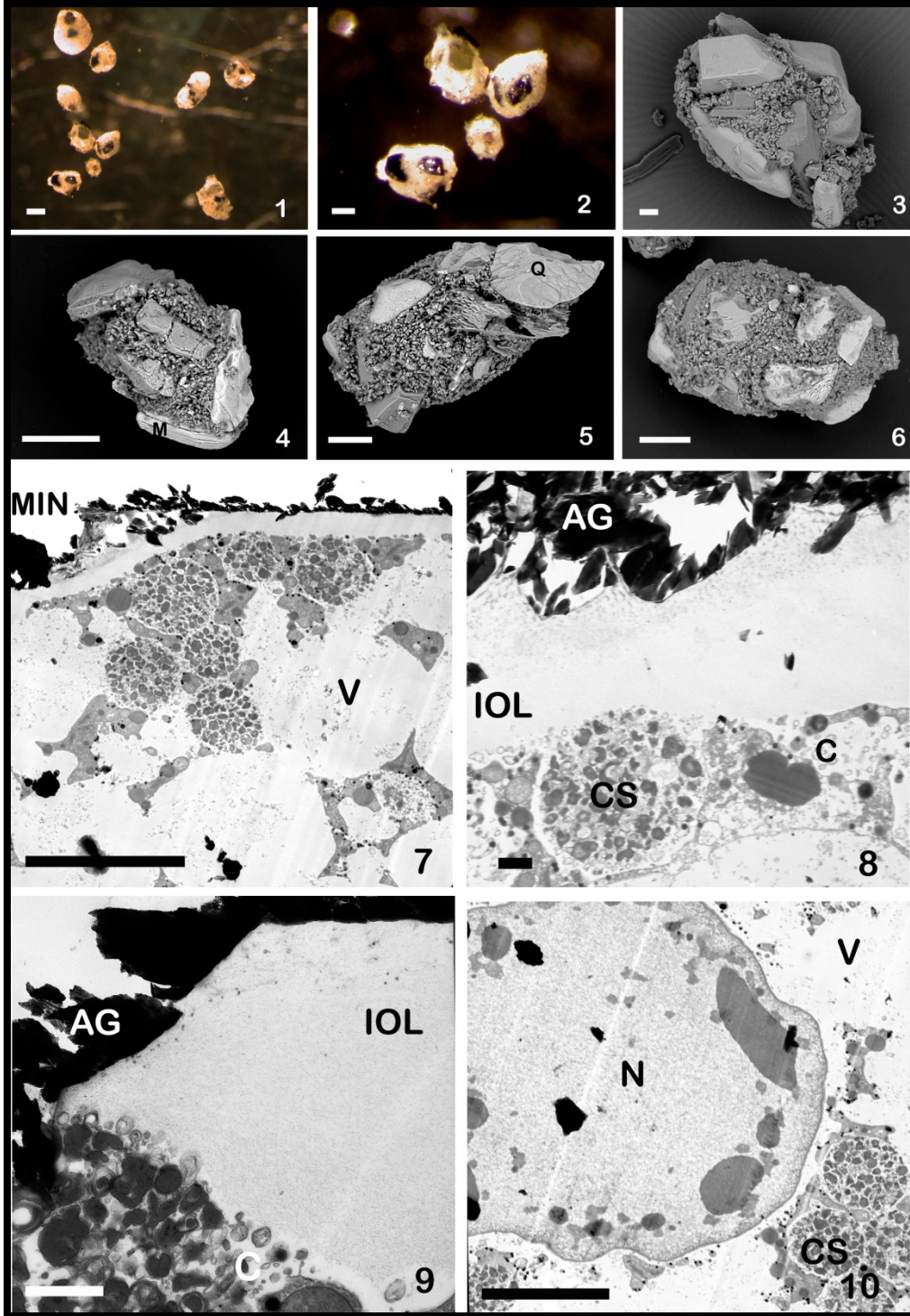


Figure 4.6 Gross morphology and ultrastructure for the “Fruitcake” monothalamid. 1-2 Living individuals showing variable size and shape. (scale bars = 200 μ m and 100 μ m respectively). 3-6 Scanning electron micrographs showing large mica (M) and other large questionable (Q) mineral grains (scale bars 3 = 20 μ m; 4-6 = 100 μ m). 7-10 Transmission electron micrographs of chemical preparations. Cytoplasm (C) containing stercomata (CS) large vacuoles (V) and a single nucleus (N). The inner organic lining (IOL) separates the agglutinated layer (AG) that contains small presumably quartz grains and large minerals that were removed during sectioning (MIN). The IOL is electron opaque and densely fibrous (scale bars 7, 10 = 100 μ m; 8= 10 μ m, 9 = 1 μ m).

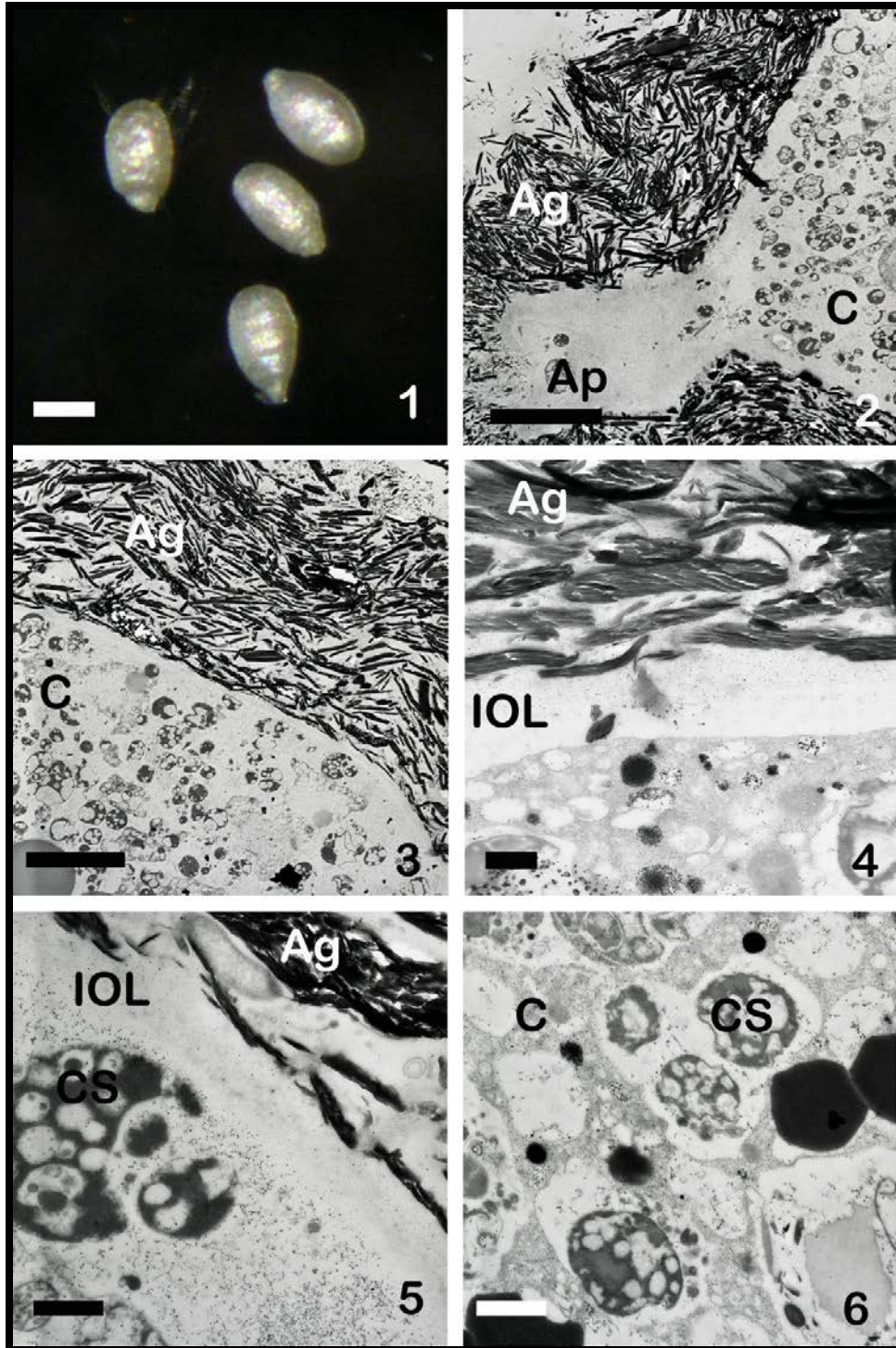


Figure 4.7 Gross morphology and ultrastructure for the “Chocolate silver saccamminid” monothalamid. 1 Living individuals ovate to pyriform shape, showing pearlescent sheen (scale bar = 100 μ m). **2-6** Transmission electron micrographs of chemically prepared specimens. **2-3** Sections through aperture (Ap) and wall showing thick agglutinated layer (Ag) and cytoplasm (C) (scale bars 2-3 = 10 μ m). **4** Higher magnification view of the very thin, electron opaque, moderately fibrous inner organic lining (IOL). The IOL is separating the agglutinated layer (Ag) from the cytoplasm (C) but is in direct contact with the plasma membrane. **5-6** The cytoplasm (C) contains numerous stercomata (CS) (scale bars 4-6 = 1 μ m).

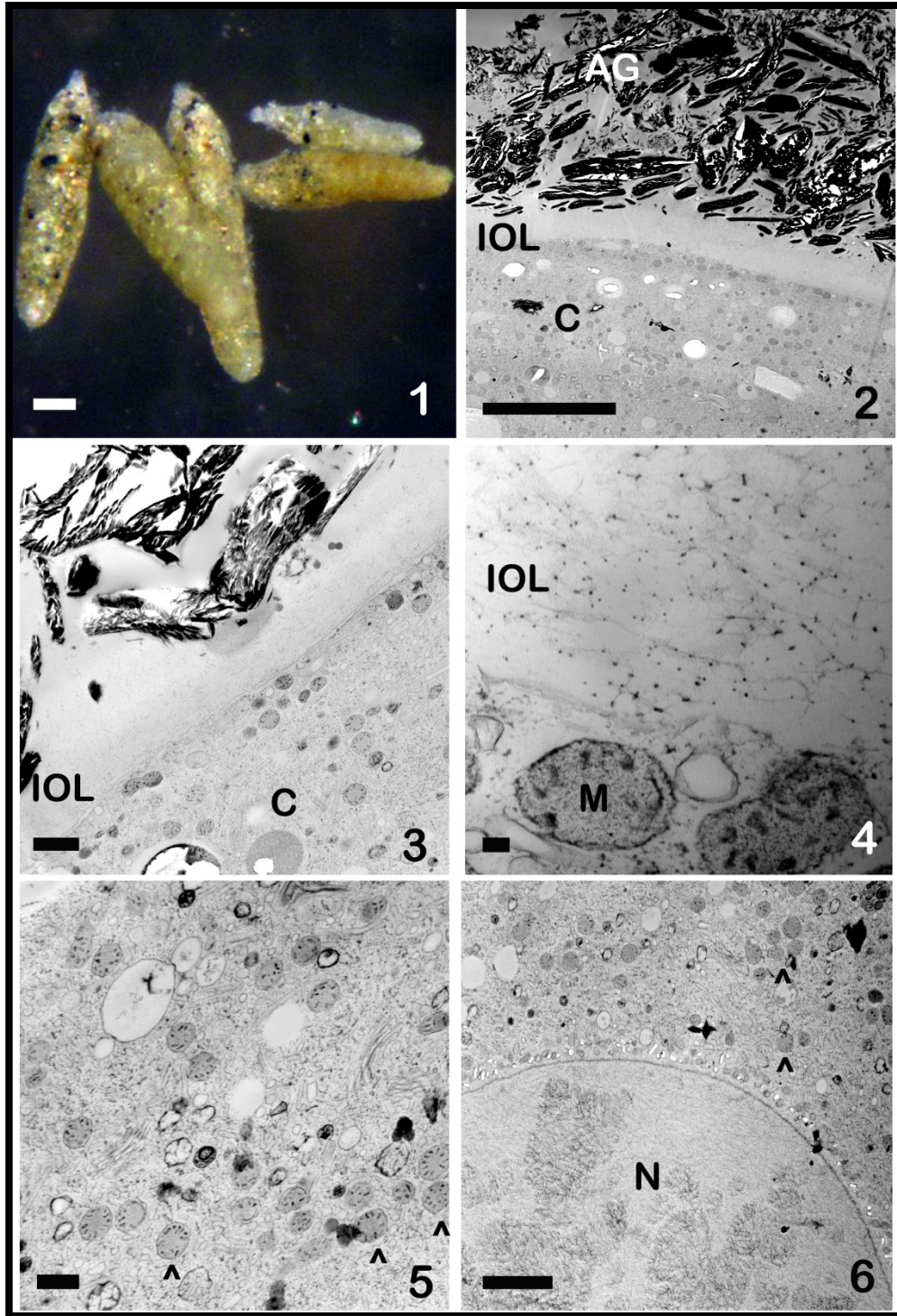


Figure 4.8 Gross morphology and ultrastructure for the “#5 Cigar” monothalamid. **1** Living individuals elongate shape with tapered abapertural end (scale bar = 300 μ m). **2-6** Transmission electron micrographs of chemically prepared specimens. **2-4** Sections through wall showing thick agglutinated layer (Ag), cytoplasm (C) densely packed with mitochondria (M) and an inner organic lining (IOL) with electron-dense fibers and particles (scale bars 10 μ m, 1 μ m and 0.1 μ m respectively). **5** Survey view of mitochondrial (^) rich cytoplasm (scale bar = 0.5 μ m). **6** View of interphase nucleus (N) with diffuse chromatin (dark patches) and perinuclear layer of endoplasmic reticulum. Mitochondrial clusters (^) are illustrated (scale bar = 2 μ m).

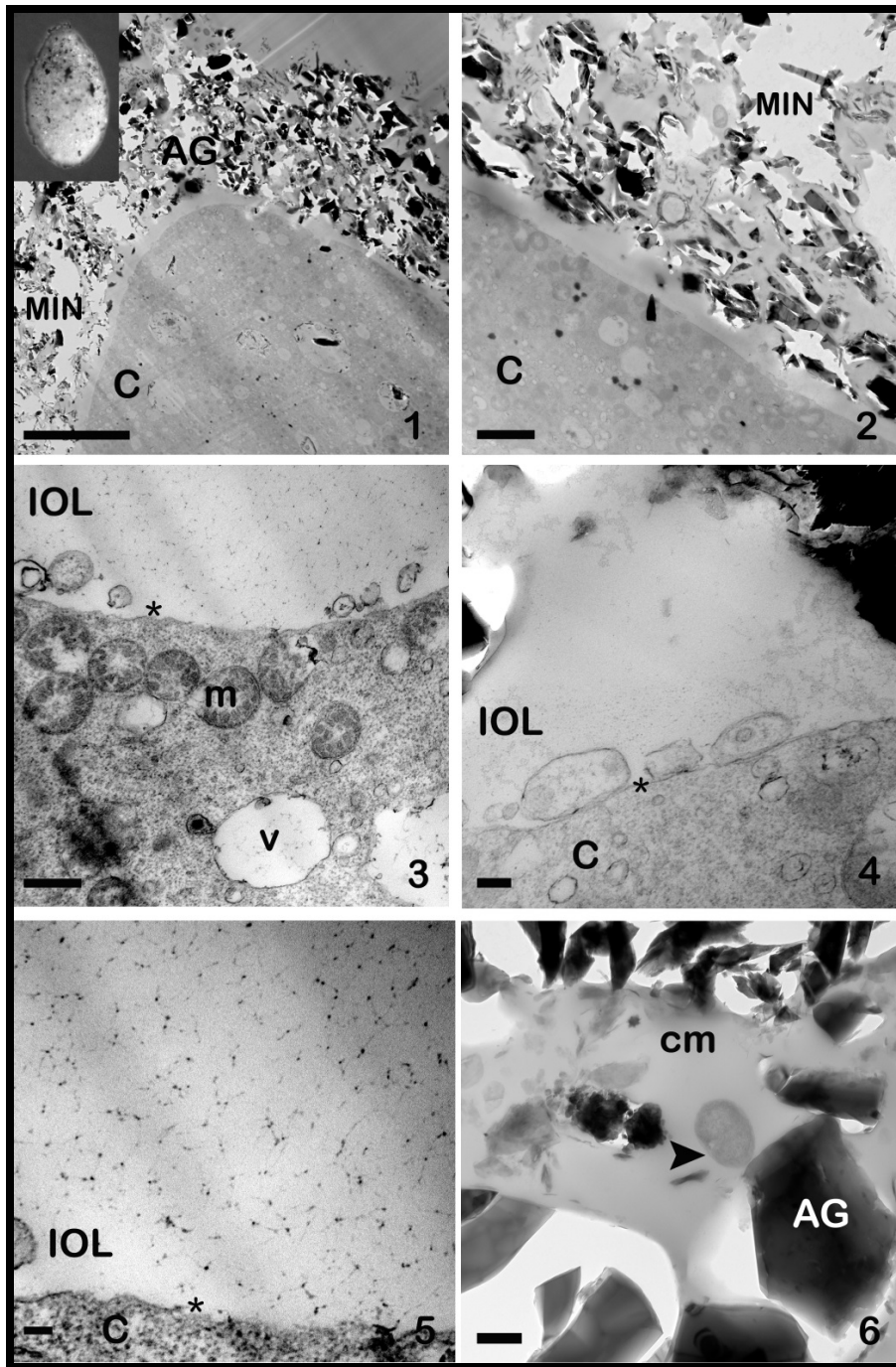


Figure 4.9 Ultrastructure for the “Timber dock black and white” monothalamid. **1** inset Living individual 500 μm in length (reprinted with permission, Habura and others, 2008). **1-6** Transmission electron micrographs of chemically prepared specimens. **1-2** Survey section of the abapertural end showing agglutinated layer (AG) thickness relative to the cytoplasm (C). Larger mineral grains commonly fall out during sectioning leaving a void behind (MIN) (scale bars 1 = 10 μm ; 2 = 2 μm). **3-5** Wall cross section showing the inner organic lining (IOL) with electron-dense fibers and particles is in direct contact with the plasma membrane (asterisk). The cytoplasm (C) contains numerous mitochondria (m) and vacuoles (v). Note that vesicles are completely transferred directly into the IOL. (scale bars 3, 4 = 0.1 μm ; 5 = 0.5 μm). **6** High magnification view of the cement (cm), agglutinated particles (AG). Note bacterial cell (arrow head) (scale bar = 0.5 μm).

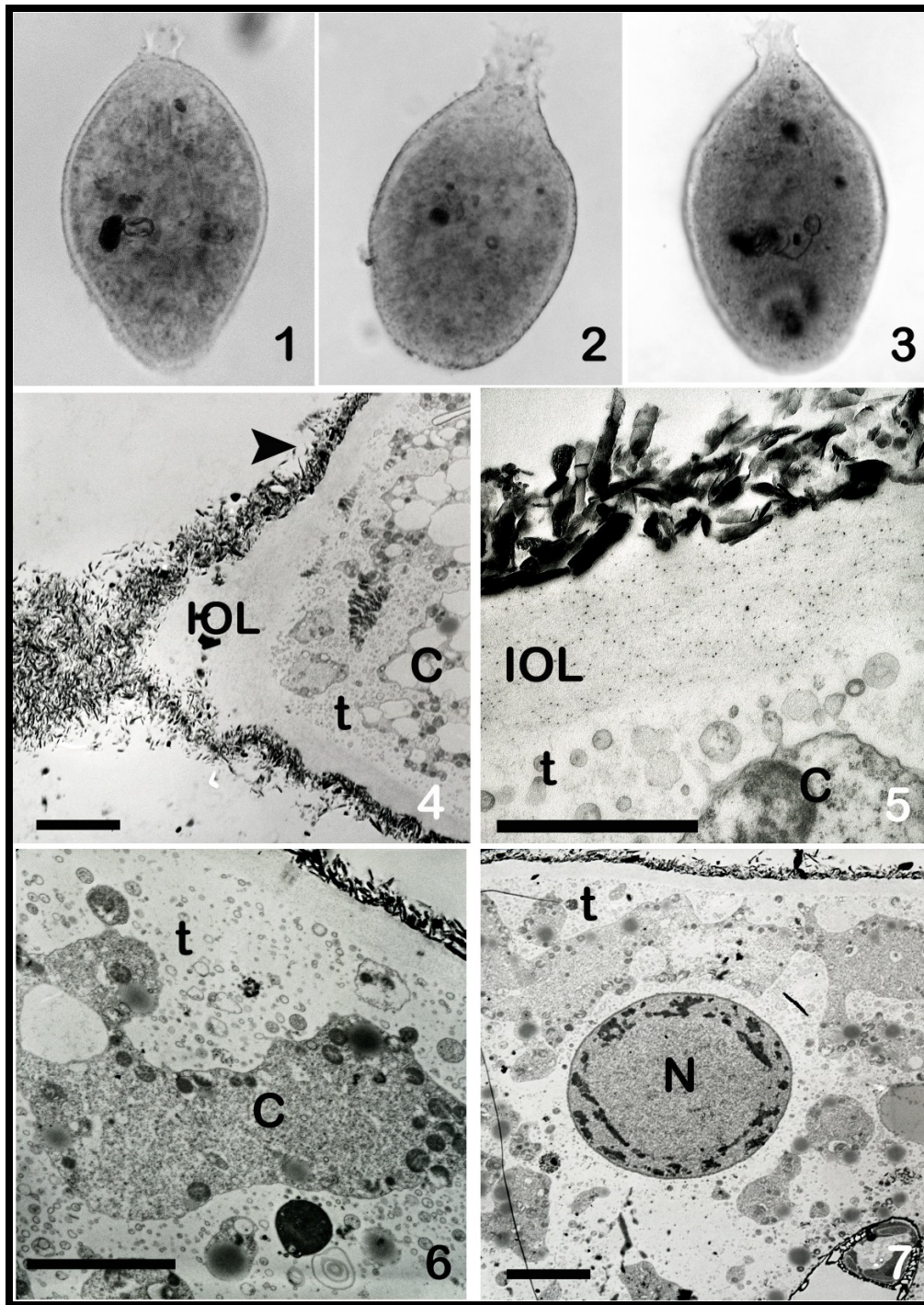


Figure 4.10 Ultrastructure for the “*Micrometula*-like” monothalamid. 1-3 Chemically fixed specimens embedded in epon-araldite resin. Individuals are 170 μm in length. 4-7 Transmission electron micrographs of chemically prepared specimens. 1 View of the apertural cytoplasm (C). Note the inner organic lining (IOL) is almost as thick as the agglutinated layer (arrow head) in this region (scale bar = 5 μm). 4-6 Sections through wall showing the cytoplasm (C) relative to the IOL and thin agglutinated layer. The IOL is composed of electron-dense fibers and particles. A possible cytoplasmic transition zone (t) of differing electron opacity and structure exists between the IOL and the cytoplasm (scale bars 2 = 1 μm ; 3 = 5 μm). 7 View of the nucleus (N) relative to the agglutinated layer running across the top of the micrograph. Electron opaque chromatin distributed as a cortical ring around the exterior of the nucleus (scale bar = 5 μm).

a primitive character state but rather a trait secondarily lost as an adaptation to freshwater habitats (Pawlowski and others, 1999a; 1999b). Molecular research has conclusively demonstrated that the degree of test complexity and overall test morphology cannot be used to infer evolutionary history for monothalamids.

The SSU rDNA Bayesian tree reported here (Fig. 4.2) returns a strongly supported (posterior probability of 0.96) ‘core’ group of taxa composed of *Psammophaga* sp., *Vellaria* spp. and *Xiphophaga* spp. A similar topology was recovered when selected groups were removed from the analysis (Fig. 4.3.A) but the entire tree collapsed upon removal of more than one clade (Fig. 4.3.B). Many systematists argue that phylogenetic accuracy is heavily influenced by taxon sampling (e.g., Hillis, 1998, Zwickl and Hillis, 2002) and in the case of clade-level monothalamids, these results concur. Introduction of distantly related taxa into the analysis improves overall resolution of the phylogenetic trees created with SSU rDNA sequences alone.

Although the core Clade E taxa are closely related based on molecular phylogenetic analysis of the SSU rDNA gene, they are not well supported in the multi-gene analysis. The species within the genera *Xiphophaga* and *Vellaria* have been formally described in the literature based on morphological characters. Interestingly, both the SSU rDNA and multi-gene trees (Fig. 4.4) suggest that, *X. allominuta*, morphologically indistinguishable to *X. minuta*, (Goldstein and others, 2010) forms a robust pairing with *V. pellucidus* and *V. pellucidus* is more closely related to the xiphophagids than its congener, *V. zucchellii*. Both the psammophagids (Arnold, 1982; Pawlowski and Majewski, 2011; Altin-Ballero and others, 2013) and xiphophagids (Goldstein and others, 2010) exhibit a voracious appetite to maintain cytoplasmic inclusions (sand and diatoms respectively) but this conspicuous biological trait is not seen in *V. pellucidus* (Gooday and Fernando, 1992; Gooday and others, 2010) and only a few mineral inclusions were reported

in *V. zucchellii* (Sabbatini and others, 2004). *Psammophaga* spp. (Arnold, 1982; Pawlowski and Majewski, 2010; Altin-Ballero and others, 2013) and *Xiphophaga* spp. (Goldstein and others, 2010) possess an agglutinated test of significant thickness (10-15 μm and 7-8 μm) whereas *V. zucchellii* is reported as having a veneer of plate-like particles (Gooday and Fernando, 1992) and *V. pellucidus* lacks an agglutinated layer all together (Sabbatini and others, 2004). All members possess a single, terminal aperture, but they all drastically vary in shape (summary of gross morphology and ultrastructure, Table 4.2). Agglutination patterns may not be a useful taxonomic tool above the generic level because the SSU rDNA based tree strongly supports a closely related core Clade E, despite the distinct agglutination patterns over such a short evolutionary history. Inconsistencies between morphology and molecules demonstrate the importance of collecting all possible information when assessing monothalamid species diversity and when formally describing new taxa.

The SSU rDNA tree also shows that the expanded monophyletic grouping (Fig. 4.2) includes previously reported Clade E members such as *Nellya rugosa* (Gooday and others, 2010) and *Niveus flexilis* (Habura and others, 2008) but also incorporates three additional taxa “Chocolate silver saccamminid”, “#5 Cigar” and “*Micrometula*-like” as reported by Habura and others (2008). The expanded, weakly supported, monophyletic grouping also exhibits a wide variation in gross morphology. The “Chocolate silver saccamminid” is pyriform to ovate in shape, opalescent in appearance and forms a clade with *N. rugosa* which is elongate or cigar-shaped composed of loosely arranged quartz grains (Gooday and others, 2010). The characteristic ‘silver’ saccamminid test is also reported in monothalamids of distinct molecular lineages such as the “sapp silver saccamminid” of clade D (Habura and others, 2008) and *Ovammina opaca* (Dahlgren, 1962a) of Clade L. The “*Micrometula*-like” taxon is pyriform in

shape with a remarkably thin (0.5 μm -1.0 μm) agglutinated layer of moderately packed clay and the “#5 Cigar” is elongate in shape with a 20 μm thick agglutinated layer of loosely packed clay with some quartz. The SSU rDNA based tree excludes the “Fusiform”, “Duplin quartzball”, “Fruitcake” and “Timber dock black and white” taxa from Clade E as they are shown to be of some genetic distance to the core as *Hippocrepinella* spp. of clade D. These taxa can be excluded from Clade E membership.

Incongruences between the SSU rDNA and multi-gene phylogenetic trees can be the result of limiting stochastic error (incorrect sister group relationships) by way of increasing the number of genes in the analysis (Felsenstein, 1978). Stochastic error occurs when there is too little signal in the data (Swofford and others, 1996; Rokas and Carroll, 2005) which could be the case when using the SSU rDNA gene alone. With the exception of region V, the hyper-variable regions are too divergent for inter-clade comparisons because of neutral substitutions or evolutionary pressures operating on the foraminiferal SSU rDNA since their divergence in the Neoproterozoic (Pawlowski and others, 2003). Aligning potential Clade E members in this study was particularly problematic even when comparisons were made using secondary structure fold predictions. Vast portions of the divergent regions were eliminated from the analysis because these sections could not be unambiguously aligned. The remaining sequence may not provide enough phylogenetic signal to delineate deeper evolutionary relationships among the potential Clade E taxa being examined in this study. Increasing gene number provides more points of comparison and ultimately has a positive effect on phylogenetic accuracy (Rokas and Carroll, 2005).

Wall Ultrastructure and Phylogenetic Significance

To date little work has been done on wall ultrastructure of monothalamous foraminifera (see Table 1.1) even though it is regarded as containing important evolutionary information (Avnimelech, 1952; Dahlgren 1962a; Angell, 1971; Hedley and others, 1972; Loeblich and Tappan, 1987; Bowser and others, 1995; Goldstein and Richardson, 2002). Based on the information available, distinct differences between the organic walled and agglutinated forms can be observed (traditionally classified within Suborders Allogromiida and Astrorhizida respectively, Loeblich and Tappan, 1987). Consistent among the organic walled monothalamids and apparently absent in all agglutinated taxa examined in this study, is an external, electron-dense, outermost layer (described as a granulofibrillar layer in Bowser and others, 2002) that overlies either a fibrillar layer, a herringbone layer or combination of layers that comprise the entire wall. Molecular analyses conclusively demonstrate that allogromiids and astrorhizids are polyphyletic yet ultrastructural findings show that certain features of the wall, particularly the presence of the outermost electron dense layer occurs in species that cut across clades delineated by the SSU rDNA.

The most morphologically simple wall layer is that of the single 'fibrillar' region composed of electron-dense fibers oriented parallel to the cell surface that resides between the outermost electron-dense layer and the cellular plasma membrane such as in *Notodendrodes hyalinosphaira* (Clade F) (DeLaca and others, 2002), *Boderia albicollaris* (Clade G) (Schwab, 1977) and *B. turneri* (Hedley and others, 1972). The fibrous layer in *Shephaerdealla taeniformis* exhibits fibers positioned randomly (Hedley and Wakefield, 1967). The fibrillar region can be modified such that fibers are arranged in bundles running in opposite directions forming a herringbone pattern as in *Allogromia laticollaris* (Clade M), *Allogromia* sp. B, *Allogromia* sp. C

(Hedley and others, 1972), *Myxotheca* sp. (Angell, 1971; Goldstein and Richardson, 2002) and *M. arenilega* (Schwab, 1969). An additional sparsely fibrous layer containing dense electron granules overlies the distinct herringbone layer in *M. arenilega* (Schwab, 1969). The Sapelo Island, Georgia species of *Myxotheca* has very fine fibers, intertwined but predominantly parallel to the plasma membrane and coarser bundles of fibrous material in the outermost region (Goldstein and Richardson, 2002). The electron-dense layer in *Myxotheca* sp. contained fibers oriented perpendicular to the test (Goldstein and Richardson, 2002) and this subtle morphology appears absent in wall of *M. arenilega* (Schwab, 1969).

Fiber length, orientation and bundling pattern (e.g., herringbone) may be a function of cell motility or wall pliability and not a function of morphological variations due to inheritance. Hedley and others (1972) discuss how wall morphology varies with test shape. For example, tests of a fixed shape (e.g., *Allogromia laticollaris*, *Allogromia* sp. B. and *Allogromia* sp. C.) possess long thin fibrils arranged parallel to the shell surface or a herringbone pattern with thin electron-dense layer. Individuals that maintain a constant shape and aperture position but can change shape rapidly exhibit an ultrastructural morphology similar to the ‘fixed’ shape. The species *Iridia diaphana* contains one fibrillar layer that was shown to exist in three distinct morphologies: with elongated fibers oriented parallel to the plasma membrane, in a herringbone pattern and with shorter fibers randomly oriented, the latter in a specimen fixed while moving (Hedley and others, 1972). Whether or not these morphological variations in fiber length, shape and arrangement are due to exclusively to functionality is not yet known.

Considerable complexity of layering has been observed in several different species of monothalamids. Taxa once considered ‘astrorhizids’ because of an agglutinated in fact possess a wall or ‘theca’ reminiscent of organic walled ‘allogromiids’. To date, the most complex theca

described belongs to *Astrammmina rara* (Bowser and others, 1995). Here, the cell body is separated from the theca by a vesicular layer. A fibrous zone is situated above the vesicular layer and is composed of three sections delineated by variable packing of the fibrils. Closest to the vesicular layer they are loosely arranged, in the central region they form the herringbone pattern and fibrils are densely packed on the outer region. Atop the fibrous zone is a thin stratified layer of alternating electron-dense bands separated by lighter staining granulofibrillar matrices.

Complex layering may be evident in one species of a given genus but absent in another species of similar molecular affinities. Unlike *Notodendrodes hyalinosphaira*, the theca of *N. antartikos* is more complex evidenced by layering of an outer fibrous layer composed of loose meshwork of long, fine fibrils situated over granular material embedded in a finely filamentous matrix (Bowser and others, 2002). The wall as described in *Allogromia* sp. A is structurally more complex than those reported for other species. Here the wall consists of three layers: the electron-dense outer layer followed by an outer fibrillar layer with randomly oriented fibers and an inner fibrillar layer with fibers running parallel to the cell surface or arranged in herringbone bundles. The theca in *Astrammmina triangularis* is not nearly as complex of that of *A. rara* as it only contains two zones. The outermost electron-dense granulofibrillar layer overlies an inner layer of thick fibers oriented parallel to the cell surface or in a herringbone pattern increasing in density towards the periphery (Bowser and others, 2002). Although the number of layers, fibrillar structure and overall degree of wall or thecae complexity can vary within closely related taxa, members of Clade I overall have a more complex architecture. The multi-gene analysis places the “Timber dock black and white” saccamminid which possesses an IOL consistent with

the core Clade E taxa basal to Clade I suggesting that the complex thecal wall observed in *Astrammina* spp. is the derived character state.

Interesting wall structures have been described for two agglutinated monothalamous foraminifera of unknown molecular affinity. Hedley and Wakefield (1967) report an organic layer of conspicuously packed, banded, proteinaceous fibers (suspected to be collagen-like) situated between the agglutinated layer and cell body of *Haliphysema* sp. The fibers are suspected to give the test appropriate flexibility for survival in higher energy intertidal zones (Hedley and Wakefield, 1967). An unusual inner organic lining (IOL) has been reported in an undescribed species of *Hyperammina*. Here the IOL is thin and composed of crescent shaped fibers running perpendicular, but not in contact with, the plasma membrane of the cell body (Goldstein and Richardson, 2002). With the exception of microtubules found just beneath plasma membrane in both *Hyperammina* spp. and *Shephaerdella taeniformis* (Hedley and others, 1967), the ultrastructural features found in *Haliphysma* sp. and *Hyperammina* sp. have yet to be reported in any other monothalamous foraminifera.

All taxa examined via transmission electron microscopy in this study possessed an agglutinated test composed of sediment grains cemented together by a bioadhesive. Most agglutinated monothalamids examined by TEM have shown that the arenaceous test and associated bioadhesive are separated from the cytoplasm of the foraminifer by an electron transparent, inner organic lining (IOL) that remains in direct contact with the plasma membrane. The only known exception to date is the collagen-like sheath observed in *Haliphysma* sp. (Hedley and Wakefield, 1967), that replaces the more commonly found IOL. The fibrous IOL with electron-dense granules is found in all taxa examined here as well as in other Clade E species such as *Niveus flexilis* (Altin and others, 2009), *Xiphophaga* spp. (Goldstein and others,

2010), *Psammophaga sapela* (Altin-Ballero and others, 2013) in addition to two Clade L taxa *Cribrothalammina alba* (Goldstein and Barker, 1998; Goldstein and Richardson, 2002) and *Ovammina opaca* (Goldstein, unpublished observations). The IOL is 1 μm – 5 μm in thickness for most reported species including those here, but it is fairly thick in *N. flexilis* (3-8 μm) (Altin and others, 2009) and exceptionally thick in “Fruitcake” (15-20 μm). The IOL is consistently reported as being in direct contact with the plasma membrane except in *Hyperammina* sp. (Goldstein and Richardson, 2002) and in “*Micrometula*-like”. The IOL and plasma membrane of “*Micrometula*-like” are separated by an amorphous vesicular layer of much lighter electron opacity than the cytoplasm and much darker than the IOL (Figs. 4.10.5-4.10.7). Bowser and others (1995) also report a homogenous, lightly staining granular matrix containing vesicles between the fibrous zone of the theca and the cytoplasm in *Astrammina rara* (Clade I).

It is very common to find vesicles and mitochondria lining the plasma membrane in monothalamid electron micrographs. Oftentimes these vesicular structures are of varying electron density and presumably function (Goldstein and Richardson, 2002; Altin and others, 2009; Goldstein and others, 2010; Altin-Ballero and others, 2013) but the presence of mitochondria is indicative of elevated energetic requirements in the vicinity. Vesicles containing wall construction materials have been found to deliver materials to the IOL by two means. Intact vesicles can be completely transferred from the cytoplasm into the IOL as in *Myxotheca arenilega* (Schwab, 1969), *Myxotheca* sp. (Angell, 1977), *Niveus flexilis* (Altin and others, 2009), “Fruitcake” (Fig. 4.6.9) and the “Timber dock black and white” (Fig. 4.9.3-4.9.4). Alternatively, vesicles cytologically merge with the plasma membrane releasing contents directly into the IOL as seen in “Fusiform” (Fig 4.5.10), *Psammophaga sapela* (Altin-Ballero and others, 2013), *Xiphophaga* spp. (Goldstein and others, 2010), *Cribrothalammina alba* (Goldstein and

Barker, 1988) and *Ovammmina opaca* (Dahlgren, 1962a). It appears that these taxa enlarge the cell diameter by adding material along all points of the cell (Hedley, 1962; Arnold, 1982; Goldstein and Barker, 1988; Goldstein and Richardson, 2002).

Overall test shape and mineralogy vary among all taxa examined in this study as well as previously reported Clade E members. All taxa have a single terminal aperture except “Fusiform” which has two, one at each tapered end of the test. The majority of the members have ovate, pyriform and spherical test shapes but others can be variable as in “Fruitcake”, elongated as in “#5 Cigar” and *Vellaria zucchellii* (Sabbatini and others, 2004), or oval as in *Nellya rugosa* (Gooday and others, 2010). Several of the taxa including “Chocolate silver saccamminid” (Fig. 4.7.1), “*Micrometula*-like”(Figs. 4.10.1-4.10.3), *Niveus flexilis* (Altin and others, 2009), *Xiphophaga* spp. (Goldstein and others, 2010), *Psammophaga sapela* (Altin-Ballero and others, 2013) and *V. zucchellii* (Sabbatini and others, 2004) agglutinate predominantly clay minerals whereas the “#5 Cigar”(Figs. 4.8.1-4.8.3), “Fruitcake” (Figs. 4.6.1-4.6.8), “Timber dock black and white” (Figs.4.9.1-4.9.2) favor quartz minerals. The latter two also incorporate darker colored minerals into the test, but “Fruitcake” tends to agglutinate minerals significantly larger than the primary minerals making sectioning difficult. Larger minerals are lost during thin sectioning therefore accurate measurements of the agglutinated layer for “Fruitcake” is not reported. The “Fusiform” member lacked any great preference for either as both clay and quartz minerals were found composing the test (Figs. 4.5.1-4.5.7). Diatom frustule fragments were also common in the majority of the newfound taxa as well as the previously reported species *Ovammmina opaca* (Dahlgren, 1962a), *Cribrothalammina alba* (Goldstein and Barker, 1988), *N. flexilis* (Altin and others, 2009), *Xiphophaga* sp. (Goldstein and others, 2010), *P. sapela* (Altin-Ballero and others, 2013) to name a few. Members of clade C

also include individuals of great morphological heterogeneity. For example, *Toxisarcon alba* (Welding, 2002) which has a large reticulated cell body with agglutinated test that can be abandoned, forms a lineage with a large round, reflective silver saccamminid (Gooday, 1996) and the organic walled *Gloiogullmia eurystoma*. Other lineages such as clade G and clade F also comprise taxa that lack gross morphological affinities (Pawłowski and others, 2002).

The specificity of which foraminifera uptake specific arenaceous materials for test construction is observed in many monothalamids. The majority of the taxa evaluated in this study primarily agglutinate clay particles regardless of sediment composition of the ambient environment. For example, *Psammophaga sapela* is found inhabiting a wide variety of habitats from mudflats to sand bars, yet they exhibit a high degree of specificity of selection of materials for the agglutinated test regardless of environmental sediment composition. The mineralogy of the material consisting of cytoplasmic inclusions is drastically distinct from that of the test material (Altin-Ballero and others, 2013). Clade L member *Ovamina opaca* agglutinates quartz minerals closest to the IOL but specifically places clay minerals on the outermost surface of the test (unpublished observations). One undescribed species observed during this study places a high concentration of black materials at the abapertural end which gradually grades towards predominantly white minerals at the apertural end (unpublished observations). Empirical sedimentological analyses of sampling sites have not been conducted at this time but it appears that monothalamid foraminifera exhibit a high degree of selectivity for materials chosen for test construction.

Not only are foraminifera selective in minerals used in test construction, some take great care in the physical packing of the minerals. For most taxa, the agglutinated layer runs 10 μ m-20 μ m thick but *Niveus flexilis* and “*Micrometula*-like” possess an agglutinated layer much

thinner than the IOL (~0.5 μm). *N. flexilis* meticulously aligns clay platelets in close proximity to each other and orients them parallel to the cell surface (Altin and others, 2009).

“*Micrometula*-like”, however, packs the clay platelets, for the most part, in varying orientations (Figs. 4.10.4-4.10.7). The “Chocolate silver saccamminid” also tightly layers clay plates parallel to the cell surface (Figs 4.7.3-4.7.4) but these are arranged more haphazardly near the aperture (Fig. 4.7.2). Like *N. flexilis*, most taxa such as *Xiphophaga* sp. (Goldstein and others, 2010), “Fusiform” (Figs. 4.5.6-4.5.7, 4.5.9) and the “#5 Cigar” (Figs. 4.8.2-4.8.3) pack the agglutinated layer in a loose pattern.

Morphology versus the Molecule: Total Evidence

The ultimate goal of any phylogenetic analysis is to establish a well-supported and accurate hypothesis of the evolutionary history of a selected group of organisms at a specified taxonomic level. The means by which to accomplish this goal, whether by using morphological or molecular data sets, is highly debated. Whereas both data sets have advantages and disadvantages in phylogenetics, neither method can be considered more informative or accurate than the other in all circumstances (Hillis and Wiens, 2000). Although collection of molecular data requires living specimens (or in a few cases cases very well preserved material), within a short period of time, any given gene can provide a very large number of observable characters for comparison (Hillis, 1987). Collecting an equivalent volume of morphological characters and assessing multiple character states can be extraordinarily time consuming and tedious. With an exception of gene selection or alignment creation, genes can be selected and defined in an objective manner because characters and states are straightforward (Hillis and Wiens, 2000). One problem with molecular data sets can be discordance between trees based on a single gene and species trees based on morphology. If a gene evolves differently from the species (e.g.

lateral gene transfer, paralogy), when analyzed independently, molecular analyses can return a well-supported but phylogenetically inaccurate tree (Doyle, 1992). Morphology proponents support the idea that a single, observable character can be the phenotypic expression of multiple genes operating under the influence of evolutionary pressures over time. Evolution operates on many, not single genes therefore the evaluation of a single morphological character is more comprehensive than one based on a single gene alone.

In foraminifera, observable similarities in character states or a morphological feature may not be due to genetic variations but instead are functions of homoplasy. For example, of the few studies on foraminiferal reproduction, several species show test dimorphism correlating with asexual or sexual phases—but not all taxa that experience an alternation of generations show the same pattern of test dimorphism (Goldstein, 1999). Variations in morphology may also be a function of differences in environmental conditions (Holzmann and Pawlowski, 1997; Holzmann, 2000). Ecophenotypic variations of test pore size have been reported to occur in *Ammonia* sp. living in different oxygen concentrations (Holzmann, 2000). Taxa morphologically similar but genetically distinct are common in planktonic foraminifera (cryptic speciation, Huber and others, 1997; Darling and others, 1997, 1999; deVargas and others, 1999) and was also documented for the benthic monothalamid *Xiphophaga* sp. (Goldstein and others, 2010). Evolutionary trees based strictly on morphology may be phylogenetically inaccurate due to homoplasy.

Because both morphological and molecular phylogenetic approaches have their unique strengths and advantages, evolutionary hypotheses based on both should be significantly more robust than if either is used alone (Bauldauf and others, 2000; Bauldauf, 2003). Where molecular and morphological trees are incongruent, trees created with both data sets combined show

improved phylogenetic accuracy (Hillis and Wiens, 2000). Ideally the ‘Total Evidence Phylogeny Approach’ (Carnap, 1950; Kluge, 1989; Nixon and Carpenter 1996) should be employed to resolve evolutionary relations among the Clade E taxa. Here, multiple lines of data such as molecular, ultrastructural, gross morphological and any biological information (i.e., reproductive, environmental, physiological) on all available taxa are treated as a single combined data set that is evaluated simultaneously. Total evidence therefore maximizes exploratory power and informative component of that data (Kluge, 1989). Unfortunately, at this time taxon sampling for monothalamids is low, biological information on reproduction is limited and ultrastructural studies are minimal. Nonetheless, whenever possible electron microscopic methods should be employed when evaluating monothalamid foraminifera because ultrastructural morphological data contains invaluable biological and evolutionary information that should be used in conjunction with molecular data sets.

Conclusions

Phylogenetic analyses based on the SSU rDNA alone, or concatenated with protein-coding genes produced a core group of taxa that can be confidently characterized as Clade E—*Psammophaga* spp., *Vellaria* spp. and *Xiphophaga* spp. Based on the taxon sampling in this study, Clade E can be broadened into a weakly supported, larger monophyletic grouping to include *Niveus flexilis*, *Nellya rugosa*, and other undescribed taxa in the SSU rDNA based tree. A multi-gene analysis eliminates the monophyletic Clade E produced by the single gene tree, recovers the core ‘E’ clade and incorporates the “Fusiform”-“Duplin quartzball” sister taxa with high support. Additional genes may decrease support in some instances but increase overall phylogenetic accuracy. Clade level phylogenetic analyses of monothalamous foraminifera are heavily influenced by taxon sampling.

All taxa evaluated in this study exhibit consistent ultrastructural architecture of the wall yet no gross morphological affinities are shared among them. Further, formally described species of one genus can be of closer molecular affinity to members of a different genus despite obvious morphological inconsistencies. It is imperative that all newfound taxa are adequately sampled for molecular characterization and ultrastructural observations as keys to their evolutionary history are evidently absent from their gross morphology. Whenever possible as much biological information should be gathered (i.e., reproduction, ecological) and used as a check and balance control for molecular based hypotheses because evolution does not operate on one gene or a single morphological character alone.

Acknowledgments

We sincerely thank Mark Farmer for utilization of equipment and lab space for the molecular portion of this project; Sam Bowser and Sarah Jardeleeza for assistance; Elizabeth Richardson, Mary Ard and John Shields for their advisement on electron microscopic techniques and Jan Pawlowski for sharing his Clade E SSU rDNA alignment. The thoughtful recommendations of reviewers significantly improved this manuscript. This research was funded in part by National Science Foundation grants DEB0445181 to S. S. Bowser and S. T. Goldstein, and OCE0850505 to S. T. Goldstein; and by graduate research awards to D. Z. Altin-Ballero: Loeblich and Tappan Award (Cushman Foundation for Foraminiferal Research), Lerner-Gray Award (American Museum of Natural History), Rodney M. Feldmann Award (Paleontological Society), Student Research Award (Geological Society of America), Levy Award for Marine Geology and Watts-Wheeler Grants-In-Aid (UGA Geology Department) the Friends the of University of Georgia Marine Institute Award. This is contribution number 1033 of the University of Georgia Marine Institute, Sapelo Island, Georgia.

CHAPTER 5

CONCLUSIONS

Monothalamid foraminifera have gained attention in the scientific literature over the past decade. As descendents of one of the earliest groups of eukaryotic protists, they can provide key information regarding paleoecology and paleobiology of deep time. Several new, undescribed monothalamid taxa with questionable membership to Clade E were recovered along various salt marshes and mudflats of Sapelo Island, Georgia, and neighboring environs. All taxa were examined morphologically both at the gross anatomical and fine structural levels through electron microscopic methods. Attempts were made to amplify two cytoskeletal, protein-coding genes (actin and β -tubulin) along with the SSU rDNA gene for each newfound taxon to test the fidelity of membership in the clade. Molecular trees were compared with the available gross and ultrastructural data to elucidate evolutionary trends and potentially identify morphological synapomorphies. Ultimately, the research presented here greatly enhances our understanding of modern monothalamid diversity, cellular biology and evolutionary trends.

Two new monothalamid species, *Niveus flexilis* (Altin and others, 2009) and *Psammophaga sapela* (Altin-Ballero and others, 2013) have formally been described with detailed ultrastructural observations for both vegetative and reproductive individuals. *N. flexilis* is distinguished by significant gross morphological differences compared to monothalamids previously reported whereas *P. sapela* was primarily delineated from other psammophagid species on the basis of morphological, reproductive and molecular differences. The test of *N. flexilis* is small, ovate in shape, flexible and composed of a significantly thin outer agglutinated layer composed of meticulously packed clay platelets. Generally pyriform in shape, *P. sapela*

also constructs an outer agglutinated test of loosely packed clay platelets situated parallel to the plasma membrane. Asexually reproduced offspring of *N. flexilis* were grown in culture in the absence of sediments affirming that an agglutinated test is not a requirement for survival. As seen in most foraminiferal orders, both taxa have been observed undergoing sexual reproduction by releasing biflagellated gametes directly into seawater via the single aperture. As an alternative to this common theme in foraminiferal reproduction, *P. sapela* can also release a collection of gametes contained within a membrane-bound packet, which subsequently ruptures at a distance from the parental test. This dispersal method may aid in genetic mixing among members within the population.

Ultrastructural findings show a consistency of fine architectural details of the test wall for all taxa evaluated in this study despite the wide gross morphological variations. All possessed an electron-transparent inner organic lining (IOL) that contained fine fibrils and granules both of which readily took up heavy metal stains. Although the width of the IOL could vary among taxa, it was always observed to remain in contact with the plasma membrane of the cell body and the agglutinated layer. Vesicles and mitochondria commonly lined the plasma membrane. It appears that golgi-derived, test construction materials are delivered exocytotically, or as intact vesicles directly to the IOL. These ultrastructural features of the wall are consistent with previously reported Clade E and Clade L taxa with the exception that the latter agglutinate quartz grains primarily as opposed to clay. Cytoplasmic stercomata have been observed in two of the undescribed species examined here.

Despite the similarities of the fine structure of the organic component of the wall, all members exhibited some variation in mineralogy, packing and thickness of the agglutinated layer. Most taxa agglutinate clay as a primary mineral but others can incorporate significant

amounts of quartz in their test (e.g., “Timber dock black and white”, “Fruitcake”). Larger sized alternative minerals (i.e., biotite) can be found embedded in a finer grained matrix of quartz, clay or a combination of both in a few of the taxa evaluated here. Fragments and intact diatom frustules are commonly found incorporated in test materials of most taxa, but as with the larger sized alternative minerals, they comprise a small fraction of agglutinated materials. The packing of agglutinated minerals can range from a meticulous, compact layering to a spacious packing with minerals arranged in varying orientations. All taxa observed in this study possessed one aperture with an exception of “Fusiform” which had two. The gross morphology of the taxa examined did not provide a corroborating, unifying theme consistent with results of the molecular phylogenetic analyses. Aspects of the overall morphology are not taxonomically or evolutionarily informative for monothalamid foraminifera.

The SSU rDNA based phylogenetic analyses restricted membership in Clade E, to species belonging to three genera (*Psammophaga* spp., *Xiphophaga* spp. and *Vellaria* spp.). Additional taxa were placed into a broader but poorly supported, grouping that appears to have close molecular affinity to Clade E in comparison to any other clade. Although wall fine ultrastructure is consistent among all these taxa, low support in Bayesian and maximum likelihood trees for both the SSU rDNA and multi-gene analyses reject the hypothesis that they are Clade E members. At the clade-level, it appears that addition of multiple genes to the phylogenetic analysis did not improve resolution or node support, however, taxon sampling had a great influence over topology. Phylogenetic relationships among the orphan taxa evaluated in this study can be improved with increased taxon sampling.

Initially this work aimed at applying the total evidence approach to elucidate the evolutionary history and determine membership of Clade E monothalamids. A true application

of this approach would require that morphological data sets be combined and analyzed simultaneously within the Bayesian statistical program. Here, morphological and fine structural characters were qualitatively compared with the gene-based phylogenetic analyses. Ultrastructural findings were generally consistent among all taxa evaluated in this study, and fine architectural features unique to ‘core’ Clade E, or even a subset of Clade E were not found. Further, similar wall constructional themes (e.g., plasma membrane, IOL, agglutinated layer) are found outside of Clade E (i.e., Clade L). Finally, gross morphology did not mirror phylogenetic results because variations in the overall anatomy of the test were vastly different among all taxa, even in congeneric forms (e.g., *Vellaria pellucidus* and *Xiphophaga allominuta*). Indeed, additional monothalamids need to be examined at both the gross and fine structural levels, and their phylogenetic affiliations characterized by DNA analyses. Whenever possible as much biological information should be gathered (i.e., reproduction, ecology), so that it can be applied as a check and balance for comparison with evolutionary trees based on molecular data. Because evolution does not operate on a sole gene or a single morphological character alone, evolutionary hypotheses should be better refined when all available data are applied to phylogenetic inferences.

At this time, the hypothesis that Clade E phylogenetic relationships can be improved by combining multiple gene analysis and ultrastructural data remains inconclusive. Nonetheless, the research presented here is the first attempt at employing a multi-gene analysis on clade level monothalamid phylogenetics. Further, it is the first attempt at comparing ultrastructural data to molecular based phylogenies for monothalamid foraminifera. Finally, it is with great pride to report that this work has formally described two new foraminiferal species, doubled the current

number of protein coding gene sequences for monothalamids and made significant contributions to the available literature on foraminiferal ultrastructure.

REFERENCES

- ALTIN, D. Z., HABURA, A. and GOLDSTEIN, S. T., 2009, A new allogromiid foraminifer *Niveus flexilis* nov. gen., nov. sp., from coastal Georgia, USA: fine structure and gametogenesis: *Journal of Foraminiferal Research*, v. 39, p. 73-86.
- ALTIN-BALLERO, D.Z., HABURA, A. AND GOLDSTEIN, S.T., 2013, *Psammophaga sapela* n. sp., a new monothalamous foraminiferan from coastal Georgia, U.S.A.: fine structure, gametogenesis, and phylogenetic placement: *Journal of Foraminiferal Research*, v. 43, p. 113-126.
- ANGELL, R. W., 1971, Observations on gametogenesis in the foraminifer *Myxotheca*: *Journal of Foraminiferal Research*, v. 1, p. 39–42.
- ANIKEEVA, O.V., 2007, Taxonomical composition and seasonal dynamic of the soft-shelled Foraminifera in the Sevastopol Bay (the Black Sea): *Èkologiyâ Moryâ*, v. 74, p. 5-9.
- APOTHÉLOZ-PERRET-GENTIL, L., HOLZMANN, M. and PAWLOWSKI, J., 2013, *Arnoliellina fluorscens* gen. et sp. nov. – a new green autofluorescent foraminifer from the Gulf of Eilat (Israel): *European Journal of Protistology*, v. 49, p. 210-216.
- ARAUJO, J. C., TÉRAN, F. C., OLIVERIA, R. A., NOUR, E. A. A., MONTENEGRO, M. A. P., CAMPOS, J. R., and VAZOLLER, R. F., 2003, Comparison of hexamethyldisilazane and critical point drying treatments for SEM analysis of anaerobic biofilms and granular sludge: *Journal of Electron Microscopy*, v. 52, p. 429–433.

- ARCHIBALD, J. M., LONGET, D., PAWLOWSKI, J. and KEELING, P. J., 2003, A novel polyubiquitin structure in cercozoa and foraminifera: evidence for a new eukaryotic supergroup: *Molecular Biology and Evolution*, v. 20, p. 62–66.
- ARNOLD, Z. M., 1955, Life history and cytology of the foraminiferan *Allogromia laticollaris*: *University of California Publications Zoology*, v. 61, p. 167–252.
- ARNOLD, Z. M., 1982, *Psammophaga simplora* n. gen, n. sp., a polygenomic Californian saccamminid: *Journal of Foraminiferal Research*, v. 12, p. 72–78.
- ARNOLD, Z. M., 1984, The gamontic karyology of the saccamminid foraminifer *Psammophaga simplora* Arnold: *Journal of Foraminiferal Research*, v. 14, p. 171-186.
- AVNIMELECH, M., 1952, Revision of the tubular Monothalamia: *Contributions to the Cushman Foundation for Foraminiferal Research*, vol. 3, p. 60-68.
- BALDAUF, S.L., 2003, The deep roots of eukaryotes: *Science*, v. 300, p. 1703-1706.
- BALDAUF, S.L., ROGER, A.J, WENK-SIEFERT, I. and DOOLITTLE, W.F., 2000, A kingdom level phylogeny of eukaryotes based on combined protein data: *Science*, v. 290, p. 972-977.
- BÉ, A. W. H., ANDERSON, O. R., and FABER, W. W., JR., 1983, Sequence of morphological and cytoplasmic changes during gametogenesis in the planktonic foraminifer *Globigerinoides sacculifer* (Brady): *Micropaleontology*, v. 29, p. 310–325.
- BERNEY, C., and PAWLOWSKI, J., 2003, Revised small subunit rRNA analysis provides further evidence that foraminifera are related to cercozoa: *Journal of Molecular Evolution*, v. 57, p. S120–S127.
- BERNHARD, J. M., HABURA, A., and BOWSER, S. S., 2006, An endosymbiont-bearing allogromiid from the Santa Barbara Basin: implications for the early diversification of foraminifera: *Journal of Geophysical Research*, v. 111, G03002, doi: 10.1029/2005JG000158.

- BOTES, L., PRICE, B., WALDRON, M., and PITCHER, G. C., 2002, A simple and rapid scanning electron microscope preparative technique for delicate “gymnodinoid” dinoflagellates: *Microscopy Research and Techniques*, v. 59, p. 128–130.
- BOWSER, S. S., and BERNHARD, J. M., 1993, Structure, bioadhesive distribution and elastic properties of the agglutinated test of *Astrammia rara* (Protozoa: Foraminiferida): *Journal of Eukaryotic Microbiology*, v. 40, p. 121–131.
- BOWSER, S. S., HABURA, A., and PAWLOWSKI, J., 2006, Molecular evolution of foraminifera, in Katz, L. A. and Bhattacharya, D. (eds.), *Genomics and Evolution of Microbial Eukaryotes*: Oxford University Press, New York, p. 78–93.
- BOWSER, S. S., GOODAY, A. J., ALEXANDER, S. P. and BERNHARD, J. M., 1995, Larger agglutinated foraminifera of McMurdo Sound, Antarctica: are *Astrammia rara* and *Nododendrodes antarctikos* allogromiids incognito?: *Marine Micropaleontology*, v. 26, p. 75–88.
- BOWSER, S. S., BERNHARD, J. M., HABURA, A., and GOODAY, A. J., 2002, Structure, taxonomy and ecology of *Astrammia triangularis* (Earland), an allogromiid-like agglutinated foraminifera from Explorers Cove, Antarctica: *Journal of Foraminiferal Research*, v. 32, p. 364–374.
- BOZZOLA, J. J., and RUSSELL, L. D., 1998, *Electron Microscopy*, 2nd Ed., Jones and Bartlett Publishers, Boston; 670 p.
- BRADY, H. B., 1881, Notes on some of the reticularian Rhizopoda of the Challenger Expedition, Part III, 1. Classification, 2. Further notes on new species, 3. Note on *Biloculina* mud: *Quarterly Journal of Microscopical Science*, New Series, v. 21, p. 31-71.

- BRADY, H. B., 1884, Reports on the foraminifera dredged by H.M.S. Challenger during the years 1873-1876: Report of the Scientific Results of the Voyage of H.M.S. Challenger 1873-1876, Zoology, v. 9, p. 1-814, pls 1-115.
- BUCHANAN, J. B., and HEDLEY, R. H., 1960, A contribution to the biology of *Astrammmina limicola* (Foraminifera): Journal of the Marine Biological Association, U.K., v. 39, p. 549–560.
- BURKI, F., KUDRYAVTSEV, A., MATZ, M.W., AGLYAMOVA, G.V., BULMAN, S., KEELING, P.J. and PAWLOWSKI, J., 2010, Evolution of rhizaria: new insights from phylogenomic analysis of uncultivated protists, BMC Evolutionary Biology, v. 10, p.377.
- BURKI, F., and PAWLOWSKI, J., 2006, Monophyly of Rhizaria and multigene phylogeny of unicellular bikonts: Molecular Biology and Evolution, v. 23, p. 1922-1930.
- BURKI, F., SHALCHIAN-TABRIZI, and PAWLOWSKI, J., 2008; Phylogenomics reveals a new ‘megagroup’ including most photosynthetic eukaryotes: Biology Letters, v. 4, p. 366-369.
- CARNAP, R., 1950, Logical foundations of probability. University of Chicago Press, Chicago.
- CAVALIER-SMITH, T., 2002, The phagotrophic origin of eukaryotes and the phylogenetic classification of Protozoa: International Journal of Systematic and Evolutionary Biology, v. 52, p. 297–354.
- CEDHAGEN, T., GOODAY, A.J. and PAWLOWSKI, J., 2009, A new genus and two new species of saccamminid foraminiferans (Protista, Rhizaria) from the deep Southern Ocean: Zootaxa, v. 2096, p. 9-22.
- CEDHAGEN, T., And PAWLOWSKI, P., 2002, *Toxiscaron synusuicidica* n. gen., n. sp., a large monothalamous foraminiferan from the west coast of Sweden: Journal of Foraminiferal Research, v. 312, p. 351-357.

CESANA, D., 1972, Ultrastructure des gamètes chez un Foraminifère: *Irdia lucida* Le Calvez:

Academie des Sciences (Paris): Comptes Rendus, v. 274, p. 1044-1047.

CUSHMAN, J.A., 1927, An outline of a reclassification of the Foraminifera: Contributions from the

Cushman Laboratory for Foraminiferal Research, v. 3, p. 1-105.

CUSHMAN, J.A., 1928, Foraminifera: Their Classification and Economic Use, 2th ed.: Cushman

Laboratory for Foraminiferal Research, Special Publication, v. 1, p. 1-401.

CUSHMAN, J.A., 1933, Foraminifera: Their Classification and Economic Use, 2th ed.: Cushman

Laboratory for Foraminiferal Research, Special Publication, n. 4, 349 p.

CUSHMAN, J.A., 1940, Foraminifera: Their Classification and Economic Use, 3th ed.: Harvard

University Press, Cambridge, Massachusetts.

CUSHMAN, J.A., 1948, Foraminifera: Their Classification and Economic Use, 4th ed.: Harvard

University Press, Cambridge, Massachusetts, 588 p.

DAHLGREN, L., 1962a, A new monothalamous foraminifer, *Ovammia opaca* n. gen., n. sp.,

belonging to the family Saccamminidae: Zoologiska Bidrag från Uppsala, v. 33, p. 197–200.

DAHLGREN, L., 1962b, *Allogromia crystallifera* n. sp., a monothalamous foraminifer: Zoologiska

Bidrag från Uppsala, v. 35, p. 451–455.

DAHLGREN, L., 1964, On the nuclear cytology and reproduction in the monothalamous foraminifer

Ovammia opaca Dahlgren: Zoologiska Bidrag från Uppsala, v. 36, p. 315–334.

DARLING, K.F., WADE, C.M, KROON, D. and LEIGH-BROWN, A.J., 1997, Planktic foraminiferal

molecular evolution and their polyphyletic origins from benthic taxa: Marine

Micropaleontology, v. 30, p. 251-266.

- DARLING, K.F., WADE, C.M, KROON, D., LEIGH-BROWN, A.J. and BIJMA, J., 1999, The diversity and distribution of modern planktic foraminiferal small subunit ribosomal RNA genotypes and their potential as tracers of present and past oceanic circulation: *Paleoceanography*, v. 14, p. 3-12.
- DELACA, T. E., 1986, The morphology and ecology of *Astrammmina rara*: *Journal of Foraminiferal Research*, v. 16, p. 216–223.
- DELACA, T. E., Bernhard, J. M., Reilly, A., and Bowser, S. S., 2002, *Notodendrodes hyalinosphaira* (sp. nov.): structure and autecology of an allogromiid-like agglutinated foraminifer: *Journal of Foraminiferal Research*, v. 32, p. 177–187.
- DEVARGAS, C., NORRIS, R., ZANINETTI, L, GIBB, S.W. and PAWLOWSKI, J., 1999, Molecular evidence of cryptic speciation in planktonic foraminifers and their relation to oceanic provinces: *Proceedings of the National Academy of Sciences*, v. 96, p. 2864-2868.
- D'ORBIGNY, A., 1826, Tableau méthodique de la Classe des Céphalopodes: *Annales des Sciences Naturelles*, Paris (Série 1), v. 7, p. 245-314.
- DOYLE, J.J., 1992, Gene trees and species trees: molecular systematics as one-character taxonomy: *Systematic Botany*, v. 17, p.144-163.
- DRUMMOND, A. J., ASHTON, B., BUXTON, S., CHEUNG, M., HELED, J., KEARSE, M., MOIR, R., STONES-HAVAS, S., THIERER, T. AND WILSON, A., 2010, Geneious v4.8, Available from <http://www.geneious.com/>
- DUJARDIN, F., 1835, Recherches sur les organismes inférieurs: *Annales Des Sciences Naturelles*, v. 4, p. 343-377.
- FELLENSTEIN, J., 1978, Cases in which parsimony or compatibility methods will be positively misleading: *Systematic Zoology*, v. 27, p. 401-410.

- FØYN, B., 1936, Foraminiferenstudien I. Der lebenszyklus von *Discorbis vilardeboana* d'Orbigny: Bergens Museums årbok, Naturvidensk rekke, v. 2, p. 1-22.
- FLAKOWSKI, J., BOLIVAR, I., FAHRNI, J., and PAWLOWSKI, J., 2005, Actin phylogeny of foraminifera: *Journal of Foraminiferal Research*, v. 35, p. 93–102.
- GOLDSTEIN, S. T., 1988, On the life cycle of *Saccammina alba* Hedley, 1962: *Journal of Foraminiferal Research*, v. 18, p. 311–325.
- GOLDSTEIN, S. T., 1997, Gametogenesis and the antiquity of reproductive pattern in the Foraminiferida: *Journal of Foraminiferal Research*, v. 27, p. 319–328.
- GOLDSTEIN, S. T., 1999, Foraminifera: A biological overview, in Sen Gupta, B. (ed.), *Modern Foraminifera*: Kluwer Academic Publishers, Boston, p. 37-55.
- GOLDSTEIN, S. T., and ALVE, E., 2011, Experimental assembly of foraminiferal communities from coastal propagule banks: *Marine Ecology Progress Series*, v. 437, p. 1-11.
- GOLDSTEIN, S. T., AND BARKER, W.W., 1988, Test ultrastructure and taphonomy of the monothalamous agglutinated foraminifer *Cribrorhammina*, n. gen., *alba* (Heron-Allen and Earland), *Journal of Foraminiferal Research*, v. 18, p. 130-136.
- GOLDSTEIN, S. T., and BARKER, W.W., 1990, Gametogenesis in the monothalamous agglutinated foraminifer *Cribrorhammina alba*: *Journal of Protozoology*, v. 37, p. 20–27.
- GOLDSTEIN, S. T., HABURA, A., RICHARDSON, E. A., and BOWSER, S. S., 2010, *Xiphophaga minuta*, and *X. allominuta*, nov. gen., nov. spp., new monothalamid foraminifera from coastal Georgia (USA): cryptic species, gametogenesis, and an unusual form of chloroplast sequestration: *Journal of Foraminiferal Research*, v. 40, p. 3-15.

- GOLDSTEIN, S. T., and MOODLEY, L., 1993, Gametogenesis and the life cycle of the foraminifer *Ammonia beccarii* (Linné) forma *tepida* (Cushman): *Journal of Foraminiferal Research*, v. 23, p. 213–220.
- GOLDSTEIN, S. T., and RICHARDSON, E. A., 2002, Comparison of test and cell body ultrastructure in three modern allogromiid Foraminifera: application of high pressure freezing and freeze substitution: *Journal of Foraminiferal Research*, v. 32, p. 375–383.
- GOLDSTEIN, S. T., WATKINS, G. T., and KUHN, R. M., 1995, Microhabitats of salt marsh foraminifera: St. Catherine's Island, Georgia, USA: *Marine Micropaleontology*, v. 26, p.17-29.
- GOODAY, A.J., 2002, Organic-walled allogromiids: aspects of their occurrence, diversity and ecology in marine habitats: *Journal of Foraminiferal Research*, v. 32, p. 384-399.
- GOODAY, A.J., ARANDA DA SILVA, A., KOHO, K.A., LECROQ, B. and PEARCE, R.B., 2010., The 'mica-sandwich'; a remarkable new genus of Foraminifera (Protista, Rhizaria) from the Nazaré Canyon (Portugese margin, NE Atlantic): *Micropaleontology*, v. 56, p. 345-357.
- GOODAY, A.J., ANIKEEVA, O.V. AND PAWLOWSKI, J., 2011, New genera and species of monothalamous foraminifera from Balaclava and Kazach'ya Bays (Crimean Peninsula, Black Sea): *Marine Biodiversity*, v. 41, p. 481-494.
- GOODAY, A.J., BOWSER, S.S. AND BERNHARD, J.M., 1996, Benthic foraminiferal assemblages in Explorer's Cove, Antarctica: a shallow water site with deep sea characteristics: *Progress in Oceanography*, v. 37, p. 117-166.
- GOODAY, A.J., BOWSER, S.S., CEDHAGEN, T., CORNELIUS, N., HALD, M., KORSUN, S., and PAWLOWSKI, J., 2005, Monothalamous foraminiferans and gromiids (Protista) from western Svalbard: a preliminary survey: *Marine Biology Research*, v. 1, p. 290-310.

- GOODAY, A.J. and FERNANDO, O.J., 1992, A new allogromiid genus (Rhizopoda: Foraminiferaida) from the Vellar Estuary, Bay of Bengal: *Journal of Micropaleontology*, v. 11, o, 233-239.
- GOODAY, A.J., KITAZATO, H., HORI, S. and TOTOFUKU, T., 2001, Monothalamous soft-shelled foraminifera at an abyssal site in the north Pacific: a preliminary report: *Journal of Oceanography*, v. 57, pp. 377-384.
- GOODAY, A.J., LEVIN, LISA A., LINKE, P. and HEEGER, T. 1992, The role of benthic foraminifera in deep-sea food webs and carbon cycling. *In* Rowe, G. T and Pariente, V. (eds.) *Deep-Sea Food Chains and the Global Carbon Cycle*, Kluwer Publishers, p. 63-91.
- GOODAY, A.J., NOMAKI, H. and KITAZATO, H. 2008, Modern deep-sea benthic foraminifera: a brief review of their morphology-based diversity and trophic diversity: *Geological Society of London, Special Publications*, v. 303, p. 97-119.
- GOODAY, A.J. and PAWLOWSKI, J. 2004, *Conqueria laevis* gen. and sp. nov., a new soft-walled, monothalamous foraminiferan from the deep Weddell Sea: *Journal of the Marine Biological Association of the United Kingdom*, v. 84, p. 919-924.
- GRELL, K. G., 1967, Sexual reproduction in protozoa, *in* Chen, T. T., (ed.), *Research in Protozoology*: Pergamon Press, Oxford, v. 2, p. 149-213.
- GRELL, K. G., 1973, *Protozoology*: Springer-Verlag, New York, 554 p.
- HABURA, A., GOLDSTEIN, S. T., BRODERICK, S., and BOWSER, S. S., 2008, A bush not a tree: the extraordinary diversity of cold-water basal foraminiferans extends to warm-water environments: *Limnology and Oceanography*, v. 53, p. 1339-1351.

- HABURA, A., GOLDSTEIN, S.T., PARFREY, L.W. AND BOWSER, S.S., 2006, Phylogeny and Ultrastructure of *Miliammina fusca*: Evidence for secondary loss of calcification in a miliolid foraminifer. *Journal of Eukaryotic Microbiology*, 53 (3):204-210.
- HABURA, A., ROSEN, D. R. AND BOWSER, S.S., 2004, Predicted secondary structure of the foraminiferal SSU 3' major domain reveals a molecular synapomorphy for granuloreticulosean protists: *Journal of Eukaryotic Microbiology*, v. 51, p. 464-471.
- HANSEN, H.J., 1999, Shell construction in modern calcareous foraminifera. In Sen Gupta, B.K., *Modern Foraminifera*: Kluwer Academic Publishers, Boston, pp. 57-89.
- HEDLEY, R.H., 1958, A contribution to the biology and cytology of *Haliphysema* (Foraminifera): *Proceedings of the Zoological Society of London*, vo. 130, p. 569-576.
- HEDLEY, R.H., 1962, The significance of "an inner chitinous lining" in saccamminid organization, with special reference to a new species of *Saccammina* (Foraminifera) from New Zealand: *New Zealand Journal of Science*, v. 5, p.375-389.
- HEDLEY, R. H., and BERTAUD, W. S., 1962, Electron microscopic observations of *Gromia oviformis* (Sarcodina): *Journal of Protozoology*, v. 9, p. 79-87.
- HEDLEY, R. H., OGDEN, C. G., and WAKEFIELD, J., ST. J., 1972, Shell ultrastructure in allogromiid Foraminifera (Protozoa): *British Museum (Natural History) Bulletin*, v. 24, p. 467-475.
- HEDLEY, R. H., PARRY, D. M., and WAKEFIELD, J., ST. J., 1967, Fine structure of *Shepherdella taeniformis* (Foraminifera: Protozoa): *Journal of the Royal Microscopical Society*, v. 87, p. 445-456.
- HEDLEY, R.H. AND WAKEFIELD, J. ST. J., 1967, A collagen-like sheath in the arenaceous foraminifer *Haliphysema* (Protozoa): *Journal of the Royal Microscopy Society*, v. 87, p. 475-481.

- HEDLEY, R. H., and WAKEFIELD, J., ST. J., 1969, Fine structure of *Gromia oviformis* (Rhizopodea: Protozoa): Bulletin of the British Museum of Natural History (Zoology), v. 18, p. 5–89.
- HERON-ALLEN, E. and EARLAND, A., 1912. On some foraminifera from the North Sea, etc. dredged by the fisheries cruiser ‘*Goldseeker*’ (international North Sea investigations-Scotland): Part I- on some new Astorhizidae and their shell-structure. Journal of the Royal Microscopy of London, p. 385.
- HILLIS, D.M., 1987, Molecular versus morphological approaches to systematics: Annual Review of Ecology and Systematics, v. 18, p. 23-42.
- HILLIS, D. M and WIENS, J.J., 2000, Molecules versus morphology in systematics: conflicts, artifacts, and misconceptions. In, Phylogenetic Analysis of Morphological Data, Wiens, J.J., ed. Smithsonian Institution Press, Washington, p. 1-19.
- HOLZMANN, M., 2000, Species concept in foraminifera: Micropaleontology, v. 46, (supplement) p. 21–37.
- HOLZMANN, M., HABURA, A., GILES, H., BOWSER, S. S., and PAWLOWSKI, J., 2003, Freshwater foraminiferans revealed by analysis of environmental DNA samples: Journal of Eukaryotic Microbiology, v. 50, p. 135–139.
- HOLZMANN, M., and PAWLOWSKI, J., 1997, Molecular, morphological and ecological evidence for species recognition in *Ammonia* (Foraminifera, Protozoa) and their evolutionary implications: Journal of Molecular Evolution, v. 43, p. 145–151.
- HOLZMANN, M., and PAWLOWSKI, J., 2002, Freshwater foraminiferans from Lake Geneva: past and present: Journal of Foraminiferal Research, v. 32, p. 344–350.
- HUBER, B.T., BIJMA, J. and DARLING, K., 1997, Cryptic speciation in the living planktonic foraminifer *Globigerinella siphonifera* (d’Orbigny): Paleobiology, v. 18, p. 551-557.

- HUELSENBECK, J.P. AND RONQUIST, F., 2001, MRBAYES: Bayesian inference of phylogeny: *Bioinformatics*, v. 17, p. 754-755.
- JEPPE, M. W., 1942, Studies on *Polystomella* Lamarck (Foraminifera): *Journal of the Marine Biological Association of the United Kingdom*, v. 25, p. 607–666.
- KLUGE, A.G., 1989, A concern for evidence and a phylogenetic hypothesis of relationships among Epicrates (Boidae, Serpentes): *Systematic Zoology*, v. 38, p.7-25.
- KNUDSEN, B. and HEIN, J.J., 1999, Using stochastic context free grammars and molecular evolution to predict RNA secondary structure: *Bioinformatics*, v. 15, p. 446-454.
- KNUDSEN, B. and HEIN, J.J., 2003, Pfold: RNA secondary structure prediction using stochastic context-free grammars: *Nucleic Acids Research*, v. 31, p. 3423-3428.
- KORSUN, S., 2002, Allogromiids in foraminiferal assemblages on the western Eurasian arctic shelf: *Journal of Foraminiferal Research*, v. 32, p. 400-413.
- LANGER, M. R., 1992, Biosynthesis of glycosaminoglycans in foraminifera: a review: *Marine Micropaleontology*, v. 19, p. 245–255.
- LANGEZAAL, A.M., JANNINK, N.T., PIERSON, E.S. AND VAN DER ZWAAN, G.J., 2005, Foraminiferal selectivity towards bacteria: an experimental approach using a cell-permeant stain: *Journal of Sea Research*, v. 54, p. 256-275.
- LARKIN, K.E. AND GOODAY, A.J., 2004, Soft-shelled monothalamous foraminifera are abundant at an intertidal site on the south coast of England, *Journal of Micropaleontology*, v. 23, p. 135-137.

- LECROQ, B., LEJZEROWICZ, F., BACHAR, D., CHRISTEN, R., ESLING, P., BAERLOCHER, L., ØSTERÅS, M., FARINELLI, L and PAWLOWSKI, J., 2011, Ultra-deep sequencing of foraminiferal microbarcodes unveils hidden richness of early monothalamous lineages in deep-sea sediments: *Proceedings from the National Academy of Sciences*, v. 108, p. 13177-13182.
- LEE, J. J., 1980, Nutrition and physiology of the foraminifera, *in* Levandowsky, M. and Hunter, S. H. (eds.) *Biochemistry and Physiology of Protozoa*, v. 3: Academic Press, New York, p. 43-66.
- LEE, J. J., 1990, Phylum Granuloreticulosa (Foraminifera), *in* Margulis, L., Corliss, J. O., Melkonian, M., and Chapman, D. J. (eds.) *Handbook of Protoctista*: Jones and Bartlett, Boston, p. 524–548.
- LEJZEROWICZ, F., PAWLOWSKI, J., FRAISSINET-TACHET, L., MARMEISSE, R., 2010, Molecular evidence for widespread occurrence of foraminifera in soils, *Environmental Microbiology*, v. 12, p. 2518-2526.
- LOEBLICH, A. R., and TAPPAN, H., 1964, Sarcodina, Chiefly Thecamoebians and Foraminiferida (2 v.), *in* Moore, R.C. (ed.), *Treatise on Invertebrate Paleontology, Part C, Protista 2*: Geological Society of America and University of Kansas Press, Lawrence, KS, 900 p.
- LOEBLICH, A. R., and TAPPAN, H., 1987, *Foraminiferal Genera and Their Classification*: Van Nostrand Reinhold Company, New York, 2 v., 970 p. (imprinted in 1988).
- LOEBLICH, A. R., and TAPPAN, H., 1992, Present status of foraminiferal classification, *in* Takayanagi, Y., and Saito, T. (eds.), *Studies in Benthic Foraminifera, Proceedings of the Fourth International Symposium on Benthic Foraminifera, Sendai, 1990 (Benthos '90)*: Tokai University Press, Tokyo, Japan, p. 93–102.

- LONGET, D., ARCHIBALD, J. M., KEELING, P. J., and PAWLOWSKI, J., 2003, Foraminifera and cercozoa share a common origin according to RNA polymerase II phylogenies: *International Journal of Systematic and Evolutionary Biology*, v. 53, p. 1735–1739.
- LONGET, D., BURKI, F., FLAKOWSKI, J., BERNEY, C., POLET, S., FAHRNI, J., and PAWLOWSKI, J., 2004, Multigene evidence for close evolutionary relations between *Gromia* and foraminifera: *Acta Protozoologica*, v. 43, p. 303–311.
- LONGET, D. and PAWLOWSKI, J., 2007, Higher-level phylogeny of Foraminifera inferred from the RNA polymerase II (RPB1) gene: *European Journal of Protistology*, v. 43, p. 171–177.
- LUFT, J.H., 1971, Ruthenium red and violet, I. Chemistry, purification, methods of use for electron microscopy and mechanism of action: *Anatomical Records*, v. 171, p. 347–368.
- MCENERY, M.E. and LEE, J.J., 1976, *Allogromia laticollaris*: a foraminiferan with an unusual apogamic metagenic life cycle: *Journal of Protozoology*, v. 23, p. 94–108.
- MEISTERFIELD, R., HOLZMANN, M., and PAWLOWSKI, J., 2001, Morphological and molecular characterization of a new terrestrial allogromiid species: *Edaphoallogromia australica* gen. et spec. nov. (Foraminifera) from Northern Queensland (Australia): *Protist*, v. 152, p. 185–192.
- MELKONIAN, M., 1978, Structure and significance of cruciate flagellar root systems in green algae: comparative investigations in species of *Chlorosarcinopsis* (Chlorosarcinales): *Plant Systematics and Evolution*, v. 130, p. 265–292.
- MELKONIAN, M., 1979, Structure and significance of cruciate flagellar root systems in green algae: zoospores of *Ulva lactuca* (Ulvales, Chlorophyceae): *Helgoland Marine Research*, v. 32, p. 425–435.

- MEYERS, E. H., 1940, Observations on the origin and fate of flagellated gametes in multiple tests of *Discorbis* (Foraminifera): *Journal of the Marine Biological Association, U.K.*, v. 24, p. 201–226.
- MOREIRA, D., VON DER HEYDEN, S., BASS, D., LOPEZ-GARCÍA, P., CHAO, E., and CAVALIER-SMITH, T., 2007, Global eukaryote phylogeny: combined small- and large-subunit ribosomal DNA trees support monophyly of Rhizaria, Retaria and Excavata: *Molecular Phylogenetics and Evolution*, v. 44, p. 255-266.
- NIKOLAEV, S. I., BERNEY, C., FAHRNI, J. F., BOLIVAR, I., POLET, S., MYLNIKOV, A. P., ALESHIN, V. V., PETROY, N. B., and PAWLOWSKI, J., 2004, The twilight of Heliozoa and rise of Rhizaria, an emerging supergroup of amoeboid eukaryotes: *Proceedings of the National Academy of Sciences of the United States of America*, v. 101, p. 8066–8071.
- NIXON, K.C. and CARPENTER, J.M., 1996, On simultaneous analysis: *Cladistics*, v. 12, p. 221-241.
- NYHOLM, K.G., 1974, New monothalamous foraminifera: *Zoon*, v. 2, p.117-122.
- NYHOLM, K. G., and NYHOLM, P. G., 1975, Ultrastructure of monothalamous foraminifera: *Zoon*, v. 3, p. 141–150.
- PAGE, R.D.M., 1996, TREEVIEW: an application to display phylogenetic trees on personal computers. *Computer Applications in the Biosciences*, v. 12, p. 357-358.
- PARFREY, L.W., GRANT, J., TEKLE, Y.I., LASEK-NESSELQUIST, E., MORRISON, H.G., SOGIN, M.L., PATTERSON, D.J., and KATZ, L.A., 2010, Broadly sampled multigene analyses yield a well-resolved eukaryotic tree of life: *Systematic Biology*, v. 59, p. 518-533.
- PAWLOWSKI, J., 2000, Introduction to the molecular systematics of foraminifera: *Micropaleontology*, v. 46 [supplement 1], p. 1-12.

- PAWLOWSKI, J., BOLIVAR, I., BERNEY, C., FAHRNI, J., CEDHAGEN, T., and BOWSER, S. S., 2002, Phylogeny of allogromiid foraminifera inferred from SSUrRNA gene sequences: *Journal of Foraminiferal Research*, v. 32, p. 334–343.
- PAWLOWSKI, J., BOLIVAR, I., FAHRNI, J., DEVARGAS, C., and BOWSER, S. S., 1999a, Naked foraminiferans revealed: *Nature*, v. 399, p. 27.
- PAWLOWSKI, J., BOLIVAR, I., FAHRNI, J., DEVARGAS, C., and BOWSER, S. S., 1999b, Molecular evidence that *Reticulomyxa filosa* is a freshwater naked foraminifer: *Journal of Eukaryotic Microbiology*, v. 46, p. 612–617.
- PAWLOWSKI, J., BOLIVAR, I., FAHRNI, J., DEVARGAS, C., GOODAY, A. J., CEDHAGEN, T., HABURA, A., and BOWSER, S. S., 2003, The evolution of early foraminifera: *Proceedings of the National Academy of Sciences of the United States of America*, v. 100, p. 11,494–11,498.
- PAWLOWSKI, J. AND HOZMANN, M., 2002, Molecular phylogeny of Foraminifera—a review: *European Journal of Protistology*, v. 38, p. 1-10.
- PAWLOWSKI, J., and HOLZMANN, M., 2008, Diversity and geographic distribution of benthic foraminifera: a molecular perspective: *Biodiversity and Conservation*, v. 17, p. 317-328.
- PAWLOWSKI, J., HOLZMANN, M. and TYSZKA, J., 2013, New supraordinal classification of Foraminifera: Molecules meet morphology: *Marine Micropaleontology*, v. 100, p. 1-10.
- PAWLOWSKI, J., and MAJEWSKI, W., 2011, Magnetite-bearing foraminifera from Admiralty Bay, West Antarctica, with description of *Psammophaga magnetica*, sp. nov.: *Journal of Foraminiferal Research*, v. 41, p. 3-13.
- PAWLOWSKI, J., MAJEWSKI, W., LONGET, D., GUIARD, J., CEDHAGEN, T., GOODAY, A. J., KORSUN, S., HABURA, A. and BOWSER, S. S., 2008, Genetic differentiation between Arctic and Antarctic monothalamous foraminiferans: *Polar Biology*, v. 31, p. 1205-1216.

- POE, S. and SWOFFORD, D. L., 1999, Taxon sampling revisited: *Nature*, v. 398, p. 299-300.
- ROKAS, A. and CARROLL, S.B., 2005, More genes or more taxa? The relative contribution of gene number and taxon number to phylogenetic accuracy: *Molecular Biology and Evolution*, v. 22, p. 1337-1344.
- ROTHER, N., GOODAY, A.J., CEDHAGEN, T., FAHRNI, J., HUGHES, J.A., PAGE, A., PEARCE, R.A. and PAWLOWSKI, J., 2009, Three new species of deep-sea *Gromia* (Protista, Rhizaria) from the bathyal and abyssal Weddell Sea, Antarctica: *Zoological Journal of the Linnean Society*, v. 157, p. 451-469.
- SABBATINI, A., PAWLOWSKI, J., GOODAY, A., STEFANO, P., BOWSER, S., MORIGI, C., and NEGRI, A., 2004, *Vellaria zucchellii* sp. nov., a new monothalamous foraminifer from Terra Nova Bay, Antarctica: *Antarctic Science*, vol. 16, p. 307-312.
- SABBATINI, A., MORIGI, C., NEGRI, A. and GOODAY, A.J., 2007, Distribution and biodiversity of living benthic Foraminifera, including monothalamous taxa, from Tempelfjord, Svalbard: *Journal of Foraminiferal Research*, v. 37, p.93-106.
- SCHAUDINN, F., 1893, *Myxotheca arenilega* nov. gen. nov. sp. Ein neuer mariner Rhizopode: *Zeitschrift für Wissenschaftliche Zoologie* v. 57, p. 18–31.
- SCHWAB, D., 1969, Elektronenmikroskopische untersuchung an der Foraminifere *Myxotheca arenilega* Schaudinn: *Zeitschrift für Zellforschung und Mikroskopische Anatomie*, v. 96, p. 295-324.
- SCHWAB, D., 1974, Elektronenmikroskopische untersuchung an der Foraminifere *Allogromia laticollaris* Arnold, *Protoplasma*, v. 80, p. 305-322.
- SCHWAB, D., 1976, Gametogenesis in *Allogromida laticollaris*: *Journal of Foraminiferal Research*, v. 6, p. 251-257.

- SCHWAB, D., 1977, Light and electron microscopic investigations on monothalamous foraminifer *Boderia albicollaris* n. sp., *Journal of Foraminiferal Research*, v. 7, p. 188-195.
- SEN GUPTA, B. K., 1999, Systematics of modern foraminifera, in Sen Gupta, B. K., (ed.), *Modern Foraminifera*: Kluwer Academic Publishers, Boston, p. 7–36.
- SERGEEVA, N.G. AND ANIKEEVA, O.V., 2006, Soft-shelled foraminiferan (Protozoa: Rhizopoda, Allogromiinae) from the Black Sea: species composition and distribution: *Èkologiyâ Moryâ*, v. 2, p. 57-64.
- SINNINGER, F., LECROQ, B., MAJEWSKI, W., and PAWLOWSKI, J., *Bowseria arctowskii* gen. et sp. nov., a new monothalamous foraminiferan from the Southern Ocean: *Polish Polar Research*, v. 29, p. 5-15.
- SLITER, W. V., 1968, Shell material variation in the agglutinated foraminifer *Trochammina pacifica* Cushman: *Tulane Studies in Geology*, v. 6, p. 80–84.
- SWOFFORD, D.L, OLSEN, G.J., WADDELL, P.J. and HILLIS, D.M., 1996, Phylogenetic inference, in Hillis, D.M., Moritz, C., Mable, B.K. (eds.) *Molecular systematics*, Sunderland, Ma., Sinauer Associates, p. 407-514.
- TAMURA, K., PETERSON, D., PETERSON, N., STECHER, G., NEI, M., AND KUMAR, S., 2011. MEGA5: molecular evolutionary genetics analysis using maximum likelihood, evolutionary distance and maximum parsimony methods: *Molecular Biology and Evolution* v.28, p. 2731-2739.
- TAPPAN, H., and LOEBLICH, A. R., 1988, Foraminiferal evolution, diversification and extinction: *Journal of Paleontology*, v. 62, p. 695–714.

- TAKISHITA, K., INAGAKI, Y, TSUCHIYA, M, SAKAGUCHI, M and MARUYAMA, T., 2005, A close relationship between Cercozoa and Foraminifera supported by phylogenetic analyses based on combined amino acid sequences of three cytoskeletal proteins (actin, α -tubulin, and β -tubulin): *Gene*, v. 362, p. 153-160.
- TAYLOR, F.J.R., 1999, Ultrastructure as a control for protistan molecular phylogeny: *The American Naturalist*, v. 154, p. S125-S136.
- TRIEMER, R. E., and OTT, D. W., 1990, Ultrastructure of *Diplonema ambulator* Larsen and Patterson (Euglenozoa) and its relationship to *Isonema*: *European Journal of Protistology*, v. 25, p. 316–320.
- TSUCHIYA, M. GOODAY, A.J., HIDETAKA, N., OGURI, K. and KITAZATO, H., 2013, Genetic diversity and environmental preferences of monothalamous foraminifers revealed through clone analysis of environmental small-subunit ribosomal DNA sequences: *Journal of Foraminiferal Research*, v. 43, p. 3-13.
- WIENS, J.J. and MOEN, D.S., 2008, Missing data and the accuracy of Bayesian phylogenetics: *Journal of Systematics and Evolution*, v. 46, p. 307-314.
- WILDING, T.A., 2002, Taxonomy and ecology of *Toxiscaron alba* sp. nov. from Loch Linnhe, west coast of Scotland, UK: *Journal of Foraminiferal Research*, v. 32, p. 358-363.
- WOESE, C. R., KANDLER, O., and WHEELIS, M. L., 1990, Towards a natural system of organisms: proposal for the domains Archaea, Bacteria and Eukarya: *Proceedings of the National Academy of Sciences of the United States of America*, v. 87, p. 4576–4579.
- WOOD, A., 1949, The structure of the wall of the test in the foraminifera: its value in classification: *Quarterly Journal of the Geological Society of London*, v. 104, p. 229–255.

ZUKER, M., 2003, Mfold web server for nucleic acid folding and hybridization prediction: *Nucleic Acids Research*, v. 31, p. 3406-3415.

ZWICKL, D.J., and HILLIS, D.M., 2002, Increased taxon sampling greatly reduces phylogenetic error: *Systematic Biology*, v. 51, p. 588-598.